Modeling, analysis, and control of microalgae growth in dense cultures

Carlos Martinez von Dossow

École Doctorale des Sciences de l'Environnement d'Ile-de-France

PhD Thesis

submitted in partial fulfillment of the requirements for the degree of doctor of

Sorbonne Université

Scpecialized in: Oceanography

By:

Carlos Alexander Martínez von Dossow

on May 13th 2019

Modeling, analysis, and control of microalgae growth in dense cultures

Supervisor	Antoine Sciandra	Laboratoire d'Océanographie de Villefranche
Co-supervisor	Olivier Bernard	INRIA Sophia Antipolis
Co-supervisor	Francis Mairet	IFREMER Nantes
Reviewer	Alain Rapaport	INRA Montpellier
Reviewer	Héctor Ramírez	Universidad de Chile
Examiner	Sakina-Dorothée Ayata	Laboratoire d'Océanographie de Villefranche
Examiner	Gail Wolkowicz	McMaster University
Examiner	Claude Lobry	Université Côte d'Azur

École Doctorale des Sciences de l'Environnement d'Ile-de-France

Thèse de doctorat

pour obtenir le grade de docteur délivré par

Sorbonne Université

Spécialité doctorale: Océanographie

présentée et soutenue publiquement par

Carlos Alexander Martínez von Dossow

le 13 Mai 2019

Modélisation, analyse et contrôle de la croissance microalgale en cultures à haute densité

Jury

M. Antoine Sciandra	Directeur de recherche	Directeur
M. Olivier Bernard	Directeur de recherche	Co-directeur
M. Francis Mairet	Cadre de recherche	Co-encadrant
M. Alain Rapaport	Directeur de recherche	Rapporteur
M. Héctor Ramírez	Professeur	Rapporteur
Mme. Sakina-Dorothée Ayata	Maître de conférences	Examinatrice
Mme. Gail Wolkowicz	Professeure	Examinatrice
M. Claude Lobry	Professeur	Examinateur

Acknowledgments

Firstly, I would like to thank my PhD supervisor Olivier Bernard for the continuous support before and during my PhD, for encouraging me and allowing me independence to pursue my own ideas. Similarly, I would like to thank my co-supervisor Francis Mairet for his support, especially at the beginning of my PhD when I was barely able to speak a different language from Spanish. I am very grateful to both of you for the time invested correcting my work with meticulous comments and for helping me to grow scientifically. I also would like to thank Antoine Sciandra for accepting to be my "official" supervisor. Even if we did not interact very much, he was always willing to help me.

I would like to thank Sakina-Dorothée Ayata and Claude Lobry for being part of my "comité de thèse" and for participating as members of the jury in my PhD defense. Special thanks are owed to Sakina for all the reports that she wrote for the doctoral school. I am also grateful to Alain Rapaport, Héctor Ramírez, and Gail Wolkowicz for being part of my jury. Thanks to all of you for investing time in reading my thesis and for your useful feed-backs.

I would like to thank BECAS CHILE (CONICYT) for financing my PhD, and also the team Greencore, and the projects IPL Algae in Silico and PHYCOVER for giving me the chance of participating in scientific meetings and financing my participation in conferences and courses.

I am grateful to the team BIOCORE that provided me a nice place for doing my research. Special thanks go to the friends that I made during these years: Agustin, Elena, Ivan, Lucie, Marjorie, Ouassim, and Sofia. Thanks to all of you for the nice moments.

I would also like to thank some people I have met in Nice, specially my chilean friends Sofía and Sebastian. Thanks for all those moments laughing, doing sport, or drinking until very late. In some sense that was necessary for finishing my PhD.

Finally, I wish to thank my family for their support and encouragement throughout my PhD.

Contents

CHAPTER 1

Introduction

From a biogeochemical viewpoint, the most important aquatic photosynthetic organisms are the phytoplankton [9]. Phytoplankton consist in single oxygenic cells drifting in aquatic mediums (from Greek *phyton*, plant, and *planktos*, drifter). They comprise microalgae (eukaryotic cells) and cyanobacteria (prokaryotic cells) that can all do photosynthesis. Phytoplankton biomass in the oceans corresponds to less than 2% of the total global plant carbon. Nonetheless, these organisms collectively capture approximately 40% of the global fixed carbon per year [3, 10]. This suggests microalgae (synonym of phytoplankton in biotechnology and applied phycology) cultivation as an attractive alternative for reducing greenhouse gas emissions [35]. Microalgae grow naturally in all aquatic environments, including oceans, lakes, ponds, and rivers. They can be used for production of compounds such as food complements, colorants, antioxydants, pharmaceuticals, or at longer time scale they might be grown for producing molecules for green chemistry, including biofuels [22, 24, 27]. They are also used for nutrient removal in wastewater treatment systems [1] where they play a central role: in addition to capturing the inorganic elements (nitrogen and phosphorus), they produce the oxygen necessary for the heterotrophic bacteria, avoiding the use of oxygenation systems. For all these applications, microalgae are mass cultivated in closed or open reactors named photobioreactors (PBR). Nevertheless, full-scale implementation of phytoplankton is still challenging due to the early stage of technological development of this innovative approach. Mathematical models have already revealed themselves to be a very efficient tool for guiding the development and optimization of several biotechnological processes. There are however specific challenges to control

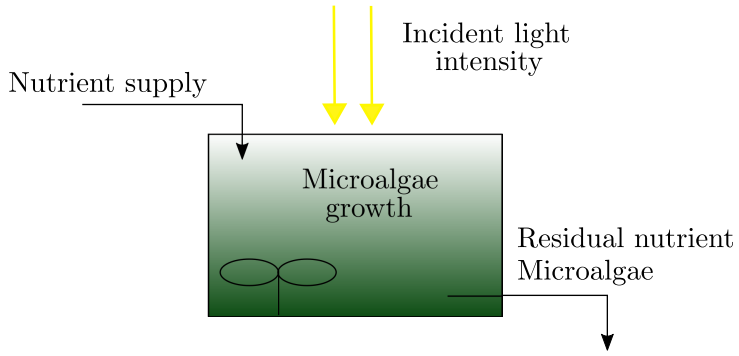

Figure 1.1: Scheme of the light-limited chemostat.

and optimize outdoor microalgae cultures, especially maintaining optimal growth conditions to cope with the diel and seasonal fluctuations of light. Developing accurate mathematical models is the first crucial stage towards this optimization objective. Obtaining a better understanding of the dynamics of phytoplankton is also key for more accurately describing the dynamics of carbon fixation by photosynthesis in oceanic ecosystems. Even if these fields seem very different, the models, and often the experimental tools to study phytoplankton in the laboratory are very similar.

The chemostat is a very interesting tool used to perform experiments that can further support model developments for microorganisms. This device is a perfectly mixed reactor, permanently fed with a nutrient rich medium and simultaneously emptied so that the culture volume is kept constant. This experimental tool was introduced in the 1950s for bacterial cultures, independently by Monod [23] and Novick and Szilard [25]. Microorganisms develop in the reactor and the dynamics of their population results from the balance between net growth (*i.e.* gross growth rate minus the losses due to

mortality) and dilution. A scheme for growth of microalgal in the chemostat is shown in Figure 1.1. Generally, all the nutrients are in excess except one that will become the limiting nutrient. The chemostat may be operated at different dilution rates and different concentrations of the influent limiting nutrient [33]. The main advantage is that, at steady state, when net growth rate perfectly equals dilution rate, the population reaches a stationary level. This is a marked difference with experiments carried out in batch mode where maximum growth rate could only last for a few tens of generation, and then growth rate progressively reduces after one of the factors necessary for growth becomes limiting. Using the chemostat is a way to maintain indefinitely a non zero growth rate, and therefore to study the organisms under various constant growth rates.

Chemostat studies supported the work of Monod for modelling bacterial populations [23]. The first studies of microalgae grown in a chemostat environment, appeared in the late 1960s with the works of Droop [7] and Caperon [5]. Droop used a chemostat to measure the internal cell quota of vitamin B_{12} required to support growth of the microalgae *Monochrysis lutheri* (see Figure 1.2). Caperon studied the growth response of *Isochrysis galbana* under nitrogen limitation. Since then, the chemostat has been widely used in microalgae research [12, 18, 20, 26]. In the words of Waltman [31], "the chemostat is the best laboratory idealization of nature for population studies". The models developed for the chemostat were generally mathematically tractable so that theory could be derived from models and could then be compared to experimental outcomes. Chemostat theory provided

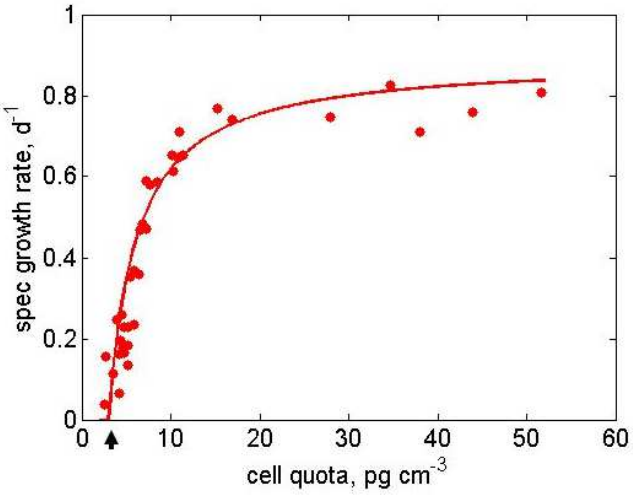

Figure 1.2: Growth rate as a function of B_{12} vitamin quota measured in a chemostat culture of *Monochrysis lutheri*. From [8].

the basis to understand and predict steady-state concentrations of biomass and the residual concentration of the limiting substrate for various dilution rates or influent concentrations [28]. Chemostat studies of photosynthetic microorganisms are however slightly more complex since light enters into the game. For example, in a series of papers, Huisman and collaborators studied microalgae growth under limitation by light [15, 17, 32]. They developed the theory of the light-limited chemostat [16]. This theory proposes fundamental concepts to help to understand the dynamic behaviour of light-limited cultures and serves as a basis for many theoretical and experimental studies in continuous photobioreactors [6, 13, 19, 34]. Moreover, models of the chemostat are the starting point for many variations that yield more realistic biological models and interesting mathematical problems.

In the natural environment, the main resources limiting microalgae growth rate are light and nutrients such as nitrogen and phosphorus. Nutrient limitation has been studied in the chemostat and often represented by the Monod model [23] or the Droop (or Cell Quota) model [8]. The former relates the growth rate to the nutrient concentration in the medium, while the latter relates the growth rate to an intracellular pool of the limiting element known as the cell quota. The applicability of the Monod model for phytoplankton is limited to steady state conditions [29]. The Droop model turned out to represent a broader range of situations, and has successfully described the growth rate even under fluctuations of the environmental conditions [4, 8, 11]. Light-limitation differs considerably from nutrient-limitation. Light rapidly decreases as it passes through the microalgae culture due to absorption and scattering by algal cells and other substances such as organic matter in the growth medium. This results in a light gradient whose pattern varies with the microalgae concentration. Additionally, microalgae may adapt their chlorophyll content to the light conditions [2]. This dynamical process is known as photoacclimation and occurs in a time scale of days [14]. This strategy limits the dramatic impact of an excess of light on cell metabolism. Indeed, when too much light reaches the photosynthetic antenna, it causes severe cell damage, resulting in the so called photoinhibition process [21, 30]. At very high light, an increase of light intensity often results in a decrease of the growth rate due to this photoinhibition.

Chemostat models are generally based on ordinary differential equations. Their main advantage is that they accurately represent the mass conserva-

tion of the limiting nutrient (which is often the sum of the dissolved and particulate compartments). The first two questions that a chemostat model can address are: (I) does the population survive or wash out in the long-term? (II) If the population survives, how does the population behave in long-term? The theory of dynamical system is used to tackle these questions. Under constant environmental conditions and constant operation of continuous photobioreactors, two types of equilibria (steady states) usually occur representing species extinction and survival. Depending on initial conditions, parameters or inputs (dilution rate, influent concentration or light intensity), the microalgae population either approaches the extinction equilibrium or the survival equilibrium. In outdoor cultures, microalgae face variable environmental conditions. These cultures are subject to a light phase (day) and a dark phase (night) that follow a periodic pattern. Thus, the growth rate, that depends on light availability, becomes a periodic function in time. Periodicity of the models can also be induced by water temperature or nutrient supply fluctuations. Not much is known about the dynamics of microalgae models with periodic forcing.

The purpose of this thesis is to better understand how different factors may affect the dynamics of microalgae in continuous photobioreactors. We focus on the following objectives:

a) To understand, under light limitation, the impact of different factors affecting microalgae growth rate: depth (or light path-length), background turbidity, incident light intensity, microalgae population density, shape of the PBR.

b) To understand the dynamics of microalgae populations when their growth is limited both by light and nutrients. In particular, to understand how the dynamics is affected by periodic variations of the environmental conditions and transitions from light-limitation to photoinhibition.

c) To give some insight into the optimization of biomass productivity by controlling the depth of the culture or the light source.

d) To propose a simple model to describe microalgae growth under the triple limitation by nitrogen, phosphorus, and light, a situation that often appears in nature or in some processes such as wastewater treatment.

This manuscript is organized as follows. In **Chapter 2**, we present a review of the existing chemostat models accounting for light and/or nutrient limitation and a survey of results regarding the mathematical analysis of these models. In **Chapter 3**, we study the growth rate of microalgae under light limitation. In **Chapter 4** and **Chapter 5**, we study the dynamics of a microalgae population whose growth is limited by light and substrate. In Chapter 4, we do not consider photoinhibition and we assume a periodic forcing (forcing by light, nutrient supply, temperature, etc.). In Chapter 5, we study chemostat with microalgae suffering from photoinhibition. **Chapter 6** and **Chapter 7** are concerned with the maximization of biomass productivity. In Chapter 6, microalgae growth is only limited by light, while in Chapter 7, microalgae growth is also limited by a substrate. Finally, in **Chapter 8**, we propose and validate a model accounting for light, phosphorus, and nitrogen limitation.

Most of the chapters have already been published or accepted (Chapters 3, 6, and 7) or have been submitted (Chapters 4, 5, 8). Introductions have been shorten and adapted to avoid redundancies. Some notation has been changed to be consistent within the manuscript. The original abstract of the corresponding papers are given in the presentation of each chapter.

Bibliography

[1] N. Abdel-Raouf, A. Al-Homaidan, and I. Ibraheem. Microalgae and wastewater treatment. *Saudi journal of biological sciences*, 19(3):257–275, 2012.

[2] T. Anning, H. L. MacIntyre, S. M. Pratt, P. J. Sammes, S. Gibb, and R. J. Geider. Photoacclimation in the marine diatom skeletonema costatum. *Limnology and Oceanography*, 45(8):1807–1817, 2000.

[3] W. Berger. Global maps of ocean productivity, productivity of the ocean: Present and past wh berger, vs smetacek, g. wefer, 429–455, 1989.

[4] G. Bougaran, O. Bernard, and A. Sciandra. Modeling continuous cultures of microalgae colimited by nitrogen and phosphorus. *Journal of theoretical biology*, 265(3):443–454, 2010.

[5] J. Caperon. Population growth response of isochrysis galbana to nitrate variation at limiting concentrations. *Ecology*, 49(5):866–872, 1968.

[6] M. Cuaresma, M. Janssen, C. Vílchez, and R. H. Wijffels. Productivity of chlorella sorokiniana in a short light-path (slp) panel photobioreactor

under high irradiance. *Biotechnology and bioengineering*, 104(2):352–359, 2009.

[7] M. Droop. Vitamin B 12 and marine ecology iii. an experiment with a chemostat. *Journal of the Marine Biological Association of the United Kingdom*, 46(3):659–671, 1966.

[8] M. R. Droop. Vitamin B 12 and marine ecology. iv. the kinetics of uptake, growth and inhibition in monochrysis lutheri. *Journal of the Marine Biological Association of the United Kingdom*, 48(3):689–733, 1968.

[9] P. G. Falkowski. The role of phytoplankton photosynthesis in global biogeochemical cycles. *Photosynthesis research*, 39(3):235–258, 1994.

[10] P. G. Falkowski and A. D. Woodhead. *Primary productivity and biogeochemical cycles in the sea*, volume 43. Springer Science & Business Media, 2013.

[11] R. J. Geider, H. L. Maclntyre, and T. M. Kana. A dynamic regulatory model of phytoplanktonic acclimation to light, nutrients, and temperature. *Limnology and oceanography*, 43(4):679–694, 1998.

[12] E. M. Grima, J. S. Pérez, F. G. Camacho, J. F. Sevilla, and F. A. Fernandez. Effect of growth rate on the eicosapentaenoic acid and docosahexaenoic acid content of isochrysis galbana in chemostat culture. *Applied Microbiology and Biotechnology*, 41(1):23–27, 1994.

[13] F. Grognard, A. R. Akhmetzhanov, and O. Bernard. Optimal strategies for biomass productivity maximization in a photobioreactor using natural light. *Automatica*, 50(2):359–368, 2014.

[14] B.-P. Han. A mechanistic model of algal photoinhibition induced by photodamage to photosystem-ii. *Journal of theoretical biology*, 214(4):519–527, 2002.

[15] J. Huisman, R. R. Jonker, C. Zonneveld, and F. J. Weissing. Competition for light between phytoplankton species: experimental tests of mechanistic theory. *Ecology*, 80(1):211–222, 1999.

[16] J. Huisman, H. C. Matthijs, P. M. Visser, H. Balke, C. A. Sigon, J. Passarge, F. J. Weissing, and L. R. Mur. Principles of the light-limited chemostat: theory and ecological applications. *Antonie van Leeuwenhoek*, 81(1):117–133, Dec 2002.

[17] J. Huisman and F. J. Weissing. Light-limited growth and competition for light in well-mixed aquatic environments: an elementary model. *Ecology*, 75(2):507–520, 1994.

[18] M. IEHANA. Kinetic analysis of the growth of spirulina sp. on continuous culture. *Journal of fermentation technology*, 61(5):457–466, 1983.

[19] W. E. A. Kardinaal, L. Tonk, I. Janse, S. Hol, P. Slot, J. Huisman, and P. M. Visser. Competition for light between toxic and nontoxic strains of the harmful cyanobacterium microcystis. *Appl. Environ. Microbiol.*, 73(9):2939–2946, 2007.

[20] Y.-K. Lee and C.-W. Soh. Accumulation of astaxanthin in haematococcus lacustris (chlorophyta) 1. *Journal of phycology*, 27(5):575–577, 1991.

[21] S. Long, S. Humphries, and P. G. Falkowski. Photoinhibition of photosynthesis in nature. *Annual review of plant biology*, 45(1):633–662, 1994.

[22] J. J. Milledge. Commercial application of microalgae other than as biofuels: a brief review. *Reviews in Environmental Science and Bio/Technology*, 10(1):31–41, 2011.

[23] J. Monod. La technique de culture continue: theorie et applications. 1950.

[24] N.-H. Norsker, M. J. Barbosa, M. H. Vermuë, and R. H. Wijffels. Microalgal productiona close look at the economics. *Biotechnology advances*, 29(1):24–27, 2011.

[25] A. Novick and L. Szilard. Description of the chemostat. *Science*, 112(2920):715–716, 1950.

[26] S. J. Pirt, Y.-K. Lee, A. Richmond, and M. W. Pirt. The photosynthetic efficiency of chlorella biomass growth with reference to solar energy utilisation. *Journal of Chemical Technology and Biotechnology*, 30(1):25–34, 1980.

[27] S. A. Razzak, M. M. Hossain, R. A. Lucky, A. S. Bassi, and H. de Lasa. Integrated co2 capture, wastewater treatment and biofuel production by

microalgae culturinga review. *Renewable and sustainable energy reviews*, 27:622–653, 2013.

[28] H. L. Smith and P. Waltman. *The theory of the chemostat: dynamics of microbial competition*, volume 13. Cambridge university press, 1995.

[29] U. Sommer. A comparison of the droop and the monod models of nutrient limited growth applied to natural populations of phytoplankton. *Functional Ecology*, pages 535–544, 1991.

[30] S. Takahashi and N. Murata. How do environmental stresses accelerate photoinhibition? *Trends in plant science*, 13(4):178–182, 2008.

[31] P. Waltman. *Competition models in population biology*, volume 45. Siam, 1983.

[32] F. J. Weissing and J. Huisman. Growth and competition in a light gradient. *Journal of theoretical biology*, 168(3):323–336, 1994.

[33] C. L. Winder and K. Lanthaler. The use of continuous culture in systems biology investigations. In *Methods in enzymology*, volume 500, pages 261–275. Elsevier, 2011.

[34] S. Yang and X. Jin. Critical light intensities for microcystis aeruginosa, scenedesmus quadricauda and cyclotella sp. and competitive growth patterns under different light: N: P ratios. *Journal of Freshwater Ecology*, 23(3):387–396, 2008.

[35] Y.-S. Yun, S. B. Lee, J. M. Park, C.-I. Lee, and J.-W. Yang. Carbon dioxide fixation by algal cultivation using wastewater nutrients. *Jour-*

nal of Chemical Technology & Biotechnology: International Research in Process, Environmental AND Clean Technology, 69(4):451–455, 1997.

CHAPTER 2

State of the art: Modeling microalgae growth in chemostats

Contents

2.1 Introduction

Mathematical modelling is of great help towards understanding microalgae growth and biomass production in continuous bioreactors. Modelling phytoplankton or microalgae has been the subject of much work since the pioneering work of [21]. Modelling was carried out either to better understand the evolution of phytoplankton in the sea, or in a first stage for further optimizing the industrial production of microalgae. The systems are different in size, but the models are similar. Many dynamical models in the literature attempt to describe microalgae growth and its dependence on different factors such as light, temperature, nutrient availability, pH, salinity, etc. (see the reviews [5, 6, 17, 36]). Most of them consider growth in perfectly mixed reactors (often batch or continuous reactors, also called chemostats), and therefore they are described by ordinary differential equations. These models have been validated in lab scale experiments and sometimes at larger scale for biotechnological applications [4, 10, 29, 45].

This chapter presents a review of the existing dynamical models accounting for light and/or nutrient limitation and a survey of mathematical results regarding their dynamics.

In the first section of this chapter (Section 2.2), we review existing models that describe microalgae growth limited by different factors: first, under light-limitation, then under nutrient limitation, and finally under co-limitation by light and nutrients. In Section 2.3, we review mathematical

results regarding the dynamics of microalgae cultures in a chemostat.

2.2 Microalgae modeling

Let us consider a continuous reactor perfectly mixed (chemostat) with a biomass $x(t)$ of microalgae. Microalgae growth may be limited by light and/or nutrients. The light is provided by an external light source (artificial or natural) and its intensity can vary with time. The nutrients are supplied from an external reservoir at the volumetric flow rate Q_{in}. The dilution rate is the ratio $D := Q_{in}/V$ with V the volume of the culture. The evolution of x can be derived from a mass balance, leading to the following generic equation:

$$\frac{dx}{dt} = [\mu(\cdot) - D]x, \tag{2.1}$$

with $\mu(\cdot)$ the specific growth rate. The specific growth rate considers the net growth i.e.

$$\mu = p - m, \tag{2.2}$$

with p known as the specific gross growth rate or specific production rate (per unit of biomass), and m the loss or maintenance rate. If x is the mass of algal carbon, then p corresponds to the carbon uptake rate and m the specific carbon loss rate.

Equation (2.1) is common to any model of well mixed cultures described by ordinary differential equations. Additional differential equations may be coupled to (2.1) depending on the factors determining the growth rate. In

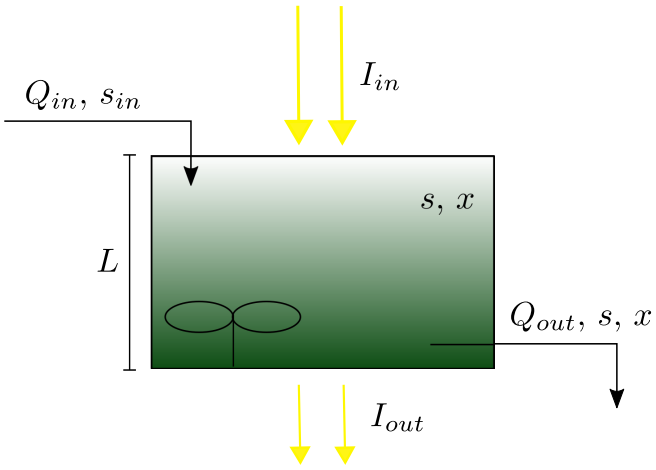

Figure 2.1: Scheme of a simplified planar continuous well-mixed microalgae culture illuminated with an incident light I_{in} and fed with a nutrient supply s_{in} at the volumetric flow rate Q_{in}.

the following, we review the different mathematical models proposed in the literature for $\mu(\cdot)$ under light and/or nutrients limitation.

2.2.1 Light limitation

First we consider the case where light is the limiting factor. Modeling microalgae growth under light limitation one must consider the response of microalgae to light intensity and the distribution of the light intensity in the medium. Light intensity decreases progressively in the culture medium due to light absorption and scattering by light-absorbing substances [8, 11, 34]. Thus, only microalgae near the surface perceive the light intensity at which the culture is illuminated, while microalgae at the darkest zone of the reactor may perceive almost no light.

The specific gross growth rate p as a function of the light intensity I perceived by microalgae (or the P-I curve) has been described by different models in the literature. For example by the Monod model:

$$p(I) = p_{max}\frac{I}{K_I + I}, \tag{2.3}$$

with p_{max} the maximal specific gross growth rate and K_I a half saturation constant. Model (2.3) assumes a positive response to light even for high light intensities. However, high light intensities may result in inhibition [51] which is known as photoinhibition. There are different functions that account for inhibition. For example the classical model of Steele [49]:

$$p(I) = p_{max}\frac{I}{I^*}e^{1-\frac{I}{I^*}}, \tag{2.4}$$

with I^* the light intensity at which p reaches its maximum value, or Haldane-type models [1] like the one presented in [9]:

$$p(I) = p_{max}\frac{I}{I + \frac{p_{max}}{\alpha}\left(\frac{I}{I^*} - 1\right)^2}, \tag{2.5}$$

where α is the initial slope of p. These examples illustrate the essential properties of any P-I curve. We refer the reader to the review [5] for an extensive list of models describing the function p. To illustrate the applicability of the Haldane model, Table 2.1 shows kinetic parameters for (2.5) for three different microalgae species, and Figure 2.2 shows its form with kinetic parameters from Table 2.1 for *C.vulgaris*.

[1] By a Haldane-type model, we mean $p(I) = \frac{I}{aI^2+bI+c}$ with $a, c > 0$.

Parameters	*Chlorella vulgaris*	*Chlorella pyrenoidosa*	*Scenedesmus. crassus*	Unit
p_{max}	1.63	2	1.32	d^{-1}
I^*	87.2	275	119	$\mu mol\, m^{-2}\, s^{-1}$
α	0.027	0.05	0.086	$\mu mol^{-1}\, m^2\, s\, d^{-1}$

Table 2.1: Kinetic parameters of p in (2.5) for different microalgae species; *Chlorella vulgaris* at $25°C$ [51], *Chlorella pyrenoidosa* at optimal temperature [9], and *Scenedesmus crassus* at $25°C$ [20].

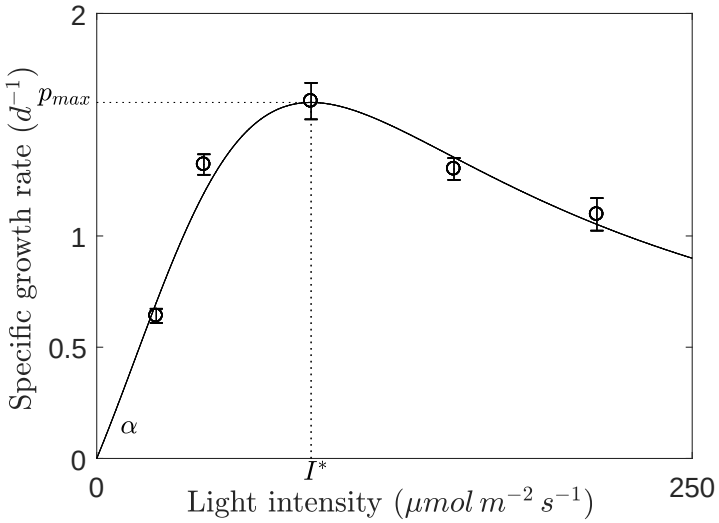

Figure 2.2: Carbon uptake rate (see (2.5)) for *Chlorella vulgaris* with experimental data from [51].

The most studied case is when the reactor is illuminated from above with a light intensity I_{in}. For low-dense cultures it is often assumed that all microalgae perceive the same light intensity equal to I_{in} as done in [33]. However, in the context of industrial applications and aquatic environments, a gradient of light is observed in the culture. As a first approximation, the

law of Lambert-Beer has been used by many authors to determine the light intensity I at any position in the growth medium:

$$I(z) = I_{in}e^{-\xi z}, \ z \in [0, L], \tag{2.6}$$

with $\xi \geq 0$ an extinction coefficient that is usually correlated to the microalgae population density x [34]:

$$\xi = kx + K_{bg}, \tag{2.7}$$

with $k > 0$ the specific light extinction coefficient of the microalgae species and $K_{bg} \geq 0$ the background turbidity that summarizes the light absorption and difussion due to all non-microalgae components i.e. suspended solids and dissolved colored material. Typical values of the coefficient k for some microalgae species are given in Table 2.2. To use expression (2.7), the density of the culture must be low enough so that most of the photons are diffused at most once. For multi diffusion regimes, which characterize industrial reactors, the latter condition is generally not satisfied [23]. Various empirical expressions have therefore been developed to macroscopically account for multi scattering (see Table 6 in [5]). For example, in [52] the following expression is proposed:

$$\xi = \frac{k_1 x}{k_2 + x},$$

with k_1 and k_2 empirical parameters.

To account for the light gradient in the culture in the description of

Extinction coefficient ($m^2\, gC^{-1}$)	Algae
0.214	*Monodus subterraneu*
0.175	*Spirulina platensis*
0.150	*Porphyridium cruentum*
0.200	*Chlorella pyrenoidosa*

Table 2.2: Values of the specific light attenuation coefficient for different microalgae species [5]

μ, some authors assume that microalgae cells in the culture respond to an average light intensity [52]. Thus, the growth rate is described by $\mu = p(\bar{I}) - m$ with $\bar{I}$ the average light intensity given by:

$$\bar{I} = \frac{1}{L}\int_0^L I(z)dz. \tag{2.8}$$

However, experimental evidence in perfectly mixed photobioreactors shows that photosynthetic efficiency increases with depth [30], consequently microalgae cells respond almost instantaneously to all light intensities within the culture medium and not to an average light intensity. Thus, an appropriate way to model the growth rate, consists in accounting for the differences in local growth rates to obtain the average growth rate:

$$\mu = \frac{1}{L}\int_0^L p(I(z))dz - m. \tag{2.9}$$

This way of modeling μ is a trade-off between simple models and complicated models accounting for photosynthesis dynamics [19] which are more difficult to handle and to analyse. Huisman et al.(2002) [30] used this model for constructing the theory of light-limited chemostats.

2.2.2 Photoacclimation

Microalgae adapt their pigment content to the light conditions of the medium [38]. Models accounting for photoacclimation consider the variable θ representing the chlorophyll to carbon ratio and they assume that θ adapts towards a value θ^*. The evolution of θ has been described by the following first-order dynamics [22, 24]:

$$\frac{d\theta}{dt} = \delta(\cdot)(\theta^*(\cdot) - \theta), \tag{2.10}$$

with $\delta(\cdot)$ a photoacclimation rate. The following form of θ^* is proposed in [24]:

$$\theta^*(I) = \theta_{max} - (\theta_{max} - \theta_{min})\frac{I}{I + I_c}, \tag{2.11}$$

with I a certain light intensity, θ_{min} and θ_{max} extreme values of θ, and I_c a constant. A different approach is given in [7, 39]. The authors consider a conceptual variable I_0 representing the irradiance at which the cells are photoacclimated. The evolution of I_0 is then given by:

$$\frac{dI_0}{dt} = \delta'(\cdot)(\bar{I} - I_0), \tag{2.12}$$

with $\bar{I}$ the current average light irradiance, and δ' a photoacclimation rate. In this case, $\theta^*(\cdot)$ is obtained as a function of I_0 and the nitrogen-to-carbon content q_n:

$$\theta^*(\cdot) = \gamma_m q_n \frac{k_I}{k_I + I_0}, \tag{2.13}$$

with γ_m and k_I photoacclimation parameters.

For the description of the photoacclimation rates (δ or δ'), authors in [22] consider a constant positive value for δ when microalgae are illuminated and zero in the absence of light, while [39] considers δ' to be proportional to the specific growth rate μ.

The form of p (or the P-I curve) may depend on the chlorophyll content θ. Figure 2.3 shows the photosynthetic rate curves of *Skeletonema costatum* for different chlorophyll quotas. Table 2.3 shows the parameters associated with the curves shown in Figure 2.3 when they are fitted with (2.5). In [41], it was highlighted that the maxima of the P-I curves normalized to chlorophyll are connected by a line passing through the origin (see Figure 2.3B). In [8], it was highlighted that the initial slope of p, α, depends on θ in the following way

$$\alpha(\theta) = \alpha^{Chl}\theta, \tag{2.14}$$

with α^{Chl} the initial slope of the chlorophyll-specific production rate $p^{Chl} := p/\theta$ which is independent of θ.

The specific microalgae extinction coefficient depends also on θ [8].

Table 2.3: Kinetic parameters associated with Figure 2.3.

Parameter	$\theta = 0.07$	$\theta = 0.02$	Unit
p_{max}	5.21	3.31	d^{-1}
I^*	472.57	973.85	$\mu mol\, m^{-2}\, s^{-1}$
α	0.030	0.0083	$\mu mol^{-1}\, m^2\, s\, d^{-1}$

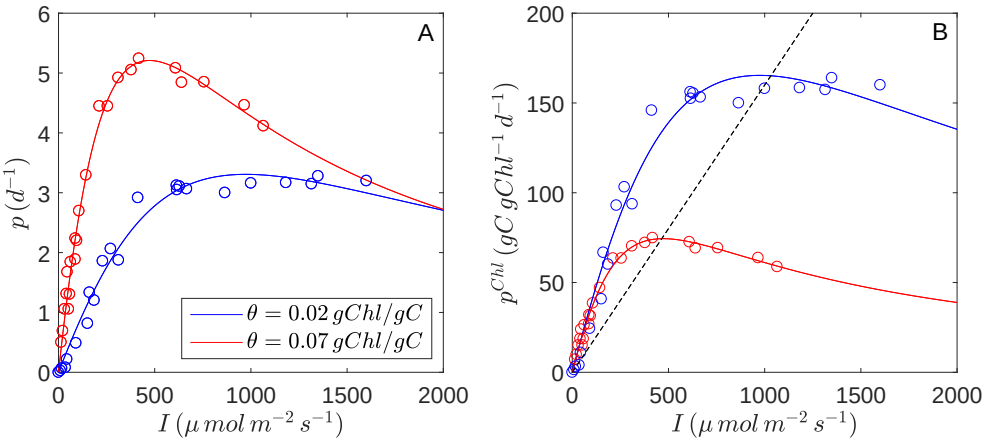

Figure 2.3: A. Photosynthetic rate of *Skeletonema costatum* for different values of θ. B. Chlorophyll-specific production rate for different values of θ. The maxima of the curves are connected by a line passing through the origin [2].

2.2.3 Nutrient limitation

We assume now that microalgae growth is only limited by nutrients. There are two different approaches for describing microalgae growth under nutrient limitation, the Monod and the Droop (or Variable Cell Quota) models. In the case of limitation by only one nutrient at concentration s, the classical model of Monod [40], initially intended for bacterial cultures, states that the specific growth rate is directly related to s in the following way:

$$\mu(s) = \mu_{max}\frac{s}{s + K_s}, \tag{2.15}$$

with μ_{max} the maximal growth rate and K_s a half-saturation constant. The applicability of (2.15) has been shown in different works [27, 37, 50]. Alternative versions of μ are proposed in the literature. For example, the Haldane

version [1] that takes into account inhibition effects, or the following version:

$$\mu(s) = \frac{\mu_{max} s + \mu'_{max} K_s}{s + K_s} \tag{2.16}$$

with μ'_{max} a positive parameter, arising from the reported fact that growth rate not immediately ceases when the concentration of nutrients dropps to zero [13]. See [17] for an extensive list of models for (2.15). From a mass balance, the dynamics of s is described by:

$$\frac{ds}{dt} = D(s_{in} - s) - \frac{1}{Y}\mu(s), \tag{2.17}$$

with s_{in} the input nutrient supply, and Y a yield coefficient.

The Droop approach [21] states that $\mu(\cdot)$ depends on an internal pool of nutrient, denoted by q, in the following way:

$$\mu(q) = \mu_{max}\left(1 - \frac{q_0}{q}\right), \tag{2.18}$$

with q_0 the minimum quota for life (or subsistence) that represents the value of q at which growth ceases. The cell quota q decreases with microalgae growth and increases with nutrient uptake. The classical Droop model states

that the evolution of q is given by:

$$\begin{aligned} \frac{dq}{dt} &= \rho(q,s) - \mu(q)q, \\ \frac{ds}{dt} &= D(s_{in} - s) - \rho(q,s)x, \end{aligned} \tag{2.19}$$

where ρ is the nutrient uptake rate function. For modeling ρ, Michaelis-Menten kinetics is most generally used [14]. More recently, a term to represent the uptake down regulation at high internal quota has been introduced. This term avoids reaching infinite quota, especially in conditions (such as darkness) when growth rate ceases. This model reads [35]:

$$\rho(\cdot) = \begin{cases} \rho_{max} \frac{q_L - q}{q_L - q_0} \frac{s}{s+K_s} & if \quad q \leq q_L, \\ 0 & if \quad q > q_L. \end{cases} \tag{2.20}$$

with ρ_{max} the maximal uptake rate, q_L an hypothetical maximal quota, and K_s a half-saturation constant. Table 2.4 shows some alternative expressions for μ and some values of the associated kinetic parameters.

Literature related to co-limitation by two or more nutrients is scarce. In the case of phosphorus and nitrogen limitation, in [12, 35] the growth rate has been described by the law of the minimum (or Liebig's law):

$$\mu(q_P, q_N) = \mu_{max} \min \left\{ 1 - \frac{q_{N0}}{q_N}, 1 - \frac{q_{P0}}{q_P} \right\} \tag{2.21}$$

with q_N and q_P the cell quotas of nitrogen and phosphorus respectively. The

Model	Remark
$\mu(q) = \mu_{max}\left(1 - \frac{q_0}{q}\right)$	Nitrogen limitation [43]: *Pseudochlorococcum sp.* $\mu_{max} = 3.26\,d^{-1}$, $0.0278\,gN/gDW$
$\mu(q) = \mu_{max}\frac{q - q_0}{q_L - q_0}$	Nitrogen limitation [25]: *Thalassiosira psedonana*: $\mu_{max} = 3\,d^{-1}$,$q_0 = 0.04\,gN/gC$, $q_L = 0.2\,gN/gC$
$\mu(q) = \mu_{max}\frac{q - q_0}{K + q - q_0}$	Nitrogen limitation [15]: *Dunaliella tertiolecta*: $\mu_{max} = 1.82\,d^{-1}$,$q_0 = 0.075\,molN/molC$ $K = 0.057\,molN/molC$

Table 2.4: Different models for the specific growth rate as a function of the cell quota.

evolution of the quotas is given by:

$$\begin{aligned}
\frac{dq_N}{dt} &= \rho_N(q_N, q_P, s_N) - \mu(q_P, q_N)q_N, \\
\frac{dq_P}{dt} &= \rho_P(q_N, q_P, s_P) - \mu(q_P, q_N)q_P, \\
\frac{ds_N}{dt} &= D(s_{N,in} - s_N) - \rho_N(s_N, q_N, q_P)x, \\
\frac{ds_P}{dt} &= D(s_{P,in} - s_P) - \rho_P(s_N, q_N, q_P)x.
\end{aligned} \tag{2.22}$$

As in in the case of mono-limitation, in [35] the uptake rates increase with the respective external nutrient concentration and are down regulated with the respective quota. In [12], the authors assume that the uptake of nitrogen

is enhanced by the phosphorus quota in the following way:

$$\rho_N(\cdot) = \begin{cases} \rho_{N,max} \frac{q_P - q_{P0}}{q_{NL} - q_{P0}} \frac{q_{NL} - q_N}{q_{NL} - q_{N0}} \frac{s_N}{s_N + K_{s_N}} & if \quad q_N \leq q_{NL}, \\ 0 & if \quad q_N > q_{NL}. \end{cases} \tag{2.23}$$

2.2.4 Co-limitation by light and nutrient.

As in the case of co-limitation by different nutrients, the literature about co-limitation by light and nutrient is scarce. Passarge and collaborators [44] describe the growth rate by the law of the minimum:

$$\mu(\cdot) = \min \left\{ p_{max} \left(1 - \frac{q_0}{q} \right), \frac{1}{L} \int_0^L p(I(z)) dz \right\}, \tag{2.24}$$

with p given by (2.3). In the case of co-limitation by light and nitrogen limitation, Bernard [6] describes the co-limitation by a multiplicative function:

$$\mu(\cdot) = \left(1 - \frac{q_0}{q} \right) \frac{1}{L} \int_0^L p(I(z)) dz - m, \tag{2.25}$$

with p a Haldane-type model (see (2.5)). The evolution of the quota and nutrient concentration is described as in (2.19). The uptake rate is taken as in (2.20). However, in the case of nitrogen limitation, the nitrogen uptake may be affected by the light intensity [39, 46]. The following version of (2.20) is considered in [39] to explain these effects of the light:

$$\rho_{NO_3}(\cdot) = \begin{cases} \rho_{max} \frac{q_L - q}{q_L - q_0} \frac{s}{s + K_s} [\eta + (1 - \eta) \frac{\bar{I}^m}{\bar{I}^m + \epsilon_I}] & if \quad q \leq q_L, \\ 0 & if \quad q > q_L, \end{cases} \tag{2.26}$$

with η a reduction factor of nitrogen uptake during the night.

2.3 Dynamics of microalgae models

2.3.1 Light limitation

Huisman et al. [31] studied the following model:

$$\frac{dx}{dt} = \left(\frac{1}{L}\int_0^L p(I(z,x))dz - b - D\right)x, \tag{2.27}$$

with $I(z,x)$ given by (2.6) and (2.7), and p a strictly increasing function with $p(I) = 0$ (see for example (2.3)). Huisman and collaborators proved that (2.27) admits at most one positive equilibrium which attracts any solution with positive initial condition. Gerla et al. [26] extended this work by considering photoinhibition. They assume that $p(0) = 0$, that p is differentiable, and that there exists $I^* > 0$ such that $p'(I) > 0$ for all $I \in (0, I^*)$ and $p'(I) < 0$ for all $I > I^*$ (see for example (2.5)). In that case, they proved that (2.27) may have two equilibria $0 < x_* < x^*$ and any solution $x(t)$ of (2.27) approaches x^* if $x(0) > x_*$ and washouts if $x(0) < x^*$. This is known as bi-stability.

Bayen et al. [3] considered periodic variations of the incident light intensity I_{in}. They write (2.27) in the following reduced way:

$$\frac{dx}{dt} = f(t,x)x, \tag{2.28}$$

with $f(t,x) = \frac{1}{L}\int_0^L p(I(z,x))dz - b - D$. Thus, if $I_{in}(t)$ is an ω-periodic function, then $t \longmapsto f(t,x)$ is also an ω-periodic function. He argues that when p is strictly increasing and $I_{in} > 0$, then $x \longmapsto f(t,x)$ is strictly decreasing. Then, using results on periodic Kolmogorov equations, he finds that the following condition:

$$\int_0^\omega f(t,0)dt > 0, \tag{2.29}$$

implies the existence of a unique positive ω-periodic solution $x^*(t)$ and any solution with positive initial conditions approaches it asymptotically.

2.3.2 Nutrient limitation

When microalgae growth is only limited by one nutrient, by using a Monod approach, we have the following model:

$$\begin{array}{rcl} \dfrac{dx}{dt} & = & [\mu(s) - D - b]x, \\ \dfrac{ds}{dt} & = & D(s_{in} - s) - \dfrac{1}{Y}\mu(s)x. \end{array} \tag{2.30}$$

This model coincides with those for bacteria growth. A lot of literature describes the dynamics of (2.30) and different variations accounting for inhibition, limitation for more than one nutrient, and periodic forcing (see [48] and the references therein). In this section, we focus on models using a Droop approach.

The dynamics of the classical the Droop model:

$$\begin{aligned} \frac{dx}{dt} &= [\mu(q) - D - b]x, \\ \frac{dq}{dt} &= \rho(q,s) - \mu(q)q, \\ \frac{ds}{dt} &= D(s_{in} - s) - \rho(q,s)x, \end{aligned} \tag{2.31}$$

has been studied by some authors. For general monotone growth and uptake rate functions, Oyarzun et al. [42] proved that (2.31) admits at most one equilibrium (x^*, q^*, s^*) with $x^* > 0$. If this equilibrium exists, then any solution $(x(t), q(t), s(t))$ with $x(0) > 0$ approaches it asymptotically. Smith [47] studied the case when $b = 0$ and the nutrient supply s_{in} varies periodically in time with a period ω. He proved that (2.31) admits a unique washout ω-periodic solution $(0, q_*(t), s_*(t))$, and if the following condition holds:

$$\int_0^\omega \mu(q_*(t))dt - D > 0, \tag{2.32}$$

then (2.31) admits a unique ω-periodic solution $(x^*(t), q^*(t), s^*(t))$ with $x^*(t) > 0$ and any solution with positive initial microalgae concentration approaches to it. If $b > 0$, in [16] it was shown numerically that (2.31) may have a chaotic dynamics. Thus, even single microalgae populations may exhibit complex behavior.

In the case of multiple nutrient limitation, the following model has been studied in [18]:

$$\begin{aligned}
\frac{dx}{dt} &= [\min\{\mu_1(q_1), \mu_2(q_2)\} - D]x, \\
\frac{dq_i}{dt} &= \rho(s_i) - \min\{\mu_1(q_1), \mu_2(q_2)\}q_i,\ i = 1, 2, \\
\frac{ds_i}{dt} &= D(s_{i,in} - s_i) - \rho(s_i)x,\ i = 1, 2.
\end{aligned} \tag{2.33}$$

For a broad class of uptake and growth functions it is proved that a nontrivial equilibrium may exist. Moreover, if it exists it is unique and globally stable.

2.3.3 Co-limitation by light and nutrients

We only found two works on the dynamics of models accounting for co-limitation by light and nutrients. Using a Monod approach, Huisman et al. [32] considered the following model:

$$\begin{aligned}
\frac{dx}{dt} &= \left(\frac{1}{L}\int_0^L p(I(z,x), s)dz - D\right)x, \\
\frac{ds}{dt} &= D(s_{in} - s) - \int_0^L p(I(z,x), s)dz,
\end{aligned} \tag{2.34}$$

with $p(I, s)$ the specific gross rate depending on the availability of nutrients and light. The function p is assumed to be strictly increasing in both arguments, and $p(0, s) = p(I, 0) = 0$ for any $s, I \geq 0$. Huisman et al. proved that 2.34 admits at most one equilibrium with a positive microalgae concentration, which is locally stable.

Hsu et al. [28] considered the light-limited Droop model proposed by Passarge and collaborators [44]:

$$\begin{aligned} \frac{dx}{dt} &= [\min\{\mu_I(I_{out}(x)), \mu_s(q)\} - D]x, \\ \frac{dq}{dt} &= \rho(q,s) - \min\{\mu_I(I_{out}(x)), \mu_s(q)\}q, \\ \frac{ds}{dt} &= D(s_{in} - s_i) - \rho(q,s)x, \end{aligned} \tag{2.35}$$

where $I_{out}(x) = I_{in}e^{-(kx+K_{bg})L)}$ is the light intensity at the bottom of the culture, and μ_I and μ_s are strictly increasing functions satisfying $\mu_I(0) = \mu_s(0) = 0$. Defining σ and ξ by means of $\mu_I(\xi) = \mu_s(\sigma) = D$, Hsu et al. proved that if $\rho(s_{in}, \sigma) > D\sigma$ and $I_{in} > \xi$, then (2.35) admits a unique positive equilibrium (x^*, q^*, s^*) which is globally stable. This equilibrium satisfies either $I_{out}(x^*) = \xi$ or $q^* = \sigma$. In the former case the system is said to have a light-limited equilibrium, while in the latter a nutrient-limited equilibrium.

2.4 Discussion and conclusions

A common result related to the dynamics of all the population models is that when there exists a unique steady state, then any solution of the model approaches this steady state. The unique situation in which more than one positive (with microalgae) steady-state has been identified is when photo-inhibition is not ignored. In such a case, a minimal initial microalgae concentration is needed to avoid the washout of the system. There is scarce literature when periodic forcing is considered. We found only two works focusing on periodic light variations, and two on periodic nutrient supply. There are

no studies on the dynamics of models considering photo-acclimation, and only one study on the light-limited Droop model.

Bibliography

[1] J. F. Andrews. A mathematical model for the continuous culture of microorganisms utilizing inhibitory substrates. *Biotechnology and Bioengineering*, 10(6):707–723, 1968.

[2] T. Anning, H. L. MacIntyre, S. M. Pratt, P. J. Sammes, S. Gibb, and R. J. Geider. Photoacclimation in the marine diatom skeletonema costatum. *Limnology and Oceanography*, 45(8):1807–1817, 2000.

[3] T. Bayen, F. Mairet, P. Martinon, and M. Sebbah. Analysis of a periodic optimal control problem connected to microalgae anaerobic digestion. *Optimal Control Applications and Methods*, 36(6):750–773, 2015.

[4] Q. Béchet, N. Coulombier, C. Vasseur, T. Lasserre, L. Le Dean, and O. Bernard. Full-scale validation of an algal productivity model including nitrogen limitation. *Algal research*, 31:377–386, 2018.

[5] Q. Béchet, A. Shilton, and B. Guieysse. Modeling the effects of light and temperature on algae growth: state of the art and critical assessment for productivity prediction during outdoor cultivation. *Biotechnology advances*, 31(8):1648–1663, 2013.

[6] O. Bernard. Hurdles and challenges for modelling and control of mi-

croalgae for co2 mitigation and biofuel production. *Journal of Process Control*, 21(10):1378–1389, 2011.

[7] O. Bernard, F. Mairet, and B. Chachuat. Modelling of microalgae culture systems with applications to control and optimization. In *Microalgae Biotechnology*, pages 59–87. Springer, 2015.

[8] O. Bernard, F. Mairet, and B. Chachuat. *Modelling of Microalgae Culture Systems with Applications to Control and Optimization*, pages 59–87. Springer International Publishing, Cham, 2016.

[9] O. Bernard and B. Rémond. Validation of a simple model accounting for light and temperature effect on microalgal growth. *Bioresource Technology*, 123:520 – 527, 2012.

[10] W. Blanken, P. R. Postma, L. de Winter, R. H. Wijffels, and M. Janssen. Predicting microalgae growth. *Algal Research*, 14:28–38, 2016.

[11] M. A. Borowitzka. *Limits to Growth*, pages 203–226. Springer Berlin Heidelberg, Berlin, Heidelberg, 1998.

[12] G. Bougaran, O. Bernard, and A. Sciandra. Modeling continuous cultures of microalgae colimited by nitrogen and phosphorus. *Journal of theoretical biology*, 265(3):443–454, 2010.

[13] J. Caperon. Population growth response of isochrysis galbana to nitrate variation at limiting concentrations. *Ecology*, 49(5):866–872, 1968.

[14] J. Caperon and J. Meyer. Nitrogen-limited growth of marine phytoplanktonii. uptake kinetics and their role in nutrient limited growth of

phytoplankton. In *Deep Sea Research and Oceanographic Abstracts*, volume 19, pages 619–632. Elsevier, 1972.

[15] J. Caperon and J. Meyer. Nitrogen-limited growth of marine phytoplanktonii. uptake kinetics and their role in nutrient limited growth of phytoplankton. In *Deep Sea Research and Oceanographic Abstracts*, volume 19, pages 619–632. Elsevier, 1972.

[16] S. Clodong and B. Blasius. Chaos in a periodically forced chemostat with algal mortality. *Proceedings of the Royal Society of London B: Biological Sciences*, 271(1548):1617–1624, 2004.

[17] P. Darvehei, P. A. Bahri, and N. R. Moheimani. Model development for the growth of microalgae: A review. *Renewable and Sustainable Energy Reviews*, 97:233–258, 2018.

[18] P. De Leenheer, S. A. Levin, E. D. Sontag, and C. A. Klausmeier. Global stability in a chemostat with multiple nutrients. *Journal of mathematical biology*, 52(4):419–438, 2006.

[19] D. Demory, C. Combe, P. Hartmann, A. Talec, E. Pruvost, R. Hamouda, F. Souillé, P.-O. Lamare, M.-O. Bristeau, J. Sainte-Marie, S. Rabouille, F. Mairet, A. Sciandra, and O. Bernard. How do microalgae perceive light in a high-rate pond? towards more realistic lagrangian experiments. *Royal Society Open Science*, 5(5), 2018.

[20] Derraz, M., Dauta, A., Capblancq, J., and Abassi, M. Influence de la lumire et de la temprature sur les taux de croissance et de photosynthse

de scenedesmus crassus chodat, isole de la retenue eutrophe el kansera (maroc). *Ann. Limnol. - Int. J. Lim.*, 31(1):65–74, 1995.

[21] M. R. Droop. Vitamin B 12 and marine ecology. iv. the kinetics of uptake, growth and inhibition in monochrysis lutheri. *Journal of the Marine Biological Association of the United Kingdom*, 48(3):689–733, 1968.

[22] P. Falkowski and C. Wirick. A simulation model of the effects of vertical mixing on primary productivity. *Marine Biology*, 65(1):69–75, 1981.

[23] F. G. A. Fernández, F. G. Camacho, J. A. S. Pérez, J. M. F. Sevilla, and E. M. Grima. A model for light distribution and average solar irradiance inside outdoor tubular photobioreactors for the microalgal mass culture. *Biotechnology and Bioengineering*, 55(5):701–714, 1997.

[24] F. García-Camacho, A. Sánchez-Mirón, E. Molina-Grima, F. Camacho-Rubio, and J. Merchuck. A mechanistic model of photosynthesis in microalgae including photoacclimation dynamics. *Journal of theoretical biology*, 304:1–15, 2012.

[25] R. J. Geider, H. L. Maclntyre, and T. M. Kana. A dynamic regulatory model of phytoplanktonic acclimation to light, nutrients, and temperature. *Limnology and oceanography*, 43(4):679–694, 1998.

[26] D. J. Gerla, W. M. Mooij, and J. Huisman. Photoinhibition and the assembly of light-limited phytoplankton communities. *Oikos*, 120(3):359–368, 2011.

[27] H. Haario, L. Kalachev, and M. Laine. Reduced models of algae growth. *Bulletin of mathematical biology*, 71(7):1626–1648, 2009.

[28] S.-B. Hsu and C.-J. Lin. Dynamics of two phytoplankton species competing for light and nutrient with internal storage. *Discrete & Continuous Dynamical Systems-S*, 7(6):1259–1285, 2014.

[29] M. Huesemann, B. Crowe, P. Waller, A. Chavis, S. Hobbs, S. Edmundson, and M. Wigmosta. A validated model to predict microalgae growth in outdoor pond cultures subjected to fluctuating light intensities and water temperatures. *Algal Research*, 13:195–206, 2016.

[30] J. Huisman, H. C. Matthijs, P. M. Visser, H. Balke, C. A. Sigon, J. Passarge, F. J. Weissing, and L. R. Mur. Principles of the light-limited chemostat: theory and ecological applications. *Antonie van Leeuwenhoek*, 81(1):117–133, Dec 2002.

[31] J. Huisman and F. J. Weissing. Light-limited growth and competition for light in well-mixed aquatic environments: an elementary model. *Ecology*, 75(2):507–520, 1994.

[32] J. Huisman and F. J. Weissing. Competition for nutrients and light in a mixed water column: a theoretical analysis. *The American Naturalist*, 146(4):536–564, 1995.

[33] Y.-C. Jeon, C.-W. Cho, and Y.-S. Yun. Measurement of microalgal photosynthetic activity depending on light intensity and quality. *Biochemical Engineering Journal*, 27(2):127–131, 2005.

[34] J. T. O. Kirk. *Light and Photosynthesis in Aquatic Ecosystems*. Cambridge University Press, second edition, 1994. Cambridge Books Online.

[35] C. A. Klausmeier, E. Litchman, and S. A. Levin. Phytoplankton growth and stoichiometry under multiple nutrient limitation. *Limnology and Oceanography*, 49(4part2):1463–1470, 2004.

[36] E. Lee, M. Jalalizadeh, and Q. Zhang. Growth kinetic models for microalgae cultivation: a review. *Algal Research*, 12:497–512, 2015.

[37] E. Lee and Q. Zhang. Integrated co-limitation kinetic model for microalgae growth in anaerobically digested municipal sludge centrate. *Algal research*, 18:15–24, 2016.

[38] H. L. MacIntyre, T. M. Kana, T. Anning, and R. J. Geider. Photoacclimation of photosynthesis irradiance response curves and photosynthetic pigments in microalgae and cyanobacteria 1. *Journal of phycology*, 38(1):17–38, 2002.

[39] F. Mairet, O. Bernard, T. Lacour, and A. Sciandra. Modelling microalgae growth in nitrogen limited photobiorector for estimating biomass, carbohydrate and neutral lipid productivities. *IFAC Proceedings Volumes*, 44(1):10591–10596, 2011.

[40] J. Monod. The growth of bacterial cultures. *Annual Reviews in Microbiology*, 3(1):371–394, 1949.

[41] A. Nikolaou, P. Hartmann, A. Sciandra, B. Chachuat, and O. Bernard. Dynamic coupling of photoacclimation and photoinhibition in a model of microalgae growth. *Journal of theoretical biology*, 390:61–72, 2016.

[42] F. J. Oyarzun and K. Lange. The attractiveness of the droop equations ii. generic uptake and growth functions. *Mathematical biosciences*, 121(2):127–139, 1994.

[43] A. Packer, Y. Li, T. Andersen, Q. Hu, Y. Kuang, and M. Sommerfeld. Growth and neutral lipid synthesis in green microalgae: a mathematical model. *Bioresource technology*, 102(1):111–117, 2011.

[44] J. Passarge, S. Hol, M. Escher, and J. Huisman. Competition for nutrients and light: stable coexistence, alternative stable states, or competitive exclusion? *Ecological Monographs*, 76(1):57–72, 2006.

[45] J. Quinn, L. De Winter, and T. Bradley. Microalgae bulk growth model with application to industrial scale systems. *Bioresource technology*, 102(8):5083–5092, 2011.

[46] O. N. Ross and R. J. Geider. New cell-based model of photosynthesis and photo-acclimation: accumulation and mobilisation of energy reserves in phytoplankton. *Marine ecology progress series*, 383:53–71, 2009.

[47] H. Smith. The periodically forced droop model for phytoplankton growth in a chemostat. *Journal of Mathematical Biology*, 35(5):545–556, 1997.

[48] H. L. Smith and P. Waltman. *The theory of the chemostat: dynamics of microbial competition*, volume 13. Cambridge university press, 1995.

[49] J. H. Steele. Environmental control of photosynthesis in the sea. *Limnology and Oceanography*, 7(2):137–150, 1962.

[50] L. Xin, H. Hong-Ying, G. Ke, and S. Ying-Xue. Effects of different nitrogen and phosphorus concentrations on the growth, nutrient uptake, and lipid accumulation of a freshwater microalga scenedesmus sp. *Bioresource technology*, 101(14):5494–5500, 2010.

[51] K.-L. Yeh, J.-S. Chang, and W.-m. chen. Effect of light supply and carbon source on cell growth and cellular composition of a newly isolated microalga chlorella vulgaris esp-31. *Engineering in Life Sciences*, 10(3):201–208, 2010.

[52] Y.-S. Yun and J. M. Park. Kinetic modeling of the light-dependent photosynthetic activity of the green microalga chlorella vulgaris. *Biotechnology and bioengineering*, 83(3):303–311, 2003.

CHAPTER 3

Theory of turbid microalgae cultures

Contents

3.1 Chapter presentation

This chapter relies on the article *Theory of turbid microalgae cultures* published in *Journal of Theoretical Biology* in 2018 [12]. Here, we study theoretically how the growth rate of microalgae, in open ponds or photobioreactors, can be affected by different factors associated to light limitation. This is important for understanding how to enhance microalgae growth, especially within the context of wastewater treatment where light can be very limited due to the high turbidity of the medium.

An important difference between this chapter and the published version, is that the notations have been changed so that now the average growth rate (abbreviated AGR within this chapter) does not consider losses due to microalgae death or respiration. The mortality rate has been explicitly reintroduced. This allows to stay consistent with the other chapters.

This chapter focuses on the biological interpretation of a mathematical analysis based on assumptions with experimental evidence. All the results include rigorous mathematical proofs (in Appendix A), thus this chapter can serve as reference for both biological and mathematical works.

Martínez, C., Mairet, F.,& Bernard, O. (2018). Theory of turbid microalgae cultures. *Journal of Theoretical Biology*, 456, 190-200.

Abstract : *Microalgae can be cultivated in closed or open photobioreators (PBR). In these systems, light rapidly decreases as it passes through the culture due to the turbidity of the medium. Thus, microalgae experiment different light intensities depending on their position in the medium. An appropriate way to model the growth rate is with the average growth rate (AGR) over all the culture. In this chapter, we study theoretically how the AGR of microalgae is affected by different factors in a PBR such as the incident light intensity, the depth of the reactor, the turbidity of the medium (by microalgae and other substances), and the form of the reactor. We show that for different types of PBR the AGR is completely determined by the incident light intensity and the light intensity in the darkest part of the PBR. In the case of vertical cylindrical PBRs illuminated from above (e.g. race-way or panel-type reactors), we describe (and we prove under general assumptions) in details the dependence of the AGR on the aforementioned factors. Finally, we discuss some implications of our analysis; the occurrence of an Allee effect, if light ostensibly limits or inhibits the growth rate in outdoor cultures, and how the geometry of the PBR affects microalgae growth rate and productivity.*

3.2 Introduction

As discussed in Chapter 2, an appropriate way to model the growth rate in microalgae population models, consists in accounting for the differences in local growth rates to obtain the average growth rate (AGR). The main objective of this chapter is to understand how the AGR is affected by different factors such as the incident light intensity, the form of the photobioreactor (PBR), the microalgae concentration, the background turbidity, and the light path-length of the reactor (or distance between the illuminated surface and the darkest point).

In the first part of this chapter, we extend an important property of perfectly mixed cultures in flat-plate reactors to other reactors with a flat light-exposed surface and to cylindrical reactors radially enlightened. This property says that the growth rate is completely determined by the incident light intensity and the light intensity at the darkest location in the culture. This property allows to study the dynamics of microalgae populations, to scale-up theoretical results, and to set-up experiments for measuring the growth rate.

The optical depth, an important variable in our study, describes how much absorption occurs when light travels through the PBR. It includes the effects of the light path-length, the background turbidity, and the microalgae population density. In the second part of this chapter, we study how the AGR varies with the incident light and the optical depth in flat-plate

reactors (or in general vertical cylindrical PBRs illuminated from above). In our analysis, we assume that microalge may suffer from photoinhibition. Theoretical works [7, 8] show that photoinhibition can lead algae cultures to the washout, while experimental results show that photoinhibition may cause a loss in biomass productivity even in high dense outdoor cultures [15, 21]. How much microalgae are affected by photoinhibition strongly depends on temperature [19] and photoacclimation [1, 13].

The study of the AGR leads to some interesting discussions as shown in the last part of this chapter. We study the AGR as a function of the microalgae population density, which gives conditions for the occurrence of an Allee effect (i.e. a positive relationship between the AGR and the population density [5]). Then, we discuss conditions such that the incident light intensity (sunlight) ostensibly limits or inhibits the AGR in outdoor cultures. Then, based on the results of Section 3.4, we compare the AGR of flat plate PBRs with that of other PBRs. Finally, in order to compare the performance of the different PBRs, we evaluate numerically the productivity that can be reached by each PBR.

This chapter is organized as follows. In Section 3.3, we define the average growth rate and we determine which factors determine its value. In Section 3.4, we describe in details the properties of the average growth rate in the case of a vertical cylindrical PBR illuminated from above. Then, in Section 3.5, we discuss some implications of the analysis of the growth rate in PBRs and compare productivities depending on PBR design.

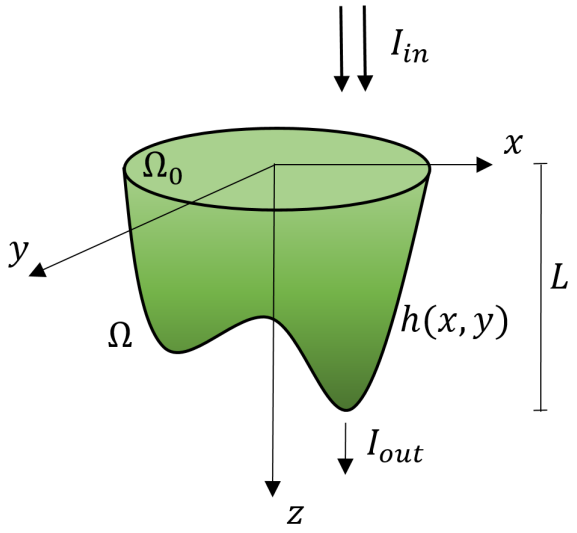

Figure 3.1: Region Ω occupied by the culture in a Cartesian coordinate system. I_{in} is the incident light intensity, $\Omega_0 \subset \mathbb{R}^2$ is the illuminated flat-surface, Ω is the volume occupied by the culture, $h(x, y)$ is the height of the culture at different positions $(x, y) \in \Omega_0$, L is the maximum depth of the culture, and I_{out} is the light intensity through the lowest part of the culture.

3.3 Average growth rate (AGR)

This section begins with the study of PBRs with a flat light-exposed surface. These PBRs serve to introduce the law of Lambert-Beer, the concept of optical depth, and the definition of AGR. Then, we briefly describe the cylindrical PBR radially enlightened. These PBRs are described by simple models which allow to obtain theoretical results. The main results of this section are given by Theorems 3.3.2 and 3.3.3. They state that the AGR is completely described by two factors; the incident light intensity and the optical depth.

Geometry of PBRs with a flat light-exposed surface Let us consider a perfectly mixed PBR having a flat surface illuminated perpendicularly with an unidirectional light field. We can described the region Ω occupied by the PBR (more precisely the volume of the culture) by

$$\Omega = \{(x, y, z)\,;\, (x, y) \in \Omega_0, z \in [0, h(x, y)]\},$$

with $\Omega_0 \subset \mathbb{R}^2$ (compact set [1]) the illuminated flat-surface of the PBR that receives the same light intensity at any point denoted I_{in} (incident light intensity) moving in the positive direction of axis z (see Figure 3.1), and $h(x, y)$ a continuous function that represents the depth of the PBR at different points $(x, y) \in \Omega_0$. In this way we can describe different PBRs [20]; a flat plate, a vertical-column (illuminated in one base), or an open pond PBR. A flat-plate PBR is described by a constant function h. By choosing adequately Ω_0 and h we can describe other kind of PBRs like a (horizontal cylindrical) triangular PBR (see Figure 3.2A) or a (horizontal cylindrical) semicircular PBR (see Figure 3.2B). In the following we will denote by L the maximum depth of the PBR that corresponds to the distance from the light-exposed surface to the lowest point of the reactor (i.e. $L := \max_{(x,y)\in\Omega_0} h(x, y)$).

Light gradient Light decreases progressively in moving deeper into the culture medium due to light absorption and scattering by light-absorbing substances [2, 4, 11]. As a first approximation, the law of Lambert-Beer can be used to determine the light intensity I at any position in the PBR. This

[1] This is necessary to ensure the existence of the maximum of h on Ω_0 and define L at the end of this paragraph.

means that multi-diffusion effects are not explicitly represented. Thus

$$\frac{\partial I}{\partial z} = -\xi I, \tag{3.1}$$

with $\xi \geq 0$ an extinction coefficient that depends on the medium. Since the culture is perfectly mixed, ξ does not depend on z. Thus, we can easily integrate (3.1) to obtain:

$$I(\xi, I_{in}, z) = I_{in} e^{-\xi z}, \text{ for all } (x, y, z) \in \Omega. \tag{3.2}$$

Here, z corresponds to the distance from the illuminated surface of the PBR to the position (x, y, z). A key variable in our study is the light intensity in the lowest (or the darkest) part of the culture, that is

$$I_{out}(I_{in}, \xi L) := I_{in} e^{-\xi L}. \tag{3.3}$$

We emphasize the fact that I_{out} depends only on the product ξL, and not on L and ξ separately.

In microalgae cultures illuminated with natural light, the incident light is in general not perpendicular to the surface. The incident flux must be computed accounting for loss due to reflection. The transmitted light fraction is then refracted into the medium. Due to the very diffusive character of the microalgae culture, we assume that it is rapidly anisotropic and therefore, we keep the Lambert-Beer approximation, assuming now an incident flux ηI_{in} with $\eta \in [0, 1]$.

Extinction coefficient In the case of a mono-culture, ξ is mainly correlated to the microalgae population density X [11]:

$$\xi(X) = kX + K_{bg}, \tag{3.4}$$

with $k > 0$ the specific light extinction coefficient of the microalgae specie and $K_{bg} \geq 0$ the background turbidity that summarizes the light absorption and difussion due to all non-microalgae components i.e. suspended solids and dissolved colored material. Typical values of the coefficient k for several microalgae species are given in Table 2.2.

AGR definition The specific gross growth rate of microalgae, denoted by p, represents the growth potential of the population. If biomass is defined in terms of cell density, p is the cell division rate. If X is a mass of algal carbon, then p is the rate of CO_2 fixation. In section 3.4 (paragraph *Assumptions over p*) some explicit expressions of p as a function of the light intensity I perceived by microalgae are presented. In this section, we only assume that I is the single factor that limits algae growth i.e $p : \mathbb{R}_+ \longrightarrow \mathbb{R}$ is a function of I. Let $V(\Omega)$ be the volume of the culture. Following [10], we compute the average (gross) growth rate (AGR) in the PBR, denoted by μ, by integrating the local specific gross growth rates over all the culture:

$$\mu(\cdot) := \frac{1}{V(\Omega)} \int_{\Omega} p(I(\xi, I_{in}, z))dxdydz. \tag{3.5}$$

We note that for $\xi = 0$ (transparent culture), expression (3.5) is reduced to

$$\mu(\cdot) = p(I_{in}). \tag{3.6}$$

This is consistent with the fact that all microalgae will perceive the same light intensity. To study the case $\xi > 0$, let us define $A_\Omega(z)$ as the area of the cross section of Ω at depth $z \in [0, L]$. The following lemma gives a useful expression for determining the AGR in different PBRs.

Lemma 3.3.1. *If $\xi > 0$, then*

$$\mu(\cdot) = \frac{1}{\xi V(\Omega)} \int_{I_{out}(\xi L, I_{in})}^{I_{in}} \frac{p(I)}{I} A_\Omega\left(\frac{1}{\xi}\ln\left(\frac{I_{in}}{I}\right)\right) dI. \tag{3.7}$$

Proof. By doing the change of variables $I = I(\xi, I_{in}, z)$ we rewrite expression (3.5);

$$\mu(\cdot) = \frac{1}{\xi V(\Omega)} \int_{(x,y)\in\Omega_0} \int_{I(\xi, I_{in}, h(x,y))}^{I_{in}} \frac{p(I)}{I} dI dx dy.$$

After changing the order of integration in the latter expression we obtain

$$\mu(\cdot) = \frac{1}{\xi V(\Omega)} \int_{I_{out}(\xi L, I_{in})}^{I_{in}} \int_{(x,y)\in\Omega_0(I)} \frac{p(I)}{I} dx dy dI. \tag{3.8}$$

$\Omega_0(I)$ corresponds to the projection onto the plane $x - y$ of the set formed by all the points of Ω at which the light intensity equals I. From Lambert-Beer law, the latter is the intersection of Ω and the plane parallel to Ω_0 that intersects $z = \frac{1}{\xi}\ln\left(\frac{I_{in}}{I}\right)$. Thus $\int_{(x,y)\in\Omega_0(I)} dxdy = A_\Omega\left(\frac{1}{\xi}\ln\left(\frac{I_{in}}{I}\right)\right)$ and we conclude the proof. □ □

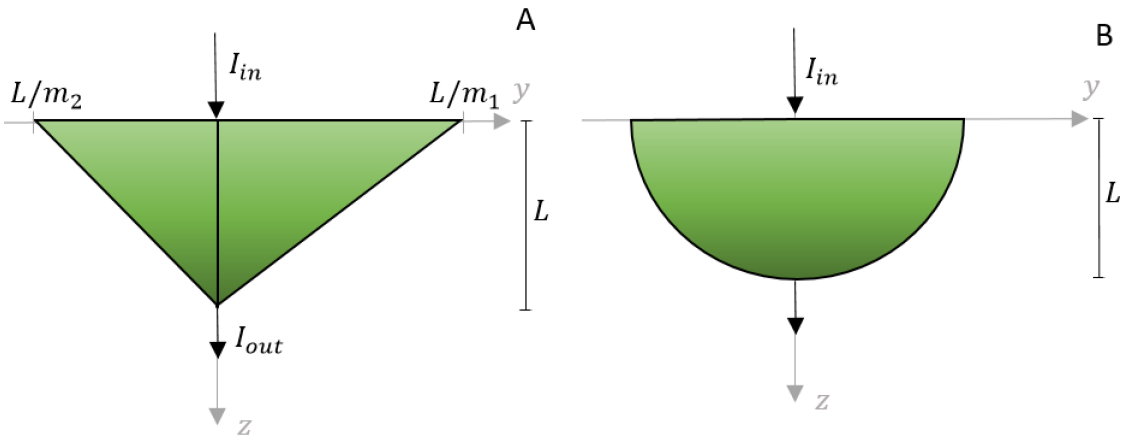

Figure 3.2: Schematic representation of a cross section through a cylindrical horizontal PBR. A. Triangular cylinder. The base measures $L(1/m_1 + 1/m_2)$ and the height L. B. Semicircular cylinder of radius L.

Flat-plate PBR In the case of a flat-plate PBR (i.e. $h(x, y) = L > 0$ for all $(x, y) \in \Omega_0$), $A_\Omega(z)$ is constant and $V(\Omega) = LA_\Omega(z)$. By using (3.7), it is straightforward to verify that

$$\mu(\cdot) = \frac{1}{\xi L} \int_{I_{out}(\xi L, I_{in})}^{I_{in}} \frac{p(I)}{I} dI. \tag{3.9}$$

This shows that in flat-plate PBRs, the AGR is completely determined by ξL and I_{in}.

Optical depth The product ξL will be denoted by θ. This variable is usually known as *optical depth*. The optical depth reflects the actual amount of light energy absorbed by the culture medium. Indeed, θ can be determined from

$$\theta = \ln(I_{in}/I_{out}(\theta, I_{in})). \tag{3.10}$$

Thus, in view of (3.9), in a flat-plate PBR, the AGR is determined by the light intensities at the top and at the bottom of the PBR.

Triangular horizontal cylinder Consider now that the PBR is a triangular horizontal cylinder (see Figure 3.2A) i.e. $h(x,y) = -m_1 y + L$ for $y \in [0, L/m_1]$ and $h(x,y) = m_2 y + L$ for $y \in [-L/m_2, 0]$ with $m_1, m_2 > 0$. So we have that $A_\Omega(z) = H\left(\frac{1}{m_1} + \frac{1}{m_2}\right)(z+L)$ and $V(\Omega) = HL^2(1/m_1 + 1/m_2)/2$ with H the length of the cylinder. Thus, Lemma 3.3.1 gives

$$\begin{aligned} \mu(\cdot) &= -\frac{2}{\theta^2}\int_{I_{out}(\theta,I_{in})}^{I_{in}} \frac{p(I)}{I}\ln\left(\frac{I_{in}}{I}\right)dI \\ &\quad +\frac{2}{\theta}\int_{I_{out}(\theta,I_{in})}^{I_{in}} \frac{p(I)}{I}dI. \end{aligned} \tag{3.11}$$

This expression shows that the family of all the triangular PBRs have the same AGR, which is determined by the incident light intensity and the optical depth (or the light intensity at the lowest point according to (3.10)). Expression (3.11) is clearly different from expression (3.9). This shows that the form of the reactor must be taken into account for determining the AGR.

Shape of a PBR We say that two PBRs have equivalent shape if one of them can be obtained by scaling the other one. Mathematically, a PBR occupying a region Ω has equivalent shape of a PBR occupying a region Ω' if there exist positive numbers s_x,s_y, and s_z such that

$$\Omega' = \{(s_x x, s_y y, s_z z)\,;\,(x,y,z) \in \Omega\}.$$

If $s_x = s_y = s_z$ we speak of an uniform scaling, otherwise of a non-uniform scaling. The following theorem shows that by fixing the shape of the PBR, we obtain the same AGR and that is determined by the incident light intensity and the optical depth.

Theorem 3.3.2. *Two PBRs with equivalent shape lead to the same AGR, which is completely determined by the incident light intensity and the optical depth.*

Proof. First we note that

$$\begin{aligned} V(\Omega) &= \int_0^L A_\Omega(z)dz \\ &= \int_{I_{out}(\theta,I_{in})}^{I_{in}} \frac{1}{I} A_\Omega\left(z = \frac{1}{\xi}\ln\left(\frac{I_{in}}{I}\right)\right) dI. \end{aligned}$$

Then, we can write

$$\mu(\cdot) = \int_{I_{out}(\xi L,I_{in})}^{I_{in}} p(I) f(I;\xi,I_{in},\Omega)dI, \tag{3.12}$$

with f defined by:

$$f(I;\xi,I_{in},\Omega) := \frac{\frac{1}{I}A_\Omega\left(\frac{1}{\xi}\ln\left(\frac{I_{in}}{I}\right)\right)}{\int_{I_{out}(\xi L,I_{in})}^{I_{in}} \frac{1}{I}A_\Omega\left(\frac{1}{\xi}\ln\left(\frac{I_{in}}{I}\right)\right) dI}. \tag{3.13}$$

Now, consider another PBR of depth $L' > L$ occupying a region Ω' obtained by scaling Ω. That is, there are $s_x, s_y > 0$ such that

$$\Omega' := \{(s_x x, s_y y, (L'/L)z);\ (x,y,z) \in \Omega\}.$$

Assume now that the extinction coefficient ξ' in this PBR satisfies $\xi L = \xi' L'$. If we note that $A_{\Omega'}(z) = s_x s_y A_\Omega((L/L')z)$, it is straightforward to verify that

$$f(I; \xi', I_{in}, \Omega') = f(I; \xi, I_{in}, \Omega). \tag{3.14}$$

Expression (3.14) indicates that the value of f is determined by I_{in}, the product ξL, and shape of the PBR. This holds of course for the AGR, since I_{out} depends only on I_{in} and ξL. □

Horizontal semicircular cylinder As a last example of a flat light-exposed surface PBR, consider a semicircular horizontal cylinder (see Figure 3.2B) i.e. $h(x, y) = \sqrt{L^2 - y^2}$. So we have that $A(z) = 2\sqrt{L^2 - z^2}$ and Lemma 3.3.1 gives:

$$\mu(\cdot) = \frac{4}{\pi\theta} \int_{I_{out}(\theta, I_{in})}^{I_{in}} \frac{p(I)}{I} \sqrt{1 - \frac{1}{\theta^2} \ln^2 \left(\frac{I_{in}}{I} \right)} dI. \tag{3.15}$$

This expression for the AGR is clearly different from that of (3.9). According to Theorem 3.3.2, this expression is also valid for semi-elliptical horizontal cylinders.

Cylindrical PBR radially enlightened The cylindrical PBR, evenly illuminated around, is also commonly used. The region Ω occupied by the PBR corresponds to a cylinder of radius R, which is radially and evenly illuminated over the sides (not over the bases). From [6], the path length of light to a point at distance r from the center as a function of the angle ϕ (see

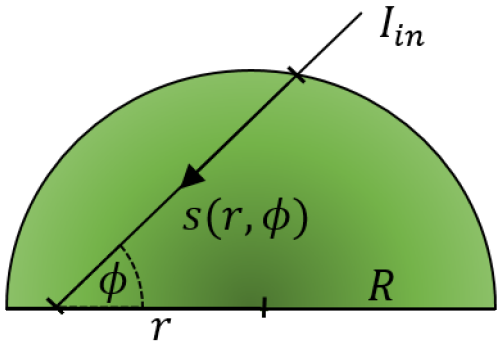

Figure 3.3: Schematic representation of one-half of a cross section through a cylindrical chemostat vessel (s, light path; R, cylinder radius; r, distance from the center; ϕ, angle of light path with line through the center.)

Figure 3.3) equals:

$$s(r,\phi) = r\cos\phi + \sqrt{R^2 - r^2\sin^2\phi}. \tag{3.16}$$

By using the law of Lambert-Beer and accounting for the light flux coming from all the directions (ϕ moving between 0 and 2π), the light intensity at a distance r from the center is given by:

$$I(r) = \int_0^{2\pi} I_{in} e^{-\xi s(r,\phi)} d\phi. \tag{3.17}$$

By using cylindrical coordinates, the AGR can be written as:

$$\mu(\cdot) := \frac{1}{\pi R^2} \int_0^{2\pi} \int_0^R p(I(r)) r dr d\phi \tag{3.18}$$

$I(r)$ is increasing as a function r (see Proof of Theorem 3.3.3). Thus, the darkest zone of the PBR is in the center ($r = 0$) and the most illuminated

zone is on the sides ($r = R$). Based on the distance between these two zones, we define the optical depth as $\theta := \xi R$. We have the following version of Theorem 3.3.2 for the cylindrical PBR.

Theorem 3.3.3. *The AGR defined in (3.18) is completely determined by the optical depth and the incident light intensity.*

Before proving Theorem 3.3.3, note that the optical depth can be obtained explicitly from:

$$\theta = \ln\left(2\pi \frac{I_{in}}{I(0)}\right). \tag{3.19}$$

This shows that Theorem 3.3.3 could be stated in terms of I_{in} and $I(0)$.

Proof. (*of Theorem 3.3.3*) Let us denote by f the first derivative of $I(r)$ i.e.

$$f(r;\xi,I_{in},R) = -\xi I_{in}\int_0^{2\pi} e^{-\xi s(r,\phi;R)}\frac{\partial}{\partial r}s(r,\phi;R)d\phi \tag{3.20}$$

Note that we explicitly indicate the dependence on the radius of the functions f and s . It is straightforward to verify that $I''(r) > 0$ for any $r \in [0,R)$. Thus, f is a strictly increasing function with respect to r. Consequently, $f(r;\xi,I_{in},R) > f(0;\xi,I_{in},R) = 0$. Thus, I is strictly increasing. The latter implies that $I(r) : [0,R] \longrightarrow [I(R),I(0)]$ has an inverse function $\varphi(I;\xi,I_{in},R) : [I(R),I(0)] \longrightarrow [0,R]$.

By integrating (3.18) with respect to ϕ and doing the change of variables $I = I(r)$, the AGR can be written as:

$$\mu(\cdot) = 2\int_{I(R)}^{I(0)} p(I)H(I;\xi,I_{in},R)dI, \tag{3.21}$$

with

$$H(I;\xi,I_{in},R)=\frac{\varphi(I;\xi,I_{in},R)}{R^2 f(\varphi(I;\xi,R);\xi,I_{in},R)}.$$

By evaluating $I(0)$ and $I(R)$, it is easy to verify that they are determined by ξR and I_{in}. It remains to prove the same for H. For this purpose, consider another PBR of radius R' and assume that the extinction coefficient ξ' in this PBR satisfies $\xi R = \xi' R'$. As in Theorem 3.3.2 we have to prove that $H(I;\xi,I_{in},R) = H(I;\xi',I_{in},R')$, but this follows rapidly after noting that $\varphi(I;\xi',I_{in},R') = \varphi(I;\xi,I_{in},R)R'/R$. □

3.4 Properties of the AGR in flat-plate PBRs.

Definition of the function g In a flat-plate PBR the AGR is given by (3.9). If $I_{in} > 0$, by substituting (3.10) in (3.9) we have:

$$\mu(\cdot) = g(I_{in}, I_{out}(\theta, I_{in})), \tag{3.22}$$

with

$$g(I_{in},I_{out})=\frac{1}{\ln(I_{in}/I_{out})}\int_{I_{out}}^{I_{in}}\frac{p(I)}{I}dI. \tag{3.23}$$

Expression (3.23) gives an explicit expression for the AGR as a function of the light intensities at the top and at the bottom of the PBR. The function g was first defined in [7] and is useful for studying the properties of the AGR. This function highlights the fundamental link between AGR and the extreme values of light intensity in the PBR.

Assumptions over p p corresponds to the carbon uptake rate. In the literature we find different models for p, for example the classical model of Steele [18]:

$$p(I) = p_{max}\frac{I}{I^*}e^{1-\frac{I}{I^*}}, \tag{3.24}$$

with p_{max} the maximum value of p, or Haldane-type models [2] like the one presented in [3]:

$$p(I) = p_{max}\frac{I}{I + \frac{p_{max}}{\alpha}\left(\frac{I}{I^*} - 1\right)^2}, \tag{3.25}$$

where α is the initial slope of p. Table 2.1 in Chapter 2 shows the kinetic parameters of model (3.25) for three different microalgae species. Figure 3.4 shows p given in (3.25) with kinetic parameters from Table 2.1 for *C.vulgaris*.

In what follows of this section, we will describe the AGR when p is given by (3.25) or (3.24). However, the theory of turbid cultures is derived for any net growth rate satisfying the following assumptions.

Assumption 3.4.1. *There exists a light intensity $I^* > 0$ such that p is strictly increasing for $I \in [0, I^*]$ and strictly decreasing for $I \in [I^*, \infty)$.*

Assumption 3.4.1 states that phytoplankton can suffer from photoinhibition. Here, I^* is the light intensity at which p reaches its maximum value.

Assumption 3.4.2. $p(0) = \lim_{I\to\infty} p(I)$.

Assumption 3.4.2 states that for high light intensities ($I \to \infty$) phytoplankton grows similarly as under absence of light ($I = 0$). Indeed, when p is given by (3.25) we have $p(0) = \lim_{I\to\infty} p(I) = 0$.

[2] By a Haldane-type model, we mean $p(I) = \frac{I}{aI^2+bI+c}$ with $a, c > 0$.

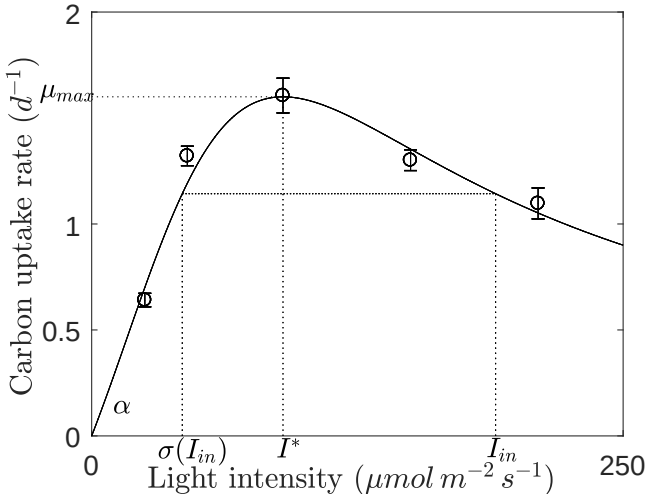

Figure 3.4: Carbon uptake rate (see (3.25)) for *Chlorella vulgaris* with kinetic parameters from Table 2.1, experimental data from [22], and graphical description of σ.

Symmetry of p We note that for any $I > 0$ different from I^*, there exists another light intensity, that will be denoted $\sigma(I)$, such that:

$$p(I) = p(\sigma(I)). \tag{3.26}$$

A graphic representation of σ is shown in Figure 3.4. It seems clear to define $\sigma(I^*) = I^*$ which ensures the continuity of σ. As we will see below, σ is relevant when describing the AGR. In the case that p is given by (3.25) we obtain a simple expression for $\sigma(I)$:

$$\sigma(I) = \frac{I^{*2}}{I}. \tag{3.27}$$

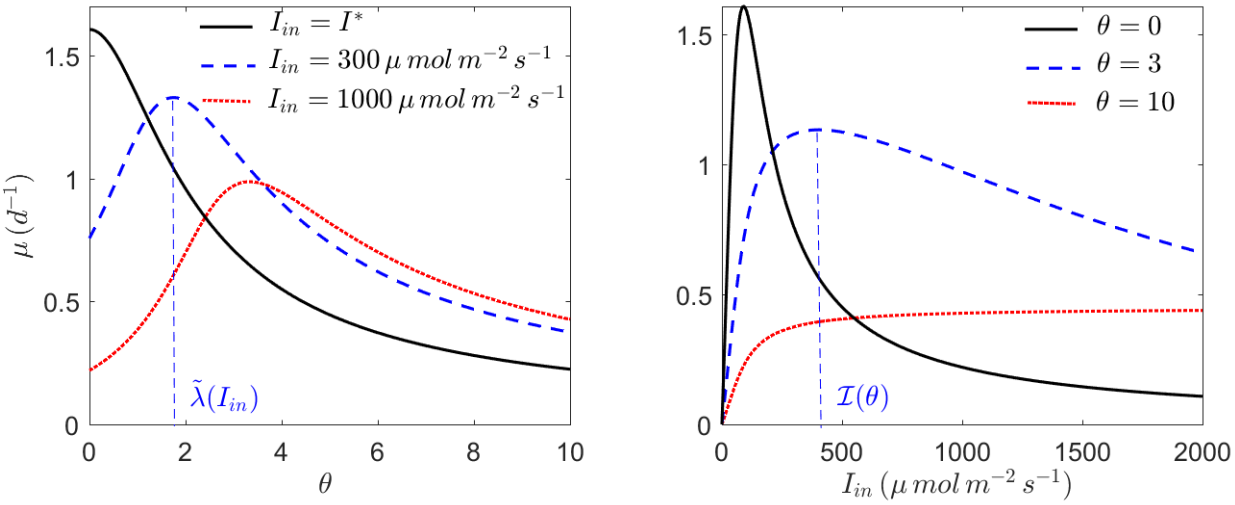

Figure 3.5: A. Plot of the AGR as a function of the optical depth for three different values of the incident light. B. Plot of the AGR as a function of the incident light intensity for three different values of the optical depth. We consider p given by (3.25) with the kinetic parameters of *C. vulgaris* given in Table 2.1.

Critical optical depth Consider that the incident light intensity I_{in} is fixed and lower than or equal to I^*. According to Lemma A1, the AGR (or the function g) increases as the light intensity at the bottom I_{out} increases. Consequently, the maximum value of the AGR is obtained when I_{out} equals I_{in}. Recalling (3.1), this equality is only possible if $\lambda = 0$ (i.e. the medium is transparent). Consider now that I_{in} is fixed at a value higher than I^*. According to Lemma A1, there exists $\gamma(I_{in}) < I^*$ such that the AGR is maximal when $I_{out} = \gamma(I_{in})$, or, in terms of the optical depth, when $\lambda = \ln(I_{in}/\gamma(I_{in}))$. Following these ideas we define the *critical optical depth*, denoted by $\tilde{\lambda}(I_{in})$, as:

$$\tilde{\lambda}(I_{in}) := \begin{cases} \ln\left(\frac{I_{in}}{\gamma(I_{in})}\right) & if \quad I_{in} > I^*, \\ 0 & if \quad I_{in} \leq I^*. \end{cases} \tag{3.28}$$

The critical optical depth (associated to a critical value if biomass) reflects the value of the optical depth for which the AGR is maximal. Figure 3.5A shows how the AGR varies with the optical depth for different incident light intensities. When $I_{in} = I^*$ (or $I_{in} < I^*$), the AGR decreases with λ. When $I_{in} > I^*$, the AGR increases with λ until reaching its maximum value at $\lambda = \tilde{\lambda}(I_{in})$ and then decreases. As λ tends to be too high, the AGR approaches the value of the specific gross growth rate in absence of light ($\lim_{\lambda\to\infty} \mu(\cdot) = p(0)$). Proposition A2 states in detail this behavior. We note that $\tilde{\lambda}$ increases with I_{in}, which is true in general as stated in Proposition A4. When p is given by (3.25), according to Proposition A4, we have that for any $I_{in} > I^*$

$$\ln\left(\frac{I_{in}}{I^*}\right) < \tilde{\lambda}(I_{in}) < 2\ln\left(\frac{I_{in}}{I^*}\right). \tag{3.29}$$

This inequality shows that $\tilde{\lambda}$ increases logarithmically. Figure 3.6 shows $\tilde{\lambda}(I_{in})$ as a function of I_{in} for three different microalgae species with kinetic parameters from Table 2.1.

Critical incident light Figure 3.5B shows the AGR as a function of the incident light for different values of the optical depth. According to Lemma A2, there is an incident light intensity $\mathcal{I}(\lambda)$, that we call *critical incident light intensity*, at which the AGR is maximal. When $\lambda = 0$, the AGR coincides with the specific gross growth rate. As λ increases, the form of the AGR becomes wider and reaches its maximum at a higher incident light intensity. At low incident light intensity (i.e. for $I_{in} < \mathcal{I}(\lambda)$), light is a limiting factor in the sense that increasing light enhances the growth rate. This notion is not straightforward since some cells (in surface) can be photoinhibited. At high light (and especially for low λ), light is globally inhibiting.

According to Proposition A2, the critical incident light intensity is such that p is the same at the top and at the bottom of the PBR (see (5)). In terms of σ this can be written as:

$$\sigma(\mathcal{I}(\lambda)) = \mathcal{I}(\lambda)e^{-\lambda}. \tag{3.30}$$

Thus, if p is given by (3.25), then

$$\mathcal{I}(\lambda) = I^* e^{\lambda/2}. \tag{3.31}$$

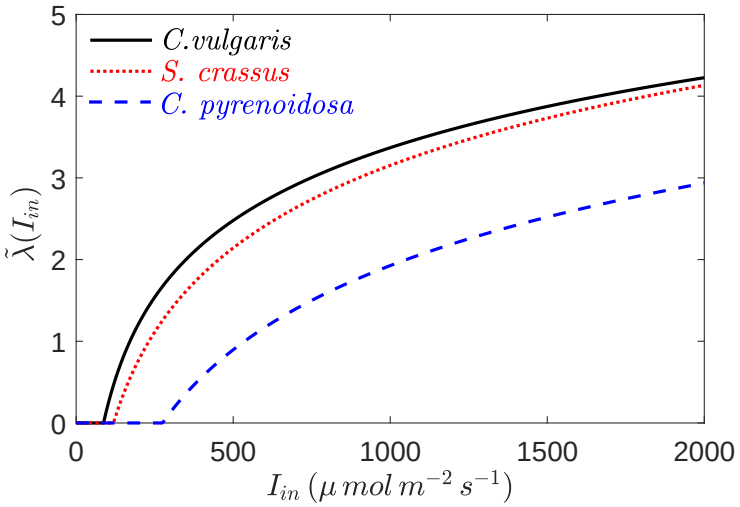

Figure 3.6: Critical optical depth $\tilde{\lambda}$ as a function of the incident light I_{in} for three different microalgae species. Kinetic parameters are taken from Table 2.1.

If p is given by (3.24), we cannot determine an explicit expression for σ, but we can determine directly from (5) (Appendix A) the form of the critical incident light intensity:

$$\mathcal{I}(\lambda) = I^* \frac{\lambda}{1 - e^{-\lambda}},$$

These expressions show that the critical incident light increases with the optical depth. This is true in the general case according to Proposition A5.

3.5 Discussion

AGR as a function of the microalgae population density Let us consider a flat-plate PBR, and assume that ξ is given by (3.4). In that case

the optical depth is given by

$$\lambda(X) = (kX + K_{bg})L.$$

From the previous section, we know that the AGR is maximal if $\lambda(X)$ equals the critical optical depth $\tilde{\lambda}$. Thus, if the optical depth in absence of microalgae $\lambda(0) = K_{bg}L$ is lower than $\tilde{\lambda}$, there is a microalgae population density $\tilde{X} = \frac{\tilde{\lambda} - K_{bg}L}{kL}$ maximizing the AGR. This shows the existence of an Allée effect, i.e. the AGR is maximal at an intermediate population density. This is illustrated in Figure 3.7 that shows the AGR as a function of X for different values of K_{bg}. Now, if $\lambda(0) = K_{bg}L \geq \tilde{\lambda}$, any increase in the microalgae population will move the optical depth further away from its optimal value. In consequence, the AGR rate is maximal when $X = 0$. In that case there is no Allee effect. From Proposition A4, $\tilde{\lambda}$ increases with I_{in}, thus, high values of I_{in} and low values of $K_{bg}L$ (low optical depth associated to the background turbidity) favor the presence of an Allee effect.

Experimental evidence of a positive optimal population density is for example described in [14]. The optimal density is $2.5\, g/L$ for a culture of *Spirulina platensis* in a glass column photobioreactor illuminated with an incident light intensity of $2000\, \mu\, mol\, m^{-2}\, s^{-1}$.

Incident light intensity as a limiting factor By a limiting factor we understand a factor such that the AGR increases with any increase of it. Figure 3.5B shows that when $\lambda = 10$, the incident light intensity is a lim-

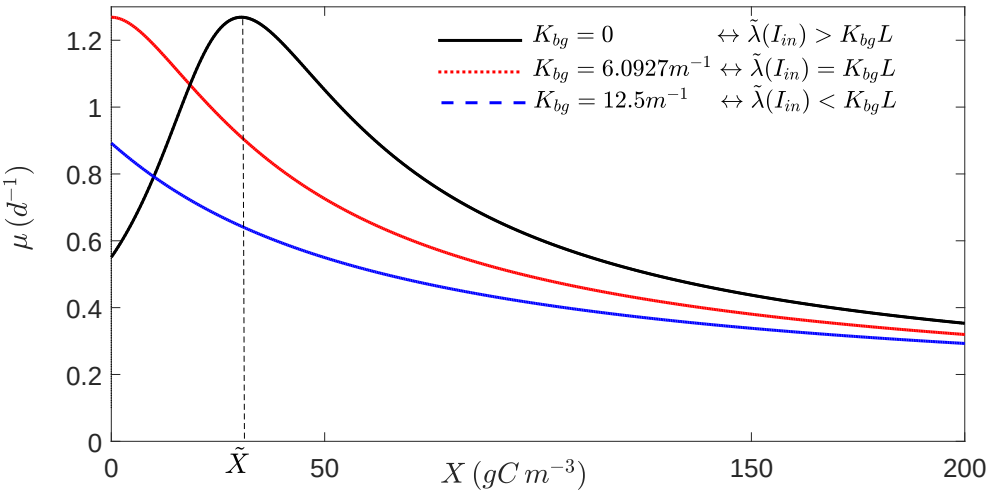

Figure 3.7: Plot of the AGR as a function of X. We consider p given by (3.25) with the kinetic parameters of *C. vulgaris* given in Table 2.1. The other parameters are taken to be $I_{in} = 500\,\mu\,mol\,m^{-2}\,s$, $k = 0.2\,m^2\,gC^{-1}$, $L = 0.4\,m$.

iting factor on the range $0 - 2000\,\mu\,mol\,m^{-2}\,s^{-1}$. This does not mean that microalgae does not suffer from photoinhibition, in fact, they do near the surface. It only means that the AGR increases. To determine if in outdoor cultures illuminated with natural light the light is a limiting factor, let us assume that I_{max} is the maximal incident light intensity (at midday) that the culture can receive. Thus, if $I_{max} \leq \mathcal{I}(\lambda)$, then light is a limiting factor during all the day. If p is given by (3.25), recalling (3.31), this is equivalent to

$$\lambda \geq 2\ln\left(\frac{I_{max}}{I^*}\right). \tag{3.32}$$

Thus, if $I_{max} = 2000\,\mu\,mol\,m^{-2}\,s^{-1}$, and $I^* = 90\,\mu\,mol\,m^{-2}\,s^{-1}$, condition (3.32) says that for cultures with $\lambda \geq 6.1$, the light is a limiting factor. In

terms of microalgae concentration, if ξ is given by (3.4), (3.32) can be put as

$$LX \geq \left(2\ln\left(\frac{I_{max}}{I^*}\right) - LK_{bg}\right)/k. \tag{3.33}$$

If $K_{bg} = 0\,m^{-1}$ and $k = 0.2\,gC\,m^{-2}$, the previous condition says that for cultures with an areal microalgal concentration higher than $30.5\,gC\,m^{-2}$ light is a limiting factor.

AGR in different geometries In section 3.4, we described some properties of the AGR in vertical cylindrical (or flat-plate) PBRs illuminated over one base. Even if we did not provide any formal demonstration for these different cases, these properties are expected to be valid for PBRs with a different shape. For sake of simplicity, we will refer to the different PBRs as flat-plate (see (3.9)), triangular (see (3.11)), semicircular (see (3.15)), and cylindrical PBR (see (3.18)). Figure 3.8A shows the AGR for different PBRs as a function of the optical depth. We can see that for low values of λ the AGR is higher in the flat-plate PBR while for high values of λ it is higher in the triangular PBR. Figure 3.8B shows the AGR for the different PBRs as a function of the incident light intensity. We can see that for high values of I_{in} the AGR is higher in the flat-plate PBR while for low values of I_{in} it is higher in the cylindrical PBR. These differences can be justified by the distribution of the microalgal culture with respect to the light gradient.

Productivity In order to compare the productivity of the different PBRs presented in this chapter, we benchmark them considering that they all have

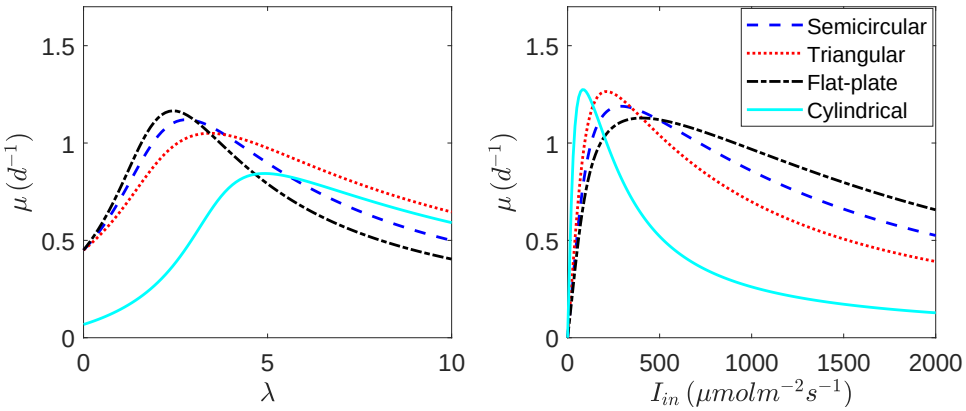

Figure 3.8: Plots of the AGR for different shapes of the PBR. A. $I_{in} = 500\,\mu\,mol\,m^{-2}\,s^{-1}$ is fixed. B. $\lambda = 3$ is fixed. We consider p given by (3.25) with the kinetic parameters of *C. vulgaris* given in Table 2.1 and $m = 0.1\,d^{-1}$.

the same volume V and the same irradiated culture area A. The depth of the flat-plate, the triangular, and the semicircular PBRs are V/A, $2V/A$, and $\frac{4}{\pi}V/A$ respectively. For the cylindrical PBR the radius is $2V/A$. $B = XV/A$ corresponds to the biomass concentration per unit of irradiated area. Thus, the biomass productivity per unit of irradiated area is:

$$P := B[\mu(I_{in}, \lambda) - m], \tag{3.34}$$

where m represents the loss rate. Writing the AGR as a function of the optical depth and the incident light intensity is justified by Theorems 3.3.2 and 3.3.3. Let us assume that the extinction coefficient is given by (3.4). Then, in the flat-plate PBR, the optical depth is given by

$$\lambda = (kX + K_{bg})V/A = kB + K_{bg}V/A. \tag{3.35}$$

Consequently, P depends on V/A but not on the values of V and A separately. The same is valid for the other PBRs. In the case that $K_{bg} = 0$, the productivity P is independent of V/A. Figure 3.9 shows the productivity as a function of B. We note that when $I_{in} > I^*$ the highest productivity is reached in the rectangular PBR. However, when $I_{in} < I^*$ the highest productivity is reached in the column PBR. The microalgae population density that yields maximal productivity is known as optimal population (or cell) density (OCD). The OCD has been studied experimentally in many works [9, 14, 16, 17].

In practice, background turbidity is not zero. It can even be very high if algae are used in wastewater treatment. In that case, the productivity varies with V/A (or with the light path-length). Figure 3.10 shows the maximal productivity for different values of V/A. As shown experimentally in [17], the productivity decreases as the light path-length increases. Note that the optical depth depends on $K_{bg}V/A$ and not on K_{bg} and V/A separately. Thus, the operational parameters determining the productivity are the incident light intensityI_{in} and the dimensionless parameter $K_{bg}V/A$ describing the background optical depth.

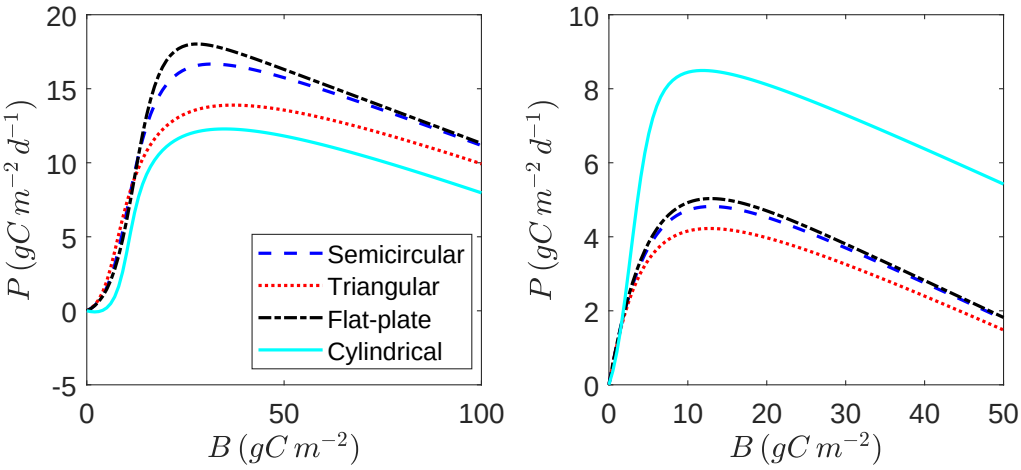

Figure 3.9: Productivity as a function of the biomass concentration per illuminated surface. A. $I_{in} = 1000\,\mu mol\,m^{-2}\,s^{-1}$ B. $I_{in} = 50\,\mu mol\,m^{-2}\,s^{-1}$. We consider p given by (3.25) with the kinetic parameters of *C. vulgaris* given in Table 2.1. The other parameters are taken to be $k = 0.2\,m^2\,gC^{-1}$, $m = 0.1\,d^{-1}$, and $K_{bg} = 0$.

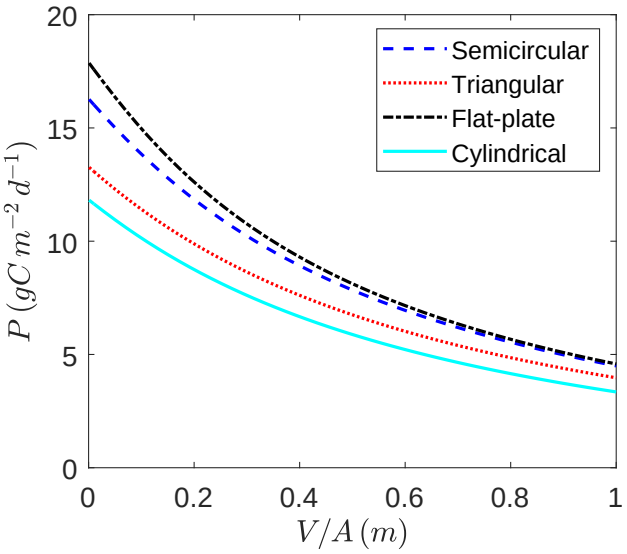

Figure 3.10: Maximal productivity as a function of V/A. p is given by (3.25) with kinetic parameters of *C. vulgaris* given in Table 2.1. Other parameters are taken to be $I_{in} = 1000\,\mu\,mol\,m^{-2}\,s$, $k = 0.2\,m^2\,gC^{-1}$, $m = 0.1\,d^{-1}$, $K_{bg} = 10\,m^{-1}$.

3.6 Conclusions

In this chapter we have described the AGR of microalgae in perfectly mixed PBRs. We showed that, given a form of the reactor, the AGR is completely determined by the incident light intensity and the optical depth. This result is due to the Lambert-Beer law and to the fact that the extinction coefficient is independent of the location in the PBR. From a mathematical point of view, our assumptions over the specific gross growth rate are very general, in particular, we did not assume that the specific gross growth rate p is differentiable as usually.

In the case of flat-plate PBRs illuminated from above, we studied in details the properties of the AGR. We showed the existence of values of the incident light intensity (critical light intensity) and the optical depth (critical optical depth) maximizing the AGR. We also studied how these values vary. These results are important for understanding how different environmental factors can affect the growth rate. In particular, they are useful for determining conditions for the occurrence of Allee effect or conditions such that the incident light intensity is a limiting factor.

Bibliography

[1] T. Anning, H. L. MacIntyre, S. M. Pratt, P. J. Sammes, S. Gibb, and R. J. Geider. Photoacclimation in the marine diatom skeletonema costa-

tum. *Limnology and Oceanography*, 45(8):1807–1817, 2000.

[2] O. Bernard, Mairet, and B. Chachuat. *Modelling of Microalgae Culture Systems with Applications to Control and Optimization*, pages 59–87. Springer International Publishing, Cham, 2016.

[3] O. Bernard and B. Rémond. Validation of a simple model accounting for light and temperature effect on microalgal growth. *Bioresource Technology*, 123:520 – 527, 2012.

[4] M. A. Borowitzka. *Limits to Growth*, pages 203–226. Springer Berlin Heidelberg, Berlin, Heidelberg, 1998.

[5] F. Courchamp, L. Berec, and J. Gascoigne. *Allee effects in ecology and conservation*. Oxford University Press, 2008.

[6] E. Evers. A model for light-limited continuous cultures: Growth, shading, and maintenance. *Biotechnology and bioengineering*, 38(3):254–259, 1991.

[7] D. J. Gerla, W. M. Mooij, and J. Huisman. Photoinhibition and the assembly of light-limited phytoplankton communities. *Oikos*, 120(3):359–368, 2011.

[8] S.-B. Hsu, C.-J. Lin, C.-H. Hsieh, and K. Yoshiyama. Dynamics of phytoplankton communities under photoinhibition. *Bulletin of Mathematical Biology*, 75(7):1207–1232, 2013.

[9] Q. Hu, N. Kurano, M. Kawachi, I. Iwasaki, and S. Miyachi. Ultrahigh-cell-density culture of a marine green alga chlorococcum littorale in

a flat-plate photobioreactor. *Applied Microbiology and Biotechnology*, 49(6):655–662, 1998.

[10] J. Huisman and F. J. Weissing. Light-limited growth and competition for light in well-mixed aquatic environments: An elementary model. *Ecology*, 75(2):507–520, 1994.

[11] J. T. O. Kirk. *Light and Photosynthesis in Aquatic Ecosystems*. Cambridge University Press, second edition, 1994. Cambridge Books Online.

[12] C. Martínez, F. Mairet, and O. Bernard. Theory of turbid microalgae cultures. *Journal of theoretical biology*, 456:190–200, 2018.

[13] J. Neidhardt, J. R. Benemann, L. Zhang, and A. Melis. Photosystem-ii repair and chloroplast recovery from irradiance stress: relationship between chronic photoinhibition, light-harvesting chlorophyll antenna size and photosynthetic productivity in dunaliella salina (green algae). *Photosynthesis Research*, 56(2):175–184, May 1998.

[14] H. Qiang, H. Guterman, and A. Richmond. Physiological characteristics of spirulina platensis (cyanobacteria) cultured at ultrahigh cell densities 1. *Journal of Phycology*, 32(6):1066–1073, 1996.

[15] H. Qiang, H. Guterman, and A. Richmond. Physiological characteristics of spirulina platensis (cyanobacteria) cultured at ultrahigh cell densities1. *Journal of Phycology*, 32(6):1066–1073, 1996.

[16] H. Qiang and A. Richmond. Productivity and photosynthetic efficiency ofspirulina platensis as affected by light intensity, algal density and rate

of mixing in a flat plate photobioreactor. *Journal of Applied Phycology*, 8(2):139–145, 1996.

[17] H. Qiang, Y. Zarmi, and A. Richmond. Combined effects of light intensity, light-path and culture density on output rate of spirulina platensis (cyanobacteria). *European Journal of Phycology*, 33(2):165–171, 1998.

[18] J. H. Steele. Environmental control of photosynthesis in the sea. *Limnology and Oceanography*, 7(2):137–150, 1962.

[19] P. Talbot, J.-M. Thébault, A. Dauta, and J. De la Noüe. A comparative study and mathematical modeling of temperature, light and growth of three microalgae potentially useful for wastewater treatment. *Water research*, 25(4):465–472, 1991.

[20] C. Ugwu, H. Aoyagi, and H. Uchiyama. Photobioreactors for mass cultivation of algae. *Bioresource technology*, 99(10):4021–4028, 2008.

[21] A. Vonshak and R. Guy. Photoadaptation, photoinhibition and productivity in the blue-green alga, spirulina platensis grown outdoors. *Plant, Cell Environment*, 15(5):613–616, 1992.

[22] K.-L. Yeh, J.-S. Chang, and W.-m. chen. Effect of light supply and carbon source on cell growth and cellular composition of a newly isolated microalga chlorella vulgaris esp-31. *Engineering in Life Sciences*, 10(3):201–208, 2010.

CHAPTER 4

Co-limitation by light and substrate under periodic forcing

Contents

4.1 Chapter presentation

This chapter relies on an article submitted to *Journal of Differential Equations* in February 2019. Here, we study the dynamics of the periodically forced light-limited Droop model that describes the growth of a single microalgae population under limitation by two resources, light and substrate. The model consists of a periodic system of ordinary differential equations. The periodicity of the model is typically induced by periodic culture operation (periodic dilution rate and/or nutrient supply) and periodic fluctuations of environmental conditions (such as the light source or the medium temperature). To the best of our knowledge, there is no study of any periodic version of the light-limited Droop model. Note also that we consider a generalized version of the classical Droop model and that we can manage non-differentiable models such as ones involving minimum laws.

The main result of this chapter consists of two theorems. Our first theorem gives conditions for the existence of a positive periodic solution i.e. a solution characterized by the presence of microalgae. It also states that if there is a unique positive periodic solution, then it is globally stable. The proof of this theorem is mainly based on persistence results for periodic Kolmogorov equations, on the theory of asymptotically periodic semiflows, and on the reduction of the model to a cooperative planar periodic system of differential equations. Our second theorem gives conditions to assure the uniqueness of positive periodic solutions. This finding is mainly based on results of the theory of monotone sub-homogeneous dynamical systems. We

include an application section to illustrate our results on a practical case and to make this chapter more intelligible for researchers and practitioners in different fields.

Martínez, C., Mairet, F.,& Bernard, O. (2019). *Dynamics of the periodically forced light-limited Droop model.* (Submitted to Journal of differential equations on Feb 4th, 2019).

Abstract : *We analyze the asymptotic behavior of the periodically forced light limited Droop model, representing microalgae growth. We consider general monotone growth and uptake rate functions. Based on a conservation principle, we reduce the model to a limiting planar periodic system of differential equations. The reduced system generates a monotone dynamical system. Combining this fact with results on periodic Kolmogorov equations, we find conditions such that any solution of the reduced model approaches to a positive periodic solution. Under these conditions, if the reduced system admits only one positive periodic solution, using the theory of asymptotically periodic semiflows, we extend the results on the limiting system to the original model. Finally, based on results of monotone sub-homogeneous dynamical systems, we give conditions to determine the uniqueness of positive periodic solutions.*

4.2 Introduction

In this chapter we study the asymptotic behavior of the periodically forced light-limited Droop model i.e. a model that results from combining the modelling approaches of Droop [2] and Huisman [3], when the growth rate, the uptake rate, the nutrient supply, and the dilution rate are periodic functions of time. This study extends the results of Smith [6] on the model (2.31) (see Chapter 2) to a much more general framework. We consider general monotone growth and uptake rate functions. In our approach, we reduce the model to a cooperative two-dimensional system to show that any solution approaches asymptomatically to a periodic solution. Following results on Kolmogorov periodic equations [8], we find conditions such that any solution of the reduced system is asymptotic to a positive periodic solution i.e. a solution characterized by the presence of microalgae. This proves the existence of positive periodic solutions for the original system. Using the theory of asymptotically periodic semiflows [10] and classical results of the theory of differential equations such as the comparison method [1], we show that if the original system admits a unique positive periodic solution, then it is globally stable. Finally, using results of the theory of subhomogeneous (or sublinear) dynamical systems [11], we give conditiones for the uniqueness of positive periodic solutions.

This chapter is organized as follows. In Section 4.3.1, we introduce the periodically forced light-limited Droop model and we state some basic results on the existence, uniqueness, and boundedness of solutions. In Section 4.4, we

study a limiting two-dimensional periodic system of the model. We prove that any solution of this system is asymptotic to a periodic solution (Proposition 4.4.3), and we give conditions for the persistence (Theorem 4.4.5). In Section 4.5, we present the main results. A first theorem (Theorem 4.5.1) is an extrapolation of the results on the limiting system to the original system, and another theorem (Theorem 4.5.2) gives conditions for the uniqueness of positive periodic solutions. In Section 4.6, we apply our results to study a model describing microalgae growth under limitation by phosphorus and light. In Section 4.7, we discuss our results and some possible extensions. In Appendix B we present some results on the asymptotic of scalar differential equations and we prove some properties of a growth rate function.

4.3 Model description and basic properties

4.3.1 Model description

Let us consider a well-mixed culture system with a biomass $x(t)$ of microalgae. Microalgae growth is only limited by light and a nutrient at concentration $s(t)$ in the medium. The light is provided by an external light source (artificial or natural) and its intensity can vary with time. The nutrient is supplied at variable concentration $s_{in}(t)$, from an external reservoir at the variable volumetric flow rate $Q_{in}(t)$. The dilution rate is the ratio $D(t) := F_{in}(t)/V(t)$ with $V(t)$ the volume of the culture. Following the Droop model [2], microalgae growth depends on the internal quota of nutrient $q(t)$. The quota increases with nutrient uptake and decreases with cell growth (by the effect of intracellular dilution). Following the theory

of light-limited chemostats [3], the growth of microalgae affects their own light environment (self-shading). Then, the cell growth rate depends on the biomass concentration $x(t)$. Since the incident light may vary over time, the growth rate depends on time. The light-limited Droop model takes the following form:

$$\begin{aligned} \frac{dx}{dt} &= [\mu(t,x,q) - D(t)]x, \\ \frac{dq}{dt} &= \rho(t,q,s) - \mu(t,x,q)q, \\ \frac{ds}{dt} &= D(t)(s_{in}(t) - s) - \rho(t,q,s)x. \end{aligned} \tag{4.1}$$

The functions μ and ρ represent the growth rate of microalgae and the nutrient uptake rate respectively. Let $J = [q_0, \infty)$ with $q_0 > 0$. We assume that $\mu : \mathbb{R}_+^2 \times J \longrightarrow \mathbb{R}$, $\rho : \mathbb{R}_+ \times J \times \mathbb{R} \longrightarrow \mathbb{R}$, and D, $s_{in} : \mathbb{R}_+ \longrightarrow \mathbb{R}_+$ are continuous functions and satisfy the following set of assumptions:

Assumption 4.3.1. *μ, ρ, D, and s_{in} are ω-periodic in t with $\omega > 0$.*

Assumption 4.3.2. *$q \longmapsto \rho(t,q,s)$ is decreasing, $s \in [0,\infty) \longmapsto \rho(t,q,s)$ is increasing, and $\rho(t,q,s) = 0$ for all $s \leq 0$.*

Assumption 4.3.3. *$\mu(t,x,q_0) \leq 0$ for any $t, x \geq 0$, and $q \longmapsto \mu(t,x,q)$ is increasing.*

Assumption 4.3.4. *For any $q > q_0$, $x \longmapsto \mu(t,x,q)$ is decreasing.*

Assumption 4.3.5. *$\lim_{q\to\infty} \rho(t,q,s) = 0$ and $\lim_{x\to\infty} \mu(t,x,q) \leq 0$, both uniformly for $t \in [0,\omega]$.*

Assumption 4.3.6. *$\int_0^\omega D(t)dt > 0$ and $\int_0^\omega D(t)s_{in}(t)dt > 0$.*

Assumption 4.3.7. *μ and ρ are locally Lipschitz uniformly for t in $[0, \omega]$.*

Assumption 4.3.8. *There exists $q' > q_0$ such that $\int_0^\omega \mu(t, 0, q')dt > 0$.*

Remark 4.3.9. *In Assumption 4.3.5, the existence of the limits is given by the monotony of μ and ρ. The limit for μ is allowed to be $-\infty$.*

Remark 4.3.10. *(Respiration rate) In hypothesis Assumption 4.3.3, the growth rate is allowed to be negative. When microalgae is measured in terms of carbon biomass, μ corresponds to the carbon gain rate i.e. $\mu = p - m$, with p the carbon uptake rate and m the specific carbon loss rate. Thus, μ may be negative, especially in absence of light when $p = 0$. Note also that if q is measured in terms of carbon (for example gN/gC), then a carbon loss results in an increase of the quota.*

Remark 4.3.11. *From a biological point of view, Assumption 4.3.8 states that there is a quota such that a very small population can grow. Hypothesis Assumption 4.3.8 is necessary to avoid the extinction of the population and unbounded values of the cell quota (see Remarks 4.3.14 and 4.3.17).*

4.3.2 Existence, uniqueness and boundedness of solutions

We define the total amount of limiting nutrient both in the substrate and in the biomass by means of $S = s + xq$. A simple calculation shows that S satisfies the differential equation:

$$\frac{dS}{dt} = D(t)(s_{in}(t) - S). \tag{4.2}$$

With respect to the solutions of (4.2), we have the following lemma.

Lemma 4.3.12. *Equation (4.2) admits a unique ω-periodic solution $s_*(t)$ which is positive and globally stable.*

Proof. From a direct calculation we have that:

$$S(t) = (S(0) + f(t))e^{-d(t)}, \tag{4.3}$$

and that $s_*(t)$ is given by:

$$s_*(t) = e^{-d(t)} \left(\frac{f(\omega)}{e^{d(\omega)} - 1} + f(t) \right), \tag{4.4}$$

with $d(t) = \int_0^\omega D(t)dt$ and $f(t) = \int_0^t e^{d(\tau)} s_{in}(\tau) D(\tau) d\tau$. Since s_{in} and D are non-negative, we have that f is a non-negative function. Since $\int_0^\omega D(t) s_{in}(t) dt > 0$ (see Assumption 4.3.6), we have that $f(\omega) > 0$. Thus, $s_*(t)$ is positive. For the global stability, it easily follows that $|S(t) - s_*(t)| \to 0$ as $t \to \infty$. □

Now we state the existence and uniqueness of solutions for system (4.1).

Lemma 4.3.13. *System (4.1) admits a unique global solution for any initial condition on $\mathbb{R}_+ \times J \times \mathbb{R}_+$.*

Proof. The local existence and uniqueness of solutions is given by Assumption 4.3.7. Let (x, q, s) be a solution of (4.1) such that $x(0), s(0) \geq 0$ and $q(0) \geq q_0$, with Δ the maximal interval of existence. It easily follows that $(x(t), q(t), s(t)) \in \mathbb{R}_+ \times J \times \mathbb{R}_+$ for any $t \in \Delta$. Since the variable $S = xq + z$ satisfies the differential equation (4.2) and (x, q, s) is non-negative, by Lemma 4.3.12, xq and s cannot be unbounded in a finite interval of time. We note

that $x(t)q(t) \geq x(t)q_0$, then $x(t) \leq S(t)/q_0$ for all $t \in \Delta$. Finally, since $dq/dt \leq \rho(t, q_0, S(t)) - \mu(t, S(t)/q_0, q_0)q$, we conclude that q cannot be unbounded in a finite interval of time. Thus, $\Delta = [0, \infty)$. □

Remark 4.3.14. *Let (x, q, s) be a solution of (4.1). If Assumption 4.3.8 does not hold, then $x(t) \to 0$ as $t \to \infty$. Indeed, since μ is decreasing in x we have that:*

$$\frac{dx(t)}{dt} \leq x(t)[\mu(t, 0, q(t)) - D(t)]. \tag{4.5}$$

Since Assumption 4.3.8 does not hold, $\int_0^{n\omega} \mu(t, 0, q(t))dt < 0$ for any integer $n \geq 1$. Thus, applying Gronwall's inequality to (4.5) on the interval $[t - \omega[t/\omega], t]$ we obtain:

$$x(t) \leq x(t - \omega[t/\omega])e^{-\alpha[t/\omega]}, \tag{4.6}$$

where $[t/\omega]$ is the greatest integer less than or equal to t/ω and $\alpha = \int_0^{\omega} D(\tau)d\tau > 0$. Letting $t \to \infty$ in (4.6) we obtain that $x(t) \to 0$.

The following lemma will be repeatedly used in the rest of this chapter.

Lemma 4.3.15. *For any non-negative continuous function σ there is $Q > 0$ such that:*

$$\int_0^{\omega} \left(\frac{\rho(t, Q, \sigma(t))}{Q} - \mu(t, 0, Q) \right) dt < 0.$$

Proof. From Assumption 4.3.5 we have that $\lim_{q\to\infty} \int_0^{\omega} \rho(t, q, s)dt = 0$ for any $s \geq 0$. Then there exists $Q > q'$ such that:

$$\int_0^{\omega} \rho(t, Q, \max_{t\in[0,\omega]} \sigma(t))dt < \epsilon := q' \int_0^{\omega} \mu(t, 0, q')dt. \tag{4.7}$$

From the monotony of μ and ρ as functions of q (see Assumptions 4.3.2 and 4.3.3), we have that:

$$Q\int_0^\omega \mu(t,0,Q)dt > q'\int_0^\omega \mu(t,0,q')dt = \epsilon \geq \int_0^\omega \rho(t,Q,\sigma(t))dt,$$

from where we conclude the proof. □

Lemma 4.3.16. *Solutions of (4.1) starting on $\mathbb{R}_+ \times J \times \mathbb{R}_+$ are uniformly bounded.*

Proof. From Theorem 8.5 in [9], the ultimate boundedness of solutions of a periodic system implies the uniform boundedness of solutions. Thus, we prove that solutions of (4.1) starting on $\mathbb{R}_+ \times J \times \mathbb{R}_+$ are ultimately bounded. Let $(\bar{x}, \bar{q}, \bar{s})$ be a solution of (4.1) with $\bar{x}(0), \bar{s}(0), \bar{q}(0) - q_0 \geq 0$. We have that $\bar{S}(t) = \bar{x}(t)\bar{q}(t) + \bar{s}(t)$ satisfies the differential equation (4.2). From Lemma 4.3.12, there is $t' > 0$ such that $\bar{S}(t) \leq s'$ for all $t \geq t'$, with $s' := 1 + \max s_*(t)$. By similar arguments as in Proof of Lemma 4.3.13, we have $\bar{x}(t) \leq s'/q_0$ and $\bar{s}(t) \leq s'$ for all $t > t'$. It remains to prove the existence of a constant β independent of initial conditions such that $\limsup_{t\to\infty} \bar{q}(t) \leq \beta$. For this purpose, let us define $h(t,q) := \frac{\rho(t,q,s')}{q} - \mu(t,0,q)$ and $g(t,q) = \frac{\rho(t,q,s')}{q} - D(t)$. From Lemma 4.3.15 and Assumption 4.3.5, there exists $Q > \bar{q}(0)$ such that:

$$\int_0^\omega h(t,Q)dt < 0 \text{ and } \int_0^\omega g(t,Q)dt < 0. \tag{4.8}$$

Now, if $\bar{q}(t) < Q$ for all $t \geq t'$, then the result holds. Then, let us assume that $\bar{q}(t_1) = Q$ for some $t_1 > t'$ and that $q(t) \geq Q$ for all $t \geq t_1$. Then we

have that $\bar{x}_s(t) := \bar{x}(t)\bar{q}(t)$ satisfies the following equation for all $t \geq t_1$:

$$\frac{dx_s}{dt} = \left(\frac{\rho(t, \bar{q}(t), \bar{s}(t))}{\bar{q}(t)} - D(t) \right) x_s \leq g(t, Q) x_s. \tag{4.9}$$

Using Gronwall's inequality on the interval $[t_1, t_1 + t], t > 0$ gives:

$$\bar{x}_s(t_1 + t) \leq \bar{x}_s(t_1 + t - \omega[t/\omega]) e^{-\alpha[t/\omega]},$$

where $[t/\omega]$ is the greatest integer less than or equal to t/ω and $\alpha = -\int_0^\omega g(\tau, Q) d\tau > 0$. Since s' is an upper bound for $\bar{x}_s$ and q_0 is a lower bound for $\bar{q}$, we obtain:

$$\bar{x}(t_1 + t) \leq \frac{s'}{q_0} e^{-\alpha[t/\omega]}. \tag{4.10}$$

Now, from Assumption 4.3.7, there exists $\delta_0 > 0$ such that:

$$|\mu(t, x, Q) - \mu(t, 0, Q)| \leq l|x|, \tag{4.11}$$

for all $t \in [0, \omega]$ and $x \in [-\delta_0, \delta_0]$, with l the Lipschitz constant of μ. Let $\epsilon := -\frac{1}{2}\int_0^\omega h(t, Q) dt$ and let us choose $t_2 > t_1$ such that $\frac{s'}{q_0} e^{-[(t_2 - t_1)/\omega]\alpha} < \min\{\delta_0, \epsilon/l\}$. Thus, from (4.10) and (4.11), we obtain that $|\mu(t, \bar{x}(t), Q) - \mu(t, 0, Q)| < \epsilon$ for all $t \geq t_2$, and consequently:

$$\frac{d\bar{q}(t)}{dt} \leq \bar{q}(t) \left(h(t, Q) + \epsilon \right). \tag{4.12}$$

Using Gronwall's inequality on the interval $[t_2, t_2 + n\omega]$ gives $\bar{q}(t_2 + n\omega) \leq \bar{q}(t_2) e^{-n\epsilon}$. Let $\gamma := \max_{t \in [0,\omega]} \frac{\rho(t, q_0, s')}{q_0} - \mu(t, s'/q_0, q_0)$. Then $d\bar{q}(t)/dt \leq \gamma \bar{q}(t)$. Applying Gronwall's inequality on the interval $[t_1, t_2]$ gives $\bar{q}(t_2) \leq Q e^{\gamma(t_2 - t_1)}$.

Consequently $\bar{q}(t_2+n\omega) \leq Qe^{\gamma(t_2-t_1)+n\epsilon}$. Thus, for $n > \gamma(t_2-t_1)/\epsilon$, we have that $\bar{q}(t_2+n\omega) < Q$. Therefore $\bar{q}$ must return to Q in a finite time smaller than $T := t_2 - t_1 + n\omega$. Since T does not depend on initial conditions, we conclude that q is ultimately bounded by $Qe^{T\gamma}$. □

Remark 4.3.17. *If Assumption 4.3.8 does not hold, then solutions of (4.1) are not bounded. Indeed, let (x,q,s) be a solution of (4.1) with $x(0), s(0) \geq 0$ and $q(0) \geq q_0$. Let us assume that q is bounded from above by $Q > 0$. Since ρ is non-negative and μ is decreasing in x, we have $\frac{dq(t)}{dt} \geq -\mu(t,0,Q)q$. Applying Gronwall's inequality on the interval $[0, n\omega]$ with $n \geq 1$ an integer, we obtain:*

$$q(n\omega) = q(0)e^{-n\int_0^\omega \mu(t,0,Q)dt}. \tag{4.13}$$

If Assumption 4.3.8 does not hold, then $\int_0^\omega \mu(t,0,Q)dt < 0$. Thus, letting $n \to \infty$ in (4.13), we conclude that q is not bounded which is a contradiction.

A solution (x,q,s) of (4.1) will be called an ω-periodic solution provided each component is ω-periodic. An ω-periodic solution with absence of microalgae is called washout periodic solution. The following proposition shows that (4.1) admits at least one washout periodic solution.

Proposition 4.3.18. *The system (4.1) has at least one washout periodic solution.*

Proof. It is not difficult to see that any washout must be of the form $(0, q(t), s_*(t))$ with $s_*(t)$ the periodic solution of (4.2). Thus, putting $x = 0$ and $s = s_*(t)$ in the second equation of (4.1) results in:

$$\frac{dq}{dt} = \rho(t,q,s_*(t)) - \mu(t,0,q)q. \tag{4.14}$$

Let us define:

$$F_0(t,q) = \frac{\rho(t,q,s_*(t))}{q} - \mu(t,0,q). \tag{4.15}$$

From Lemma 4.3.15, there exists $Q > 0$ such that $\int_0^\omega F_0(t,Q)dt < 0$. From Assumption 4.3.3 we have that $F_0(t,q_0) \geq 0$ for all $t \geq 0$. Thus, the proof follows from a direct application of Proposition B9 in Appendix B. □

Remark 4.3.19. *(Uniqueness of the washout) The uniqueness of the washout can be stated under additional assumptions over the monotony of ρ and μ. For example, consider F_0 defined in (4.15). If for some t the function $q \longmapsto F_0(t,q)$ is strictly decreasing, then we have the uniqueness of the washout.*

4.4 Reduced system

Dropping the equation for s and replacing s in (4.1) by $s = s_*(t) - xq$ results in the following limiting ω-periodic system for (x,q):

$$\begin{aligned} \frac{dx}{dt} &= [\mu(t,x,q) - D(t)]x, \\ \frac{dq}{dt} &= \rho(t,q,s_*(t) - xq) - \mu(t,x,q)q. \end{aligned} \tag{4.16}$$

In the following we study the asymptotic behavior of the limiting system (4.16). We are interested in solutions of (4.16) starting with a positive initial microalgae concentration and an internal quota not lower than q_0 i.e. solutions with initial conditions on the set:

$$P := \{(x,q)\ ;\ x > 0,\ q \geq q_0\}. \tag{4.17}$$

Our first lemma states a basic property of solutions of (4.16).

Lemma 4.4.1. *For any solution (x, q) of (4.16) starting on P we have that $x(t) > 0$ and $q(t) \geq q_0$ for all $t > 0$. Moreover, there is $t' >\geq 0$ such that $s_*(t) \geq x(t)q(t)$ for all $t \geq t'$.*

Proof. Since $\frac{dq}{dt}|_{q=q_0} \geq 0$, if $q(0) \geq q_0$ then $q(t) \geq q_0$ for all $t \geq 0$. If $x(0) > 0$, x cannot reach $x = 0$ in a finite time by the uniqueness of solutions of initial value problems. Then $x(t) > 0$ for all $t \geq 0$. The variable $x_s := xq$ satisfies the differential equation:

$$\frac{dx_s}{dt} = x_s \left(\frac{\rho(t, q, s_*(t) - x_s)}{q} - D(t) \right). \tag{4.18}$$

Thus, the variable $y(t) = s_*(t) - x_s(t)$ satisfies:

$$\frac{dy}{dt} = D(t)(s_{in}(t) - y) + (y - s_*(t))\frac{\rho(t, q, y)}{q}. \tag{4.19}$$

We note that $\frac{dy}{dt}|_{y=0} = s_{in}(t)D(t) \geq 0$, therefore if $y(t') \geq 0$ for some $t' \geq 0$ then $y(t) \geq 0$ for all $t \geq t'$ and the proof is trivial. Then we have to prove the existence of $t' > 0$ such that $y(t') \geq 0$. By contradiction, let us assume that $y(t) < 0$ for all $t \geq 0$. From (4.19) and Assumption 4.3.2 we have $dy/dt = D(t)(s_{in}(t) - y)$. From Lemma 4.3.12, y approaches asymptotically to s_*, which is a contradiction because s^* is positive. □

The following convergence results for the limiting system need the uniqueness of the washout periodic solution.

Proposition 4.4.2. *Let us assume that (4.16) admits a unique washout periodic solution $(0, q_*)$. Then, for any solution (x, q) of (4.16) satisfying*

$\lim_{t\to\infty} x(t) = 0$, *we have that* $\lim_{t\to\infty} |q(t) - q_*(t)| = 0$.

Proof. Let $(\bar{x}, \bar{q})$ a solution of (4.16). Following the proof of Proposition 4.3.18, we define $F(t,q) = \rho(t, q, s_*(t) - q\bar{x}(t))/q - \mu(t, \bar{x}(t), q)$. From Assumption 4.3.3 we have that $F(t, q_0) \geq 0$ for all $t \geq 0$. Since $\lim_{t\to\infty} \bar{x}(t) = 0$, we have that $\lim_{t\to\infty} |F_0(t,q) - F(t,q)| = 0$. Thus, the proof follows from a direct application of Proposition B9b) in Appendix B. □

Now we prove that any solution of (4.16) is asymptotic to an ω-periodic solution. The heart of the proof lies in the fact that the change of variables $x_s = xq$ leads the limiting system to a cooperative system.

Proposition 4.4.3. *If (4.16) admits a unique washout periodic solution, then any solution of (4.16) starting on P approaches asymptotically to an ω-periodic solution.*

Proof. Let $(\bar{x}, \bar{q})$ be a solution of (4.16) with $\bar{x}(0) > 0$ and $\bar{q}(0) \geq q_0$. Let $\bar{x}_s(t) := \bar{x}(t)\bar{q}(t)$. From Lemma 4.4.1, it easily follows that $\bar{x}_s(t)$ and $\bar{x}(t)$ are bounded. Considering the change of variables $x_s := qx$, we have that $(\bar{x}(t), \bar{x}_s(t))$ is a solution of the following system:

$$\begin{aligned} dx/dt &= f_1(t, x, x_s) := [\mu(t, x, x_s/x) - D(t)]x, \\ dx_s/dt &= f_2(t, x, x_s) := \rho(t, x_s/x, s_*(t) - x_s)x - D(t)x_s. \end{aligned} \tag{4.20}$$

The system (4.20) is cooperative i.e. f_1 and f_2 are increasing in x_s and x respectively. Following the proof of Theorem 4.2 in Chapter 7 in the Book [7], we have that the sequences $\bar{x}_n := \bar{x}(n\omega)$ and $\bar{x}_{sn} = \bar{x}_s(n\omega)$ are convergent. Let $l := \lim_{n\to\infty} \bar{x}_n$ and $l' := \lim_{n\to\infty} \bar{x}_{sn}$. If $l > 0$, then $l' > 0$ and consequently $\bar{q}_n := \bar{q}(n\omega) = \bar{x}_{sn}/\bar{x}_n \to l/l'$ as $n \to \infty$. Thus, $(\bar{x}_n, \bar{q}_n)$ approaches

asymptotically to an ω-periodic solution of (4.16) with initial conditions $(l, l'/l)$. Let us assume now that $l = 0$ and let $g(t) := \mu(t, \bar{x}(t), \bar{q}(t)) - D(t)$. We can write $\bar{x}(t) = \bar{x}(0)e^{\alpha(t)+\beta(t)}$, with:

$$\alpha(t) = \int_0^{\omega[t/\omega]} g(\tau)d\tau, \text{ and } \beta(t) = \int_{\omega[t/\omega]}^{t} g(\tau)d\tau.$$

Let Q be an upper bound for $\bar{q}$ given by Lemma 4.3.16, then we have $g(t) \leq \mu(t, 0, Q)$. Thus, $\beta(t) \leq b := \omega \max_{t_{0,\omega}} \mu(t, 0, Q)$. We have that $\bar{x}_n = \bar{x}(0)e^{\alpha(n\omega)}$. Since $\bar{x}_n \to 0$, we conclude that $\alpha(n\omega) \to -\infty$. Then, it is trivial that $\alpha(t) \to -\infty$ as $t \to \infty$. Thus, we conclude that $\bar{x}(t) \leq \bar{x}(0)e^{\alpha(t)+b} \to 0$ as $t \to \infty$. From Proposition 4.3.18, we conclude that $(\bar{x}, \bar{q})$ is asymptotic to an ω-periodic solution. □

Remark 4.4.4. *The monotony of μ as a function of x is not essential in the proof of Proposition 4.4.3. Indeed, the system (4.20) does not lose the property of being cooperative.*

An ω-periodic solution (x, q) of (4.16) will be called positive ω-periodic solution, if $x(t) > 0$, $q(t) \geq q_0$, and $x(t)q(t) \leq s_*(t)$ for all $t \in [0, \omega]$. The following theorem gives conditions to ensure that any solution of (4.16) approaches to a positive ω-periodic solution.

Theorem 4.4.5. *Let us assume that (4.16) admits a unique washout periodic solution $(0, q_*)$ and that $\int_0^\omega [\mu(t, 0, q_*(t)) - D(t)]dt > 0$. Then, (4.16) admits at least one positive ω-periodic solution and any solution of (4.16) starting in P approaches asymptotically to a positive ω-periodic solution.*

Proof. Along the proof we will write $u = (x, q)$. Let us define $f = (f_1, f_2)$:

$\mathbb{R}^2_+ \times J \times \mathbb{R}_+ \longrightarrow \mathbb{R}^2$ by:

$$f_1(t,u,v) = \mu(t,u) - D(t) \text{ and } f_2(t,u,v) = \hat{\rho}(t,u_2, v - u_1u_2)/u_2 - \mu(t,u), \tag{4.21}$$

with $\hat{\rho}$ a continuous extension of ρ on $\mathbb{R}_+ \times J \times \mathbb{R}$ to $\mathbb{R}^2_+ \times \mathbb{R}$ such that $\hat{\rho}$ is ω-periodic in t and locally Lipschitz in u uniformly in t. Consider the Kolmogorov periodic system:

$$\frac{du_i}{dt} = u_i f_i(t,u,s_*(t)),\ i = 1,2, \tag{4.22}$$

For initial conditions on $\mathbb{R}_+ \times [0,q_0]$, solutions of (4.22) stay on $\mathbb{R}_+ \times [0,q_0]$ or they intersect the set $\mathbb{R}_+ \times J$ for some $t > 0$. Thus, solutions of (4.22) exist for any initial condition on $\mathbb{R}^2_+$ and they are uniformly bounded. Let $\phi_0(t,u)$ be the unique solution of (4.22) with $\phi_0(0,u) = u \in \mathbb{R}^2_+$ and let $\varphi := \phi(\omega,\cdot) : \mathbb{R}^2_+ \longrightarrow \mathbb{R}^2_+$ be the Poincaré map associated to (4.22). From Lemma 1 in the appendix of [8], we conclude that there is $\delta > 0$ such that $\lim_{n\to\infty} d(\varphi^n(u),(0,q_*(0))) \geq \delta$ for all $u \in int(\mathbb{R}^2_+)$. This implies that for any $u \in (0,\infty) \times J$, $\phi(t,u)$ is not asymptotic to the washout periodic solution. From Proposition 4.4.3, we conclude that $\phi(t,u)$ approaches an ω-periodic solution (x^*,q^*) different from the washout periodic solution. From Lemma 4.4.1, we have that $x^*(t)q^*(t) \leq s_*(t)$ for all $t \geq 0$. Thus (x^*,q^*) is a positive ω-periodic solution and the proof is completed. □

We end this section with the following result that states an order of the positive periodic solutions of (4.16).

Lemma 4.4.6. *For any two periodic solutions (x_i^*,q_i^*), $i = 1,2$ of (4.16)*

with $x_i^*(0) > 0$*, we have that either*

- $x_1^*(t) \leq x_2^*(t)$ *and* $x_1^*(t)q_1^*(t) \leq x_2^*(t)q_2^*(t)$ *for all* $t \in [0, \omega]$*, or*
- $x_1^*(t) \geq x_2^*(t)$ *and* $x_1^*(t)q_1^*(t) \geq x_2^*(t)q_2^*(t)$ *for all* $t \in [0, \omega]$*.*

Proof. We write $x_{si}^* = x_i^*(t)q_i^*(t)$, $i = 1, 2$. Then, we have that $(x_i^*, x_{si}^*), i = 1, 2$ are periodic solutions of (4.20). We claim that either (a) $x_{1s}^*(t) \leq x_{2s}^*(t)$ for all $t \in [0, \omega]$ or (b) $x_{1s}^*(t) \geq x_{2s}^*(t)$ for all $t \in [0, \omega]$. Indeed, let us assume that there is $t_0 \in [0, \omega]$ such that $x_{1s}^*(t_0) = x_{2s}^*(t_0)$, otherwise the claim is trivial. Then either (I) $x_1^*(t_0) < x_2^*(t_0)$ or (II) $x_2^*(t_0) > x_1^*(t_0)$, otherwise both periodic solutions are the same. If (I) holds, then by a Kamke's Theorem argument, we have that $x_{1s}^*(t) \leq x_{2s}^*(t)$ for all $t \geq t_0$, and by the periodicity of x_{1s}^* and x_{2s}^* we conclude that (a) holds. In the same way, if (II) holds then (b) holds. Thus, the claim is proved. Now, since f_1 (see (4.20)) is increasing in x_s, we conclude that (a) implies $x_1^*(t) \leq x_2^*(t)$, and (b) implies $x_1^*(t) \geq x_2^*(t)$. This completes the proof. □

4.5 Main results

An ω-periodic solution (x^*, q^*, s^*) of (4.1) is known as positive ω-periodic solution if $x^*(t) > 0$, $q^*(t) \geq q_0$, and $s^*(t) \geq 0$. The following theorem states conditions for the existence of a positive periodic solution and for its global stability.

Theorem 4.5.1. *Let us assume that (4.1) admits a unique washout periodic solution* $(0, q_*, s_*)$ *and that* $\int_0^\omega [\mu(t, 0, q_*(t)) - D(t)]dt > 0$*. Then:*

a) System (4.1) admits a positive ω*-periodic solution*

b) If (4.1) admits a unique positive ω-periodic solution, then any solution approaches asymptotically to it.

Proof. From Theorem 4.4.5, (4.16) admits an ω-periodic solution (x^*, q^*) satisfying $x^*(t) > 0$, $q^*(t) \geq q_0$, and $x^*(t)q^*(t) \leq s_*(t)$ for all $t \in [0, \omega]$. Then, $(x^*, q^*, s_* - x^*q^*)$ is a positive ω-periodic solution of (4.1) and part a) is proved. For the part b), let us assume that (x^*, q^*, s^*) is the unique positive ω-periodic solution of (4.1). As in the proof of Theorem 4.4.5, we write $u = (x, q)$ and we consider the functions f_i, $i = 1, 2$ defined in (4.21). Consider the Kolmogorov non-autonomous system:

$$\frac{du_i}{dt} = u_i f_i(t, u, S(t)), \ i = 1, 2, \tag{4.23}$$

where $S(t)$ is the unique solution of (4.2) with $S(0) \geq u_1(0)u_2(0)$. Recalling the proof of Theorem 4.4.5, solutions of (4.22) and (4.23) exist for any initial condition on $\mathbb{R}_+$ and they are uniformly bounded. Let $\phi_0(t, s, u)$ and $\phi(t, s, u)$ be the unique solutions of (4.22) and (4.23) respectively with $\phi(s, s, u) = \phi_0(s, s, u) = u \in \mathbb{R}^2_+$. We note that for initial conditions on $\mathbb{R}_+ \times J$, (4.1) is equivalent to (4.23) (take $s(0) = S(0) - u_1(0)u_2(0)$), then we have to prove that $\lim_{t\to\infty} |\phi(t, 0, u) - (x^*(t), q^*(t))| = 0$ for any $u \in (0, \infty) \times J$. From Lemma 4.3.12, $\lim_{t\to\infty} |S(t) - s_*(t)| = 0$, and hence $\lim_{t\to\infty} |f(t, u, S(t)) - f(t, u, s_*(t))| = 0$. By Proposition 3.2 in [10], $\phi(t, s, u)$ is asymptotic to the ω-periodic semiflow $T(t) := \phi_0(t, 0, \cdot) : \mathbb{R}^2_+ \longrightarrow \mathbb{R}^2_+$, and hence $T_n(u) = \phi(n\omega, 0, u), n \geq 0$, is an asymptotically autonomous discrete dynamical process with limit discrete semiflow $\varphi^n : \mathbb{R}^2_+ \longrightarrow \mathbb{R}^2_+, n \geq 0$, where $\varphi = T(\omega)$ is the Poincaré map associated to (4.22). By Theorem 3.1

in [10], it remains to prove that $\lim_{n\to\infty} T_n(u) = u^* := (x^*(0), q^*(0))$ for any $u \in (0,\infty)\times J$. From Theorem 4.4.5, u^* is a globally attractive fixed point of φ in $(0,\infty]\times\mathbb{R}_+$. Thus, the only fixed points of φ are u^* and the washout $(0, q_*(0))$. By Theorem 2.4 in [10], the ω-limit of u is a fixed point of φ. By Lemma 2 with $n = 2$ in [8], we have:

$$\{u \in \mathbb{R}^2_+ ;\ \lim_{n\to\infty} T_n(u) = (0, q_*(0))\} \cap int(\mathbb{R}^2_+) = \phi.$$

Thus, $\lim_{n\to\infty} T_n(u) = u^*$ for any $u \in int(\mathbb{R}^2_+)$, which completes the proof. □

The following theorem gives conditions to ensure the uniqueness of positive ω-periodic solutions of (4.1).

Theorem 4.5.2. *Assume that:*

I) $\rho(t, q_0, s) > 0$ *for all* $t \in [0,\omega]$, $s > 0$,

II) for any $q > q_0$ *the function* $x \longmapsto \mu(t, x, q)$ *is strictly decreasing for some* $t \in [0,\omega]$, *and*

III) if there are $t' \geq 0, q' \geq q_0, s' \geq 0$ *such that* $\rho(t', q', s') > 0$, *then the function* $s \longmapsto \rho(t', q', s)$ *is strictly increasing.*

Then, (4.1) admits at most one ω*-periodic solution with positive* x*-component.*

Proof. Let $K := int(\mathbb{R}^2_+)$ and $\varphi : K \longrightarrow K$ be the Poincaré map associated to (4.20). We claim that for any fixed point $u \in K$ we have the following componentwise inequality:

$$\varphi(\alpha u) < \alpha\varphi(u), \text{ for all } \alpha \in (0,1). \tag{4.24}$$

Indeed, let u be a fixed point of φ and let $y(t) := \alpha\phi(t,u)$ with $\phi(t,u)$ the unique solution of (4.20) satisfying $\phi(t,0) = u$. We can easily verify that for all $, t \in [0,\omega], i = 1,2$:

$$\frac{dy_i(t)}{dt} = \alpha f_i(t, y_1(t)/\alpha, y_2(t)/\alpha) \leq f_i(t, y_1(t), y_2(t)). \tag{4.25}$$

Note that $y(t)/\alpha$ corresponds to an ω-periodic solution of (4.20), and consequently $(y_1(t)/\alpha, y_2(t)/y_1(t))$ corresponds to an ω-periodic solution of (4.16). From hypothesis I), we have that $y_2(t)/y_1(t) > q_0$ for all $t \in [0,\omega]$. Thus, from hypothesis II), for $i = 1$, the inequality in (4.25) is strict for some $t' \in [0,\omega]$. Again, since $y(t)/\alpha$ is an ω-periodic solution of (4.20), we have:

$$\int_0^\omega \rho(t, y_2(t)/y_1(t), s_*(t) - \alpha y_2(t)) = \int_0^\omega D(t)dt > 0,$$

from where there exists a interval of time $[t_1, t_2]$, $t_1 < t_2$ such that:

$$\rho(t, y_2(t)/y_1(t), s_*(t) - \alpha y_2(t)) > 0$$

for all $t \in [t_1, t_2]$. From hypothesis III), we conclude that for $i = 2$, the inequality in (4.25) is strict for some $t' \in [0,\omega]$. Thus, by a Kamke's Theorem argument, we have that $y(\omega) > \phi(\omega, \alpha u)$ i.e. $\alpha\varphi(\alpha) > \varphi(\alpha u)$. Thus, the claim is proved.

Now, let us assume that φ admits two different fixed points $u, v \in K$. From a Kamke's Theorem argument, it follows that φ is monotone. Thus, following the same arguments as in the proof of Lemma 2.3.1 in Chapter 2 in

[11], we obtain the existence of $\sigma > 0$ such that $u = \sigma v$. From Lemma 4.4.6 we can assume that $u \leq v$ (component-wise inequality). Therefore, $\sigma \in (0, 1)$. Thus, $u = \varphi(u) = \varphi(\sigma v) > \sigma\varphi(v) = \sigma v = u$, which is a contradiction. □

4.6 Application: Microalgae growth under phosphorus and light limitation.

Here we consider a periodic version of the light-limited Droop model proposed by Passarge and collaborators in [5] for describing microalgae growth under light and phosphorus limitation. The model reads:

$$\begin{aligned} dx/dt &= [\min\{\mu_I(t,x), \mu_P(q)\} - D]x, \\ dq/dt &= \rho(q,s) - \min\{\mu_I(t,x), \mu_P(q)\}\, q, \\ ds/dt &= D(s_{in} - s) - \rho(q,s)x. \end{aligned} \tag{4.26}$$

We assume that the nutrient supply s_{in} and the dilution rate D are constant and positive. $\mu_P(q) = \mu_{max}\left(1 - \frac{q_0}{q}\right)$ is the specific growth rate as described by Droop [2] under nutrient limitation, and $\mu_I(t,x) = \frac{1}{L}\int_0^L p(I(t,x,z))dz$ is the vertical average of the local specific growth rate $p(I) = \mu_{max}\frac{I}{K_I + I}$ when microalgae is only limited by light. $I(t,z,x)$ is the light intensity perceived by microalgae at a distance z from the surface of the culture vessel and is determined from the Lambert-Beer law:

$$I(t,x,z) = I_{in}(t)e^{-(kx + K_{bg})z}, \quad z \in [0, L], \tag{4.27}$$

with $I_{in}(t)$ the incident light intensity, $k > 0$ the specific light extinction coefficient of microalgae, and $K_{bg} \geq 0$ the background turbidity. A direct integration shows that:

$$\mu_I(t,x) = \frac{\mu_{max}}{(kx + K_{bg})L} \ln\left(\frac{K_I + I_{in}(t)}{K_I + I_{out}(t,x)}\right), \tag{4.28}$$

with $I_{out}(t,x) = I(t,x,L)$ the light intensity at the bottom of the culture. We consider that the incident light intensity varies periodically according to $I_{in}(t) = I_{max} \max\{0, \sin(2\pi t/\omega)\}^2$, with $\omega > 0$ the length of a day and I_{max} the maximal incident light (at midday). The uptake rate function is given by:

$$\rho(q,s) = \begin{cases} \rho_{max} \frac{s}{K_s+s} \frac{q_L - q}{q_L - q_0} & if \quad q \leq q_L, \\ 0 & if \quad q > q_L, \end{cases} \tag{4.29}$$

where ρ_{max} is the maximal uptake rate of phosphorus, q_L is the hypothetical maximal quota, and K_s is a half-saturation constant.

It is not difficult to see that (4.26) satisfies the Assumptions 4.3.1-4.3.8 presented in section 4.3 (see Appendix B for the properties of μ_I). Thus, we can apply Theorems 4.5.1 and 4.5.2 to obtain the following result.

Theorem 4.6.1. *Consider the system (4.26).*

a) There is a unique washout ω-periodic solution, $(0, q_*(t), s_{in})$.

b) If $\int_0^\omega \mu(t,0,q_*(t))dt > \int_0^\omega D(t)dt$, then (4.26) admits a unique positive ω-periodic solution $(x^*(t), q^*(t), s^*(t))$ and any solution to (4.26) with a positive initial population density approaches asymptotically to it.

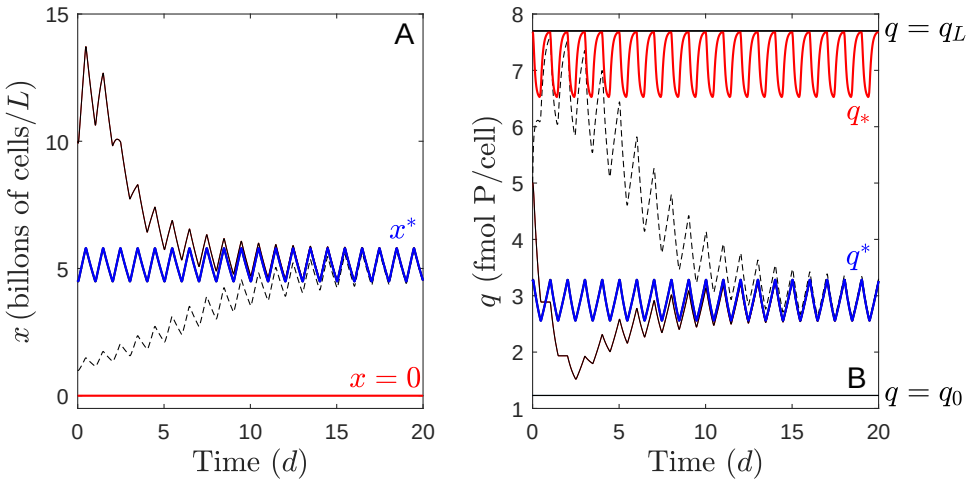

Figure 4.1: Periodic solutions of (4.26) and their stability. System (4.26) admits only two periodic solutions, the ω periodic solution represented by $x = 0$ and q_*, and a positive ω-periodic solution represented by $x^* > 0$ and q^*. Any solution starting with a positive microalgae concentration approaches the positive ω-periodic solution. In this case, x_1, q_1 and x_2, q_2 correspond to two different solutions of (4.26) with $x_1(0), x_2(0) > 0$ and $q_1(0) = q_2(0)$. We note that the cell quota remains between q_0 and q_L. A. Microalgae population density. B. Cell quota.

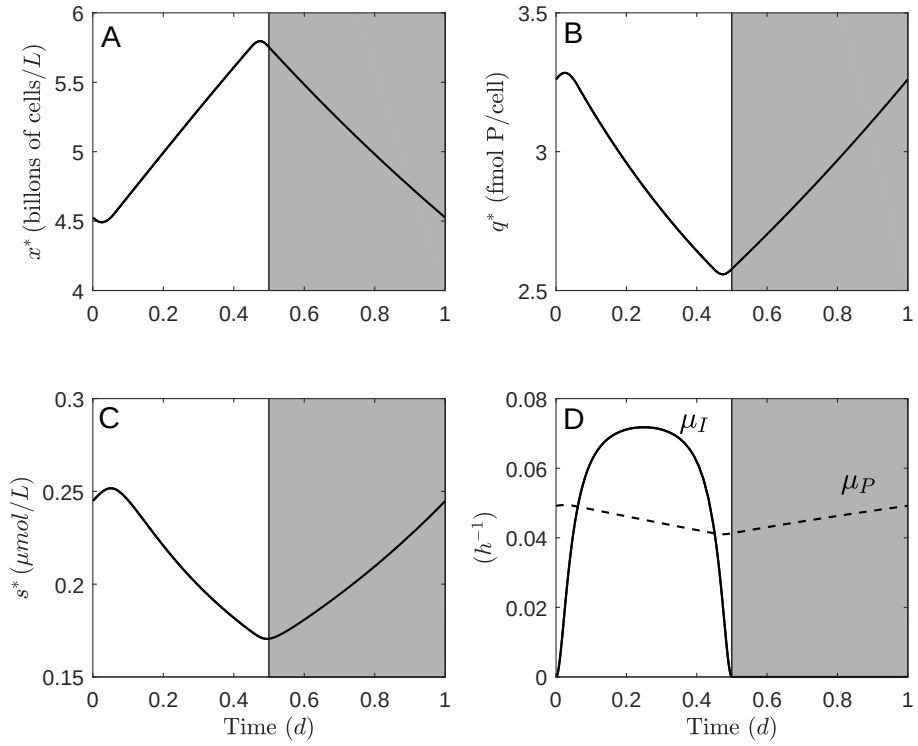

Figure 4.2: Unique positive periodic solution of (4.26). A. Population density. B. Intracellular phosphorus content. C. External phosphorus concentration. D. Light and phosphorus limitation.

Proof. We recall equation (4.14) to study the uniqueness of the washout. We note that $\int_0^\omega F_0(t, q(t))dt < 0$ for any function $q(t) \in [q_L, \infty)$. Thus, the quota associated to any washout must intersect the set $[q_0, q_L]$. Since $\mu(t, x, q) := \min\{\mu_I(t, x), \mu_P(q)\} \geq 0$, we have that $[q_0, q_L]$ is positively invariant with respect to (4.14). Thus, the quota associated to any washout stays on $[q_0, q_L]$. Since $q \longmapsto \rho(q, s_{in})$ is strictly decreasing on $[q_0, q_L]$, we have that $q \longmapsto F_0(t, q)/q$ is also strictly decreasing on $[q_0, q_L]$. This implies the uniqueness of the washout and part a) is proved.

We note that for any $q > q_0$ there is a $t' \in [0, \omega]$ such that $I_{in}(t') > 0$ and $\mu_I(t', x) \leq \mu_P(q)$ for all $x \geq 0$ i.e. $\mu(t, x, q) = \mu_I(t, x)$. Then we have that $x \longmapsto \mu(t', x, q)$ is strictly decreasing (see Proposition B10 in Appendix B). If we note that $s \longmapsto \rho(q, s)$ is strictly increasing for any $q \in [q_0, q_L]$ and that $\rho(q_0, s) > 0$ for any $s > 0$, from Theorem 4.5.2, we conclude that (4.1) admits at most one ω-periodic solution with positive x-component. Applying Theorem 4.5.1, we conclude the proof. □

To illustrate Theorem 4.6.1, let us consider the kinetic parameters for *Chlorella vulgaris* provided by Passarge [5]. The rest of parameters are chosen as $D = 0.02\, h^{-1}$, $K_{bg} = 6\, m^{-1}$, $s_{in} = 15\, \mu mol\, /L$, $L = 0.4\, m$, and $I_{max} = 2000\, \mu mol\, m^{-2}\, s^{-1}$. Figure 4.1 illustrates the microalgae population density and the cell quota associated to the periodic solutions of (4.26) and their attractiveness property. Figure 4.2 illustrates the positive periodic solution (x^*, q^*, s^*) and its evolution during one day. The shaded area corresponds to the night (i.e. $I_{in}(t) = 0$). Figure 4.2D shows that during the day ($t \in [0, 0.5]$) microalgae growth is mainly limited by phosphorus, while during the night

($t \in [0.5, 1]$), there is no growth due to the absence of light. Thus, microalgae population only grows during the day (see Figure 4.2A), and consequently the internal cell quota and external nutrient concentration decrease during the day (see Figures 4.2B and 4.2C).

4.7 Discussion and conclusions

In this work, we study the asymptotic behavior of a single microalgae model accounting for nutrient and light limitation. We found conditions such that prolonged continuous periodic culture operation (periodic dilution rate and nutrient supply) under periodic fluctuations of environmental conditions (such as the light source or the medium temperature) allows periodic concentrations to be maintained in the culture. More precisely, if (4.1) admits only one washout periodic solution $(0, q_*, s_*)$, then the following condition:

$$\int_0^\omega D(t)dt < \int_0^\omega \mu(t, 0, q_*(t))dt, \tag{4.30}$$

ensures the existence of a positive periodic solution. If this solution is the only one positive periodic solution, then it is globally stable (Theorem 4.5.1). The uniqueness of this positive periodic solution is assured under additional hypotheses over the monotony of the functions μ and ρ (Theorem 4.5.2).

As an application of our results, we gave sufficient conditions for the existence of a unique positive globally stable periodic solution for a periodic version of the model proposed by Passarge and collaborators [5]. In this model the growth rate is represented by the law of minimum. It is not diffi-

cult to obtain similar results if we describe the growth rate as a multiplicative function i.e. $\mu(t,x,q) = \mu_I(t,x)(1-q_0/q)$.

We conjecture that, under hypotheses of Section 4.3, if there is a unique washout $(0, q_*, s_*)$, then:

$$\textit{if } \int_0^\omega D(t)dt \geq \int_0^\omega \mu(t,0,q_*(t))dt, \textit{ then the washout is globally stable} \tag{4.31}$$

Following Proposition 4.4.3, the proof of the conjecture follows from proving that the limiting system (4.16) only admits the washout as periodic solution. Classical techniques based on the comparison method (see for example Proposition 1.3 in [6]) fail in our model because dq/dt is in general not monotone as a function of x in (4.16).

A possible extension of this work consist in allowing the function μ not to be monotone as a function of x. In [4] it is shown that when microalgae suffer from photoinhibiton (i.e. a decrease of the photosynthetic rate due to an excess of light), then an Allee effect may occurs i.e. μ in (4.1) is increasing as a function of x for small values of x. In such a case, the cooperativity of the limiting system (4.16) is not lost (see Remark 4.4.4). Thus, a similar result to Proposition 4.4.3 could be obtain for this new model.

Bibliography

[1] W. A. Coppel. *Stability and asymptotic behavior of differential equations*. Heath, 1965.

[2] M. R. Droop. Vitamin B 12 and marine ecology. iv. the kinetics of uptake, growth and inhibition in monochrysis lutheri. *Journal of the Marine Biological Association of the United Kingdom*, 48(3):689–733, 1968.

[3] J. Huisman, H. C. Matthijs, P. M. Visser, H. Balke, C. A. Sigon, J. Passarge, F. J. Weissing, and L. R. Mur. Principles of the light-limited chemostat: theory and ecological applications. *Antonie van Leeuwenhoek*, 81(1-4):117–133, 2002.

[4] C. Martínez, F. Mairet, and O. Bernard. Theory of turbid microalgae cultures. *Journal of theoretical biology*, 456:190–200, 2018.

[5] J. Passarge, S. Hol, M. Escher, and J. Huisman. Competition for nutrients and light: stable coexistence, alternative stable states, or competitive exclusion? *Ecological Monographs*, 76(1):57–72, 2006.

[6] H. Smith. The periodically forced Droop model for phytoplankton growth in a chemostat. *Journal of Mathematical Biology*, 35(5):545–556, 1997.

[7] H. L. Smith and P. Waltman. *The theory of the chemostat: dynamics of microbial competition*, volume 13. Cambridge university press, 1995.

[8] G. S. Wolkowicz and X.-Q. Zhao. n-species competition in a periodic chemostat. *Differential and Integral Equations*, 11(3):465–491, 1998.

[9] T. Yoshizawa. *Stability theory and the existence of periodic solutions and almost periodic solutions*, volume 14. Springer Science & Business Media, 1975.

[10] X.-Q. Zhao. Asymptotic behavior for asymptotically periodic semiflows with applications. *Communications on Applied Nonlinear Analysis*, 3(4):43–66, 1996.

[11] X.-Q. Zhao. *Dynamical systems in population biology.* CMS Books in Mathematics, 16. Springer, 2003.

CHAPTER 5

Co-limitation by light and substrate: Including photoinhibition.

Contents

5.1 Chapter presentation

This chapter relies on an article in preparation to be submitted to *Journal of Differential Equations*. Here, as in Chapter 4, we study the dynamics of a microalgae population when their growth is limited by light and substrate. The difference is that now, we do not consider periodic forcing but the effects of photoinhibition. As shown in Chapter 3 (see Figure 3.7), photoinhibition may result in an Allee effect i.e. the growth rate function is increasing for low population densities. Consequently, the assumptions over the monotony of the growth rate function in Chapter 4 (see Assumption 4.3.4) are now not satisfied. This makes the study of this new model a challenging task.

The main results of this chapter state conditions for the survival of the microalgae population independently of the initial population density, conditions for the extinction of the population, and conditions for the existence of a locally stable equilibrium characterized by the presence of microalgae. These results are mainly based on the theory of monotone dynamical systems and standard results of the theory of differential equations. With the help of numerical computation, in the last part of this chapter, we give a complete description of the dynamics of the population.

Martínez, C., Mairet, F.,& Bernard, O. (2019). *Effects of photo-inhibition on the dynamics of the light-limited Droop model. Journal of Differential Equations*

Abstract : *We study the asymptotic behavior of the light-limited Droop model when microalgae may face photoinhibition. We consider general assumptions over the growth rate and the uptake rate functions. In particular, the growth rate considers Allee effect due to photoinhibition. Thus, the growth rate reaches its maximum at a certain optimal population density. We prove that solutions of the model approach asymptotically to a single point and we find the existence of three dilution rates: a dilution rate characterizing the persistence of the population, a dilution rate characterizing the existence of equilibria with a population density higher than the optimal population density, and a dilution rate leading the system to the washout. Finally, with the help of numerical computation, we construct a bifurcation diagram with respect to the dilution rate. Our approach involves monotone dynamical systems and standard results from the theory of differential equations.*

5.2 Introduction

We study the asymptotic behavior of an autonomous version of the light-limited Droop model presented in Chapter 4 (see the model (4.1)). This new version do not consider periodic forcing but photoinhibition i.e. a decrease of the growth rate due to high light intensities. Thus, following Chapter 3 (see Figure 3.7), the growth rate function (averaged over depth) may have a peak at a certain positive optimal population density. This makes more challenging the study of the light-limited Droop model.

Under light-limitation, previously in [4], it was shown that under high light intensities, the population may face bi-stability. That is, at low density, the population may go extinct, and above a threshold population density the population can establish itself. In the case of co-limitation by light and substrate, to the best of our knowledge, there is only one theoretical study on the dynamics of microalgae populations [6]. This study does not consider inhibition by light and proves that if the model admits a positive equilibrium, then this equilibrium is globally stable.

This chapter is organized as follows. In Section 5.3 we describe the model to be studied. In Section 5.4, we show that any solution of the model converges towards a single point, and we give conditions to ensure that this single point does not correspond to the extinction of the population. In Section 5.5, we study in more details the existence of non-trivial single points. First, we give necessary conditions over the dilution rate for the existence

of non-trivial equilibria. Then, we give necessary and sufficient conditions for the existence of an equilibrium with a population density higher than or equal to the optimal population density, which is locally stable if it is unique. In Section 5.6, we determine numerically the number of steady states of the model and we describe their stability with a bifurcation diagram.

5.3 Model description

We consider the following autonomous version of the light-limited Droop model (4.1):

$$\begin{aligned} \frac{dx}{dt} &= [\mu(x,q) - D]x \\ \frac{dq}{dt} &= \rho(q,s) - \mu(x,q)q \\ \frac{ds}{dt} &= D(s_{in} - s) - \rho(q,s)x. \end{aligned} \tag{5.1}$$

Here, as usually, x stands for the microalgae population density, q for the internal cell quota, and s for the external nutrient concentration. $D > 0$ is the dilution rate and s_{in} is the nutrient supply concentration. The functions $\mu : \mathbb{R}_+ \times [q_0, \infty) \longrightarrow \mathbb{R}$ and $\rho : [q_0, \infty) \times \mathbb{R}_+ \longrightarrow \mathbb{R}_+$ represent the specific growth rate and the uptake rate respectively.

We assume that microalgae may suffer from photoinhibition. Thus, following Chapter 3, there may be the occurrence of an Allee effect i.e. the growth rate increases with low microalgae concentrations reaching a maximal value at certain microalgae concentration. In Chapter 3 (or see Proposition A2d) in Appendix A), it was also shown that in a very high dense culture, microalgae grow similarly as in absence of light i.e. their growth

rate equals the loss rate for high microalgae concentrations. Figure 5.1A illustrates these properties of μ as a function of x (see also Figure 3.7). The following assumption formally states these properties of μ.

Assumption 5.3.1. *There exists $\tilde{x} \geq 0$, $r \geq 0$, and $q_0 > 0$ such that for any $q \geq q_0$ the function $x \to \mu(x, q)$ is increasing on $[0, \tilde{x}]$ and decreasing on $[\tilde{x}, \infty)$, $\lim_{x\to\infty} \mu(x, q) = -r$ for any $q \geq q_0$, and $\mu(x, q_0) = -r$ for any $x \geq 0$.*

Note that q_0 in 5.3.1 corresponds to the minimal quota for existence. According to Droop model, microalgae growth is only possible when the cell quota q is higher than q_0. The following assumption describes the monotony of μ as a function of q.

Assumption 5.3.2. *For any $x \geq 0$, the function $q \longmapsto \mu(x, q)$ is increasing on $[q_0, \infty)$.*

The following two assumptions describes the monotony properties of ρ. They are mainly based on the classical uptake rate model presented in Chapter 2 (see (2.20)).

Assumption 5.3.3. *There exists q_L such that for any s the function $q \longmapsto \rho(q, s)$ is strictly decreasing on $[q_0, q_L]$ and $\rho(q, s) = 0$ for all $q \in [q_L, \infty)$.*

Assumption 5.3.4. *For any $q \in [q_0, q_L)$, the function $s \longmapsto \rho(q, s)$ is strictly increasing.*

The quota q_L corresponds to the theoretical maximal quota. The following assumption states that microalgae can grow for a quota q_L (Assumption 4.3.8 in Chapter 4 is a general version).

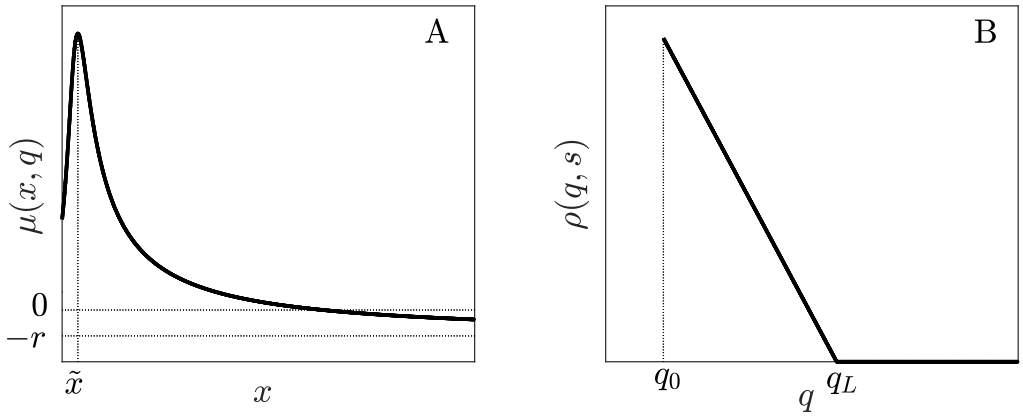

Figure 5.1: A. Plot of μ as a function of x. B. Plot of ρ as a function of q.

Assumption 5.3.5. $\mu(0, q_L) > 0$.

The following and last assumption states that we only need differentiability when $q \in [q_0, q_L]$. Later (Lemma 5.4.3) it is shown that in long-term the quota stays in this interval. Thus, for studying the asymptotic behavior of (5.1) we only need differentiability in that interval.

Assumption 5.3.6. *μ and ρ are continuously differentiable on* $[0, \infty) \times [q_0, q_L]$.

5.4 Basic properties and persistence.

Our first lemma states the existence of only one washout steady state.

Lemma 5.4.1. *There is only one washout steady state* $E_* = (0, q_*, s_{in})$ *with* $q_* \in (q_0, q_L)$.

Proof. We have to study the zeros of the function $h(q) = \rho(q, s_{in})/q - \mu(0, q)$. We have that $h(q_0) = \rho(q_0, s_{in})/q_0 + r > 0$ and $h(q) = -\mu(0, q) < 0$ for all $q \in [q_L, \infty)$. This shows that there exist $q_* \in (q_0, q_L)$ such that $h(q_*) = 0$. Now we note that h is strictly decreasing on (q_0, q_L), from where we have the uniqueness of q_*. □

Following the same ideas in Proof of Lemma 4.3.16 in Chapter 4, it can be proved the following lemma.

Lemma 5.4.2. *System (5.1) is dissipative.*

Proof. See Proof of Lemma 4.3.16. □

We define the internal stored nutrient $x_s := xq$ and the total amount of nutrient S in the reactor including both external nutrient s and stored nutrient x_s i.e. $S := x_s + s$. By combining the first two equations in (5.1) we obtain that:

$$\frac{dx_s}{dt} = \rho(q, s)x - Dx_s. \tag{5.2}$$

This equation shows that x_s only varies with the uptake of nutrient from the medium by microalgae and with the dilution rate of the system. Combining (5.2) with the last equation in (5.1), we obtain that:

$$\frac{dS}{dt} = D(s_{in} - S). \tag{5.3}$$

This equation shows that S converges to s_{in} as t goes to infinity. It is therefore natural to take advantage of the fact that the solutions of (5.1) approach the surface $s_{in} = s + xq$ by dropping the equation for s and replacing s in (5.1)

by $s_{in} - xq$ in the second equation. This results in the following reduced two-dimensional system:

$$\begin{array}{rcll} \dfrac{dx}{dt} & = & f(x,q) & := [\mu(x,q) - D]x \\ \dfrac{dq}{dt} & = & g(x,q) & := \rho(q, s_{in} - xq) - \mu(x,q)q \end{array} \tag{5.4}$$

The following result is related to the reduced system.

Lemma 5.4.3. *For any solution (x,q) of (5.4), there exists $T > 0$ such that $q(t) \in (q_0, q_L)$ for all $t \geq T$*

Proof. According to Poincaré -Bendixson Theorem, $(x(t), q(t))$ approaches to an equilibrium point or to a positive periodic solution of (5.4). It is clear that the quota in any equilibrium cannot be higher than q_L. Thus, it is enough to prove that for any positive periodic solution the quota stays on (q_0, q_L). Let (x_p, q_p) be a positive periodic solution and let $\omega > 0$ be its period. By contradiction, let us assume that $q_p(t) \geq q_L$ for some $t > 0$. Let $t_q, t_x \in [0, \omega]$ be such that $q_p(t_q) = \max_{t\in[0,\omega]} q_p(t)$ and $x_p(t_x) = \max_{t\in[0,\omega]} x_p(t)$. Since μ is increasing in q, we have that:

$$\frac{dx_p}{dt} \leq F(x_p) = [\mu(x_p, q_p(t_q)) - D]x_p, \text{ for all } t \geq 0. \tag{5.5}$$

Let y be the unique solution of the differential equation:

$$\frac{dy}{dt} = F(y), \tag{5.6}$$

satisfying $y(t_q) = x_p(t_q)$. Then, by a comparison argument, $x_p(t) \leq y(t)$ for

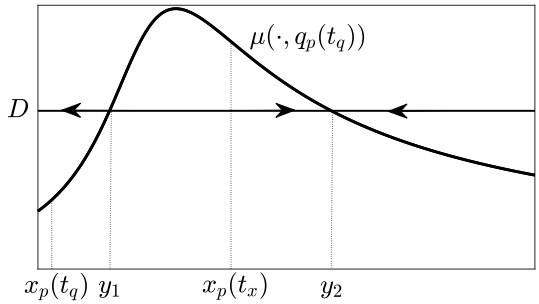

Figure 5.2: Function $y \longmapsto \mu(y, q_p(t_q))$ and illustration of the dynamics of (5.6)

all $t \geq t_q$. Since $\frac{dx_p(t_x)}{dt} = 0$, we have that:

$$D = \mu(x_p(t_x), q_p(t_x)) \leq \mu(x_p(t_x), q_p(t_q)), \tag{5.7}$$

and since $\frac{q_p(t_q)}{dt} = 0$ and $q_p(t_q) \geq q_L$, we have that $\mu(x_p(t_q), q_p(t_q)) = 0 < D$. We note that if $\mu(0, q_p(t_q)) \geq D$, then $x_p(t_x) < x_p(t_q)$, which is a contradiction. Then we have $\mu(0, q_p(t_q)) < D$. Let $y_1 := \max\{y \geq 0\,;\, \mu(y, q_p(t_q)) < D\}$. Since $x_p(t_x) > y(t_q)$ and $\mu(y(t_q), q_p(t_q)) < D$, we conclude that $y(t_q) < y_1$ (see Fig. 5.2). This implies that $y(t) \to 0$ as $t \to \infty$. Thus, $x_p = 0$ which contradicts the positiveness of x_p. Thus, $q_p(t) < q_L$ for all $t \in [0, \omega]$. □

The following result shows that (5.1) does not admit any limit cycle. This result follows from the Theory of Monotone Dynamical systems [5].

Lemma 5.4.4. *Any solution to (5.1) converges toward a single point.*

Proof. We note that:

$$\rho(q, S(t) - xq) \to \rho(q, s_{in}) \quad \text{as} \quad t \to \infty, \text{ uniformly in } (x, q).$$

Thus, according to the convergence Theorem 1.2 in [7], it is enough to prove that any solution to (5.4) converges toward a single point. Following Poincaré -Bendixson Theorem, this is equivalent to show the non-existence of non-trivial periodic solutions. By contradiction, let us assume that (5.4) admits a non-constant periodic solution (x_p, q_p) with $x_p(t) > 0$ for all $t \geq 0$. From Lemma 5.4.3, we know that $\bar{q}(t) \in (q_0, q_L)$ for all $t > 0$. Let us define $x_{sp} = x_p q_p$. We note that (x_p, x_{sp}) is a solution of the following system:

$$\begin{aligned} \frac{dx}{dt} &= f_1(x, x_s) := [\mu(x, x_s/x) - D]x \\ \frac{dx_s}{dt} &= f_2(x, x_s) := \rho(x_s/x, s_{in} - x_s)x - Dx_s. \end{aligned} \tag{5.8}$$

System (5.8) is cooperative on $\Omega := (0, \infty) \times (q_0, q_L)$, i.e.:

$$\frac{\partial f_1}{\partial x_s}, \frac{\partial f_2}{\partial x} \geq 0 \text{ on } \Omega.$$

From Theorem 3.22 in [5], there exists t^* such that $x_p(t)$ and $x_{sp}(t)$ are monotone on the interval $[t^*, \infty)$. Since a monotone periodic function is necessarily constant, we conclude that (x_p, x_{sp}) is constant, which is a contradiction. Consequently, (5.4) does not admit non-constant periodic solutions and any solution to (5.4) approaches a single point. □

The following theorem shows that the growth rate evaluated at the washout quota defines the dilution rate at which the population persists.

Theorem 5.4.5. *Let $E_* = (0, q_*, s_{in})$ be the washout given by Lemma 5.4.1 and let us define $D_* := \mu(0, q_*)$.*

a) If $D < D_*$, any solution (x, q, s) of (5.1) starting with $x(0) > 0$ converges towards a positive steady state.

b) If $D > D_*$, then E_* is locally stable.

Proof. At the washout steady state, the Jacobian matrix associated to the system (5.4) takes the form:

$$J = \begin{pmatrix} D_* - D & 0 & 0 \\ -q_* \dfrac{\partial \mu(0, q_*)}{\partial x} & a & \dfrac{\partial \rho(q_*, s_{in})}{\partial s} \\ -\rho(s_{in}, q_*) & 0 & -D \end{pmatrix}$$

with

$$a = \frac{\partial \rho(q_*, s_{in})}{\partial q} - D_* - q_* \frac{\partial \mu(0, q_*)}{\partial q}$$

Thus, the eigenvalues of J are $\lambda_1 = D_* - D$, $\lambda_2 = a$, and $\lambda_3 = -D$. If $D > D_*$, it is clear that all the eigenvalues are negative. Thus, E_* is locally stable and the part b) is proved. For the part a), we define $X_0 := \{0\} \times \mathbb{R}^2_+$ and $W^s(\{E_*\})$ be as the stable manifold of $\{E_*\}$. Since $\lambda_1 > 0$, and $\lambda_2, \lambda_3 < 0$, we have that $W^s(\{E_*\})$ is a locally manifold of dimension 2. Since X_0 has dimension 2, we conclude that $W^s(\{E_*\}) \subset X_0$. Thus any solution (x, q, s) of (5.1) starting with $x(0) > 0$ converges towards a single point different from the washout E_0. □

5.5 Existence of non-trivial steady states

In the following, we study the existence of nontrivial equilibria i.e. the existence of solutions of the algebraic system:

$$\begin{array}{rcl} \mu(x,q) & = & D \\ \frac{\rho(q,s_{in}-xq)}{q} & = & \mu(x,q) \end{array} \tag{5.9}$$

Combining both equations in (5.9) we obtain that:

$$\frac{\rho(q, s_{in} - xq)}{q} = D. \tag{5.10}$$

The following lemma gives necessary conditions for the existence of non-trivial equilibria.

Lemma 5.5.1. *Let $q_m \in (q_0, q_L)$ be defined by means of:*

$$\frac{\rho(q_m, s_{in})}{q_m} = \mu(\tilde{x}, q_m), \tag{5.11}$$

and let us define $D_m = \mu(\tilde{x}, q_m)$. If $D > D_m$ then (5.1) only admits the washout as equilibrium.

Proof. In any equilibrium the nutrient concentration $s = s_{in} - xq$ cannot be higher than s_{in} (there is no production of nutrient in the system). Since ρ is strictly increasing in s and strictly decreasing in q, the maximal value on the left side in (5.10) is $\rho(q_0, s_{in})/q_0$. Thus, if $\rho(q_0, s_{in})/q_0 < D$, the equation (5.10) is never satisfied. If $\rho(q_0, s_{in})/q_0 = D$, then the equation (5.10) is only satisfied when $q = q_0$ and $s = s_{in}$. However, in those conditions the first equation in (5.9) is not satisfied. Then, a necessary condition for the existence of a non-trivial equilibrium is:

$$\frac{\rho(q_0, s_{in})}{q_0} > D. \tag{5.12}$$

Assume that (5.12) holds, and let us define $q_{in} = q_{in}(D)$ by means of the following equation:

$$\frac{\rho(q_{in}, s_{in})}{q_{in}} = D. \tag{5.13}$$

The value of q_{in} is an upper bound for the quota of any non-trivial equilibrium. Indeed, let $E = (x_e, q_e, s_e)$ be a non-trivial equilibrium. Then $s_e := s_{in} - x_e q_e < s_{in}$, which implies:

$$\frac{\rho(q_{in}, s_{in})}{q_{in}} = D = \frac{\rho(q_e, s_e)}{q_e} < \frac{\rho(q_e, s_{in})}{q_e},$$

from where $q_e < q_{in}$. Thus, we have the following necessary condition for the existence of a non-trivial equilibrium:

$$\mu(\tilde{x}, q_{in}) \geq D \ (= \mu(x_e, q_e)). \tag{5.14}$$

Let $D_0 = \frac{\rho(q_0, s_{in})}{q_0}$ and let $g : (0, D_0) \longrightarrow \mathbb{R}$ be the function defined by $g(d) = \mu(\tilde{x}, q_{in}(d)) - d$. The function g is strictly decreasing,

$$\lim_{d \to 0^+} g(d) = \mu(\tilde{x}, q_L) \geq \mu(0, q_L) > 0,$$

and

$$\lim_{d \to D_0^-} g(d) = \mu(\tilde{x}, q_0) - D_0 = -(r + D_0) < 0.$$

This implies that there exists a unique $D' \in (0, D_0)$ such that $g(D') = 0$. By using the definition of $q_{in}(D')$ and the definition of D', we conclude that $\frac{\rho(q_{in}(D'), s_{in})}{q_{in}(D')} = \mu(\tilde{x}, q_{in}(D'))$, which implies that $q_m = q_{in}(D')$ and $D_m = D'$. Now, it remains to prove that the inequalities (5.12) and (5.14) imply $D \leq$

D_m. This follows directly from noting that if (5.14) holds, then $g(D) \geq 0$.

□

Remark 5.5.2. *If $\tilde{x} = 0$, then q_m in Lemma 5.5.1 is the quota associated to the washout of (5.1) and consequently D_m corresponds to D_* defined in Theorem 5.4.5. Moreover, if $q \longmapsto \mu(\tilde{x}, q)$ is strictly increasing, then the necessary condition can be changed by $D \geq D_m$. This follows from the fact that inequality (5.14) is now strict.*

The following result gives necessary and sufficient conditions for the existence of an equilibrium with a population density higher than or equal to $\tilde{x}$.

Lemma 5.5.3. *Assume that $\tilde{x} > 0$ and let $q_r \in [q_0, q_L]$ be defined by $\mu(\tilde{x}, q_r) = 0$. Let us define $\tilde{q}$ in the following way:*

a) if $s_{in} \leq \tilde{x} q_r$, then $\tilde{q} = q_r$,

b) if $s_{in} > \tilde{x} q_r$, then $\tilde{q} \in (q_r, s_{in}/\tilde{x})$ is the unique solution of the following equation for q:

$$\frac{\rho(q, s_{in} - \tilde{x} q)}{q} = \mu(\tilde{x}, q). \tag{5.15}$$

Now let us define $\tilde{D} = \mu(\tilde{x}, \tilde{q})$. Then (5.1) admits an equilibrium (x_e, q_e, s_e) with $x_e \geq \tilde{x}$ if, and only if, $\tilde{D} > 0$ (i.e. $s_{in} > \tilde{x} q_r$) and $D \leq \tilde{D}$.

Proof. First we show that $\tilde{q}$ and $\tilde{D}$ are well defined. If $s_{in} \leq \tilde{x} q$, then $\tilde{q} = q_r$ and consequently $\tilde{D} = 0$. If $s_{in} > \tilde{x} q$, we have to show that the function $\tilde{f}(q) = \rho(q, s_{in} - \tilde{x} q)/q - \mu(\tilde{x}, q)$ admits a unique zero on the interval $[q_0, q_L]$. This follows directly from noting that $\tilde{f}$ is strictly decreasing, $\tilde{f}(q_r) > 0$, and

$\tilde{f}(q') = -\mu(\tilde{x}, q') < 0$ with $q' := \min\{q_L, s_{in}/\tilde{x}\}$.

Let q_m and D_m the quota and the dilution rate defined in Lemma 5.5.1. Since q_m is the unique zero of $f_m(q) = \rho(q, s_{in})/q - \mu(\tilde{x}, q)$ and $\tilde{f}(q) < f_m(q)$ for all q, we conclude that $\tilde{q} < q_m$. This implies $\tilde{D} < D_m$. Thus, without loss of generality, we can assume that $D \leq D_m$ (If $D > D_m$, then the washout is the unique equilibrium of the system (5.1)).

Since $D \leq D_m$, we have that $\rho(q_0, s_{in})/q_0 > D$ (see Proof of Lemma 5.5.1). We define $s_0 \in (0, s_{in})$ by means of $\rho(q_0, s_0)/q_0 = D$, and we define q_{in} by means of $\rho(q_{in}, s_{in})/q_{in} = D$. Then, we define the function $f_q : [s_0, s_{in}] \longrightarrow [q_0, q_{in}]$ by means of $\rho(f_q(s), s)/f_q(s) = D$. We note that $f_q(s_0) = q_0$, $f_q(s_{in}) = q_{in}$, and that f_q is strictly increasing. As argued in Proof of Lemma 5.5.1, q_{in} is an upper bound of the quota associated to any equilibrium of (5.1). Now, let q' be such that $\mu(\tilde{x}, q') = D$. It is easy to see that q' is a lower bound for the quota of any equilibrium of (5.1). We define then the function $f_x : [q', q_{in}] \longrightarrow [\tilde{x}, \infty)$ with $f_x(q)$ the minimal solution of the equation for x: $\mu(x, q) = D$. We note that $f_x(s') = \tilde{x}$ and that f_x is strictly increasing. Now, the substrate associated to any equilibrium on the set $\Omega := \{(x_e, q_e, s_e); x_e \geq \tilde{x}\}$ must be a zero of the function $h : [s', s_{in}] \longrightarrow \mathbb{R}$ with $h(s) := s_{in} - s - f_x(f_q(s))f_q(s)$ and s' defined by $\rho(q', s')/q' = D$. We note that $h(s_{in}) < 0$ and that h is strictly decreasing. Thus, it remains to prove that $D \leq \tilde{D}$ is equivalent to $h(s') = s_{in} - s' - q'\tilde{x} \geq 0$.

Let us define $f : (0, D_m) \longrightarrow \mathbb{R}$ by means of $f(D) = s_{in} - s'(D) - \tilde{x}q'(D)$.

The function f is strictly decreasing, and we have:

$$\lim_{D\to 0^+} f(D) = s_{in} - \tilde{x}q_r, \text{ and } \lim_{D\to D_m^-} f(D) = -\tilde{x}q_m < 0. \tag{5.16}$$

Thus, if $s_{in} - \tilde{x}q_r \leq 0$, then $f(D) < 0$ for all $D \in (0, D_m)$ and consequently $h(s') < 0$. Thus, $\Omega = \phi$. If $s_{in} - \tilde{x}q_r > 0$, then there exists $D' \in (0, D_m)$ such that $f(D') = 0$. Now we have to prove that $D' = \tilde{D}$ to conclude the proof. From the definitions of n', q', and D' we have that $\frac{\rho(q'(D'), s_{in} - \tilde{x}q'(D'))}{q'(D')} = \mu(\tilde{x}, q'(D'))$, which implies $\tilde{q} = q'(D')$ and $\tilde{D} = D'$. □

The following proposition considers the case when μ is strictly decreasing as a function of x on the interval $[\tilde{x}, \infty)$.

Proposition 5.5.4. *Assume that the function $x \longmapsto \mu(x, q)$ is strictly decreasing on $[\tilde{x}, \infty)$ and that $\tilde{D} > 0$. Then for any $D \leq \tilde{D}$, there exists a unique equilibrium $E = (x_e, q_e, s_e)$ with $x_e \geq \tilde{x}$. Moreover, E is locally stable.*

Proof. The existence of E is given by Lemma 5.5.3. For the uniqueness, let us assume that there is another equilibrium $E' = (x'_e, q'_e, s'_e)$ with $\tilde{x} \leq x'_e$. We can assume that $x'_e > x_e$. Since $\mu(x'_e, q_e) < \mu(x_e, q_e) = D$, we conclude that $q'_e > q_e$. This implies that

$$D = \frac{\rho(q_e, s_{in} - x_e q_e)}{q_e} < \frac{\rho(q'_e, s_{in} - x'_e q'_e)}{q'_e} = D, \tag{5.17}$$

which is a contradiction.

To determine the local stability of E, we evaluate the Jacobian matrix associated to the system (5.4) at (x_e, q_e):

$$J = \begin{pmatrix} x_e \frac{\partial \mu(x_e,q_e)}{\partial x} & x_e \frac{\partial \mu(x_e,q_e)}{\partial q} \\ c & d \end{pmatrix},$$

with

$$c = -q_e \frac{\partial \rho(q_e, s_{in})}{\partial s} - q_e \frac{\partial \mu(x_e, q_e)}{\partial q}$$

and

$$d = \frac{\partial \rho(q_e, s_{in})}{\partial q} - x_e \frac{\partial \rho(q_e, s_{in})}{\partial s} - \mu(x_e, q_e) - q_e \frac{\partial \mu(x_e, q_e)}{\partial q}.$$

It is not difficult to see that the trace and the determinant of J are negative and positive respectively. Thus, the eigenvalues of J have a negative real part. Hence, E is locally stable. □

The following proposition gives a threshold result on the dynamics of (5.1) when $\tilde{x} = 0$.

Proposition 5.5.5. *Assume that $\tilde{x} = 0$ and that the function $x \longmapsto \mu(x, q)$ is strictly decreasing on $[0, \infty)$. Let D_* given in Theorem 5.4.5.*

a) if $D < D_*$, then (5.1) admits only one equilibrium $E = (x_e, q_e, s_e)$ with $x_e > 0$ and any solution (x, q, s) to (5.1) with $x(0) > 0$ converges to E.

b) if $D \geq D_*$, then (5.1) only has the washout E_0 as equilibrium which is globally stable.

Proof. By similar arguments to those given in the proof of Proposition 5.5.4, (5.1) admits at most one steady state with a positive population density.

From Theorem 5.4.5 and Lemma 5.5.1, it remains to prove that when $D = D_*$, (5.1) admits only the washout as equilibrium . By contradiction, let us assume that there exists an equilibrium $E = (x_e, q_e, s_e)$ with $x_e > 0$. Since $\tilde{x} = 0$, we have that $x \longmapsto \mu(x, q)$ is decreasing on $[0, \infty)$. Then, from the definition of D_* we have that:

$$\mu(x_e, q_*) \leq \mu(0, q_*) = D = \mu(x_e, q_e),$$

from where $q_* \leq q_e$. Similarly, from the definition of q_* and E we have:

$$\frac{\rho(q_*, s_{in})}{q_*} = D = \frac{\rho(q_e, s_{in} - x_e q_e)}{q_e} < \frac{\rho(q_e, s_{in})}{q_e}.$$

Since the function $q \longmapsto \rho(q, s_{in})/q$ is strictly decreasing, we conclude that $q_* > q_e$ which is a contradiction. □

5.6 Numerical study of the steady states.

In this section, we study numerically the existence of steady states of (5.1) and their stability. For this purpose, we consider the following growth rate function:

$$\mu(x, q) = \left(1 - \frac{q_0}{q}\right) \mu_I(x) - r, \quad \mu_I(x) = \frac{1}{L} \int_0^L p(I_{in} e^{-axz}),$$

with $p(I) = p_{max} \frac{I}{I + \frac{\mu_{max}}{\alpha} \left(\frac{I}{I^*} - 1\right)^2}$, and we consider the following uptake rate function:

$$\rho(q, s) = \begin{cases} \rho_{max} \frac{s}{K_s + s} \frac{q_L - q}{q_L - q_0} & if \quad q \leq q_L, \\ 0 & if \quad q > q_L, \end{cases}$$

The growth rate is motivated by the model presented in [2] for describing the growth of microalgae under co-limitation by light and nitrogen. The kinetic parameters are given in Table 5.1.

Table 5.1: Kinetic parameters

Parameter	Value	Unit	Reference
p_{max}	1.63	d^{-1}	[8]
I^*	90	$\mu mol\, m^{-2}\, s^{-1}$	[8]
α	0.027	$\mu mol^{-1}\, m^2\, s\, d^{-1}$	[8]
a	0.2	$m^2\, gC^{-1}$	[1]
ρ_{max}	11.2	$gN\, gC^{-1}\, d^{-1}$	[3]
q_L	0.28	$gN\, gC^{-1}$	[3]
q_0	0.07	$gN\, gC^{-1}$	[3]
K_s	15	$gN\, m^{-3}$	[3]
r	0.1	d^{-1}	-

To illustrate the number of steady states, we note that they correspond to the intercepts of the following two curves:

$$\Gamma_1 := \{(x, q)\,;\, \mu(x, q)q = \rho(q, n_{in} - xq)\}, \tag{5.18}$$

and

$$\Gamma_2(D) := \{(x, q)\,;\, D = \mu(q, x)\}. \tag{5.19}$$

Thus, plotting Γ_1 and $\Gamma_2(D)$ for different values of the dilution rate, we can determine the quantity of steady states. It can be verified that $\Gamma_2(D) := \{(x, q)\,;\, q = q_0/(1 - (D + r)/\mu_I(x))\}$. Thus, Γ_2 moves in the positive sens of q as D increases. Therefore, we only need some representatives values of D to have a global idea of the existence of steady states. We choose the

following four values of the dilution rate: D_* (defined in Theorem 5.4.5), $\tilde{D}$ (defined in Lemma 5.5.3), D_m (defined in Lemma 5.5.1), and D^* that is the highest dilution rate at which there is a positive steady state. To determine the local stability, we evaluate the Jacobian matrix associated to (5.1).

We consider three different cases that are defined by the values of the nutrient supply s_{in} and the incident light intensity I_{in}.

Table 5.2: Representative dilution rates.

Dilution rate	Case 1	Case 2	Case 3
$D_*\,(d^{-1})$	0.8533	0.2365	0.2362
$\tilde{D}\,(d^{-1})$	–	0.3981	0.0702
$D^*\,(d^{-1})$	0.8533	0.5235	0.3893
$D_m\,(d^{-1})$	0.8533	0.7643	0.7619

Case 1: $s_{in} = 15gN/m^3$ and $I_{in} = 90\mu mol\, m^{-2}\, s^{-1}$. In this case $I_{in} = I^*$, and $\tilde{x} = 0$. Thus, the asymptotic behavior is completely described by Proposition 5.5.4. The value of D_* is given in Table 5.2.

Case 2: $s_{in} = 15gN/m^3$ and $I_{in} = 500\mu mol\, m^{-2}\, s^{-1}$. In this case $I_{in} > I^*$ and $\tilde{x} > 0$. Figure 5.3A shows the intercept of Γ_1 with $\Gamma_2(D)$ for different values of D given in Table 5.2. If $D \leq D_*$ or $D = D^*$, there is only one positive steady state. For $D \in (D_*, D^*)$ there are exactly two positive steady states. As stated in Proposition 5.5.4, for $D \leq \tilde{D}$ there is a steady state with a population equal to or higher than $\tilde{x}$. To illustrate the stability of the steady states of the system, Figure 5.3B shows a bifurcation diagram of the population density with respect to the dilution rate and Figure 5.4 shows a diagram phase of the reduced system (5.4). For $D < D_*$ there is only

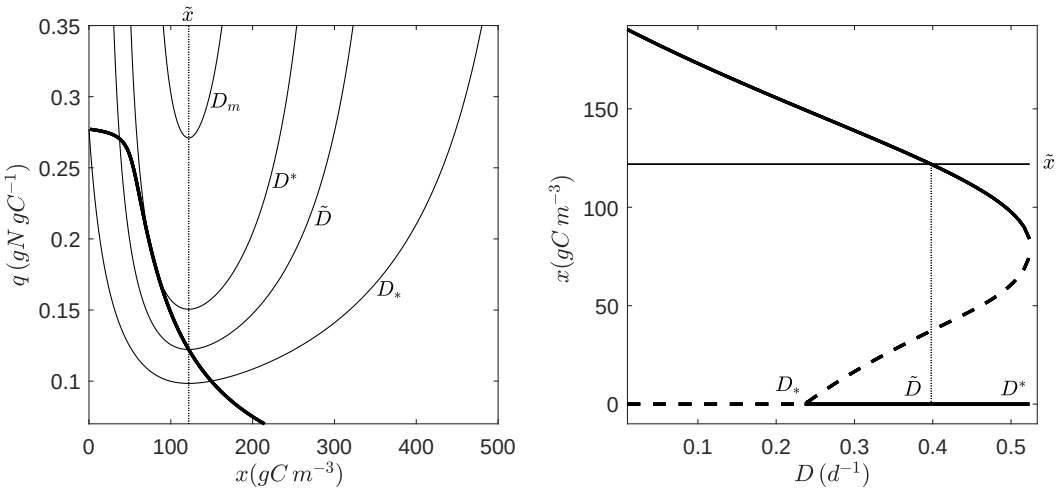

Figure 5.3: A. Intercepts of Γ_1 and $\Gamma_2(D)$ for different dilution rates in the case 2. The bold line corresponds to Γ_1. B. Bifurcation diagram of x with respect to D.

one positive steady state which is globally stable (see Theorem 5.4.5). For $D = D_*$, the unique positive equilibrium is locally stable while the washout is a non-hyperbolic equilibrium. Figure 5.4 suggest that an attracting region for the washout only exists when two positive steady states exists. Thus, the washout should be unstable. For $D \in (D_*, D^*)$ there are two positive steady states, one locally stable and one locally unstable. In this case, the washout is locally stable. From Proposition 5.5.4, we already know that for $D \leq \tilde{D}$ there is a locally stable non-trivial steady state. Finally, for $D = D^*$, the unique positive equilibrium is non-hyperbolic and the washout is locally stable. Figure 5.4 shows the existence of a region that is attracted by the positive steady state.

Case 3: $s_{in} = 10gN/m^3$ and $I_{in} = 500\mu mol\,m^{-2}\,s^{-1}$. In this case, we

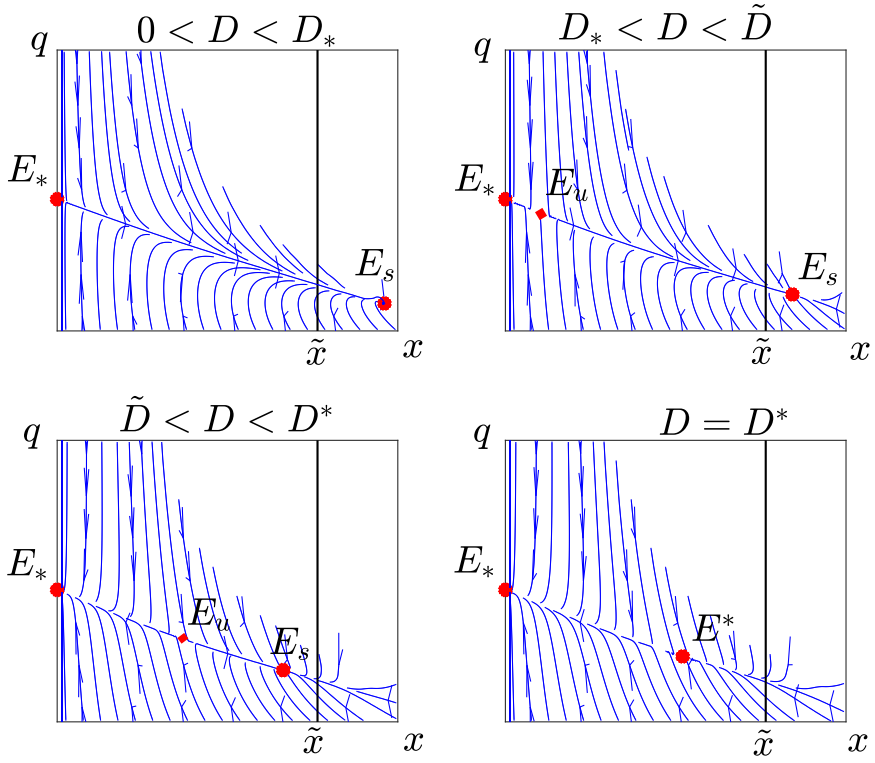

Figure 5.4: Phase diagrams for different values of D. E_* stands for the washout steady state, E_u and E_s stand for unstable and locally stable equilibria respectively, and E^* stands for the unique positive equilibrium in the case $D = D^*$.

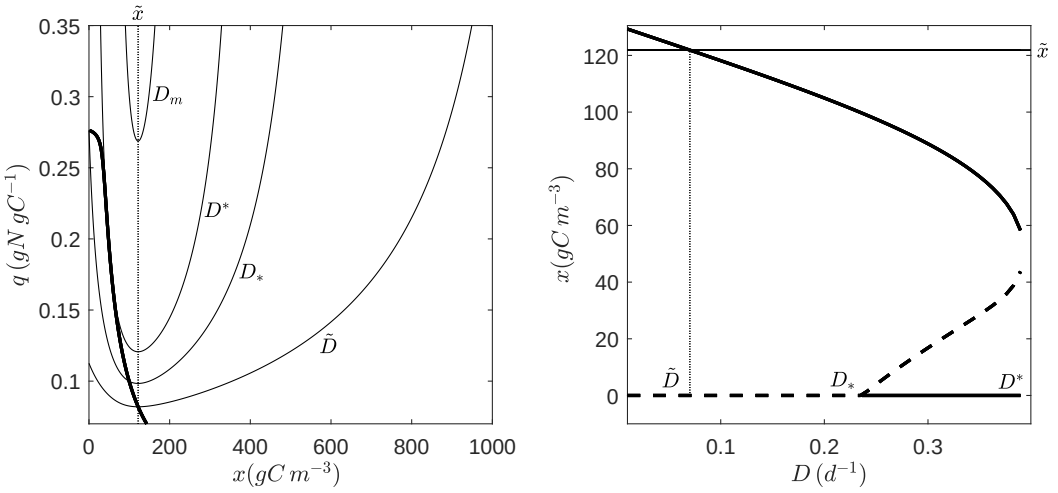

Figure 5.5: A. Intercepts of Γ_1 and $\Gamma_2(D)$ for different dilution rates in the case 2. The bold line corresponds to Γ_1. B. Bifurcation diagram of x with respect to D.

reduce the nutrient supply of nitrogen. This results in a change in the order of D_* and $\tilde{D}$ as it is shown in Table 5.2. As in the case 3, Figure 5.5 summarizes the existence of steady states and their stability.

5.7 Conclusions

In this work, we studied the asymptotic behavior of a single microalgae population model accounting for nutrient and light limitation. We assumed that microalgae may suffer from photoinhibition. We showed that the model does not admit limit cycles and that any solution approaches a steady state, the washout steady state characterized by the absence of microalgae, or a positive steady state characterized by the survival of the population. The existence and the stability of these steady states depend on the parameters of the

model.

We proved the existence of three dilution rates giving information about the dynamics of the model. A dilution rate D_* characterizing the persistence of the population (see Theorem 5.4.5). A dilution rate D_m ensuring the extinction of the population (see Lemma 5.5.1). For dilution rates higher than D_m the population goes to extinction. And a dilution rate $\tilde{D}$ characterizing the existence of a positive steady with a population density higher than the population density $\tilde{x}$ at which the growth rate is maximal (see Lemma 5.5.3).

With the help of numerical simulations and the information given by the dilution rates D_*, D_m, and $\tilde{D}$, we built a bifurcation diagram.

Bibliography

[1] Q. Béchet, A. Shilton, and B. Guieysse. Modeling the effects of light and temperature on algae growth: State of the art and critical assessment for productivity prediction during outdoor cultivation. *Biotechnology Advances*, 31(8):1648 – 1663, 2013.

[2] O. Bernard. Hurdles and challenges for modelling and control of microalgae for co2 mitigation and biofuel production. *Journal of Process Control*, 21(10):1378–1389, 2011.

[3] G. Bougaran, O. Bernard, and A. Sciandra. Modeling continuous cultures of microalgae colimited by nitrogen and phosphorus. *Journal of theoretical biology*, 265(3):443–454, 2010.

[4] D. J. Gerla, W. M. Mooij, and J. Huisman. Photoinhibition and the assembly of light-limited phytoplankton communities. *Oikos*, 120(3):359–368, 2011.

[5] M. W. Hirsch and H. Smith. Monotone dynamical systems. *Handbook of differential equations: ordinary differential equations*, 2:239–357, 2006.

[6] S.-B. Hsu and C.-J. Lin. Dynamics of two phytoplankton species competing for light and nutrient with internal storage. *Discrete Contin. Dyn. Syst. Ser. S*, 7:1259–1285, 2014.

[7] H. R. Thieme. Convergence results and a poincaré-bendixson trichotomy for asymptotically autonomous differential equations. *Journal of mathematical biology*, 30(7):755–763, 1992.

[8] K.-L. Yeh, J.-S. Chang, and W.-m. chen. Effect of light supply and carbon source on cell growth and cellular composition of a newly isolated microalga chlorella vulgaris esp-31. *Engineering in Life Sciences*, 10(3):201–208, 2010.

CHAPTER 6

Optimization of microalgae processes under light limitation

Contents

6.1 Chapter presentation

This chapter synthesizes and combines the published articles [8, 9]. Both articles are related to the maximization of microalgae productivity by controlling the light availability in the culture. In a first stage, exploiting the results presented in [9], we better understand what are the optimal incident light intensities for microalgae cultures operated at steady state. Then, based on [8] we see how to reduce natural light by shading the cultures.

Martínez, C., Mairet, F.,& Bernard, O. (2019). *Maximizing microalgae productivity in a light-limited chemostat. IFAC-PapersOnLine 51 (2), 735-740*

Abstract : *Light supply is one of the most important parameters to be considered for enhancing microalgae growth in photobioreactors (PBR) with artificial light. However, most of the mathematical works do not consider incident light as a parameter to be optimized. In this work based on a simple model of light-limited growth, we determine optimal values for the dilution rate and the incident light intensity in order to maximize the steady-state microalgal surface productivity in a continuous culture. We also show that in optimal conditions there is a minimal initial microalgal concentration (and we give a simple expression to determine it) to guarantee the persistence of the population. Finally, in the context of enhancing microalgae productivity by reducing light absorption by microalgae, we conclude our work by studying the influence of the chlorophyll-carbon quota on the maximal productivity.*

Martínez, C., Mairet, F.,& Bernard, O. (2019). *Maximizing microalgae productivity by shading outdoor cultures. IFAC-PapersOnLine 50 (1), 8734-8739*

Abstract : *Outdoor microalgae cultures can undergo a photoinhibitory process that can result in a loss in biomass productivity. This loss can be reduced by shading the culture such that the incident photon flux decreases. Based on a simple model of light-limited growth, we look for a control strategy to shadow the culture in order to maximize the biomass productivity. The strategy results in a feedback control that depends on the microalgae strain, the microalgae concentration, and the incident light. In the case that the incident light and the loss rate vary periodically in time, we give conditions for the existence of a positive periodic solution that is globally stable. We show the performance of the feedback control by means of numerical simulations.*

6.2 Introduction

Light supply is one of the most important factors affecting microalgae growth. Howewer, excess light can result in photoinhibition, that is, a decrease in the rate of photosynthesis due to high light intensities [5]. Thus, light should be provided at an appropriate intensity to enhance microalgae growth [2]. In outdoor microalgae cultures, photoinhibition may cause a loss in biomass productivity in the midday, even in high dense cultures [11]. Indeed, [12] demonstrated that by shading dense *Spirulina platensis* cultures grown in outdoor and protecting them from full exposure to solar radiation higher productivities could be achieved. This shows that by shading adequately outdoor cultures, the biomass productivity can increase. Despite the importance of the incident light intensity, most of the mathematical works concerned with the optimization of microalgae cultures only focus on the control of the dilution rate. See for example the works [4, 7, 10].

This chapter is concerned with the optimization of biomass productivity when microalgae growth is only limited by light. We consider an indoor culture where the incident light can be directly controlled, and an outdoor culture illuminated with natural light, where we cannot directly control the incident light. For the indoor culture, we determine optimal values for the dilution rate and the incident light intensity in order to maximize the biomass productivity at steady state operation. In the case of the outdoor culture, we determine a strategy to shadow the culture to reduce the photoinhibitory process during the midday in order maximize biomass productivity.

In the literature, we can find some works where the incident light is directly modulated. For example, in [6] the incident light is modulated to maintain a constant light at the bottom of the culture, while in [3] the incident light is controlled to maximize the biomass productivity.

This chapter is organized as follows. In Section 6.3, we briefly describe a model for light-limited cultures. We recall some aspects from Chapter 3. In Section 6.4, we study the indoor culture. First, we study the dynamics of the model when it is operated at constant dilution rate and constant incident light intensity. Then, we determine the maximal productivity at steady state. Finally, in Section 6.5, we consider the outdoor culture. We begin determining the control strategy. Then, we study the dynamics of the controlled culture. Finally, we evaluate numerically the efficiency of the control strategy.

6.3 Modeling light-limited growth of microalgae.

Let us consider a perfectly mixed microalgae culture of depth L where microalgae grow (see Figure 6.1). Let us assume that light is attenuated exponentially with depth according to the Lambert-Beer law i.e. at a distance $z \in [0, L]$ from the illuminated surface, the corresponding light intensity $I(x, I_{in}, z)$ satisfies:

$$I(x, I_{in}, z) = I_{in} e^{-kxz}, \tag{6.1}$$

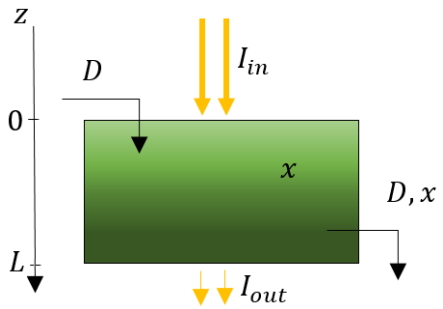

Figure 6.1: Scheme of the light-limited chemostat.

where x denotes the microalgae concentration, I_{in} is the incident light intensity, and $k > 0$ is the specific light attenuation coefficient.

Let us denote by p the specific gross growth rate of microalgae. We assume that nutrients and carbon dioxide are such that light is the single factor that limits growth i.e. $p : \mathbb{R}_+ \longrightarrow \mathbb{R}_+$ is a function of the light intensity I perceived by microalgae. Following Chapter 3, we compute the average growth rate function (AGR) in the reactor, denoted now by μ, by integrating the local growth rate over all the reactor minus a loss rate m:

$$\mu(x, I_{in}) := \frac{1}{L} \int_0^L p(I(x, I_{in}, z))dz. \tag{6.2}$$

Considering a dilution rate D and a mortality rate m, the evolution of the microalgae concentration x is given by:

$$\dot{x} = [\mu(x, I_{in}) - m - D]x. \tag{6.3}$$

As shown in Chapter 3 (see Section 3.4), we can write:

$$\mu(\cdot) = g(I_{in}, I_{out}(x, I_{in})), \tag{6.4}$$

with

$$g(I_{in}, I_{out}) = \frac{1}{\ln(I_{in}) - \ln(I_{out})} \int_{I_{out}}^{I_{in}} \frac{p(I)}{I} dI. \tag{6.5}$$

6.4 Maximizing microalgae productivity: Indoor case.

In this section, we assume that p is given by the Haldane-type model introduced in Chapter 2:

$$p(I) = p_{max} \frac{I}{I + \frac{p_{max}}{\alpha} \left(\frac{I}{I^*} - 1\right)^2}, \tag{6.6}$$

with α the initial slope of the light response curve, p_{max} the specific maximal gross growth rate, and I^* the light intensity at which p reaches p_{max}. The advantage of using (6.6) relies on the following lemma that gives some properties of p and g.

Lemma 6.4.1. *Assume that p is given by (6.6) and let us define $\sigma(I) = I^{*2}/I$. Then:*

a) $p(I_1) = p(I_2)$ if, and only if $I_1 = I_2$ or $I_2 = \sigma(I_1)$.

b) If $I_{in} > I^*$, then $g(I_{in}, \sigma(I_{in})) = g(I_{in}, I^*)$.

c) If $\Delta := 4\frac{p_{max}}{\alpha I^*} - 1 > 0$, *then:*

$$g(I_{in}, I_{out}) = \frac{2p_{max}/\sqrt{\Delta}}{\ln(I_{in}/I_{out})} \left[\tan^{-1}(\kappa(I_{in})) - \tan^{-1}(\kappa(I_{out}))\right], \tag{6.7}$$

with $\kappa(I) = \frac{2p_{max}}{\alpha I^* \sqrt{\Delta}} \left(\frac{I}{I^*} - 1\right) + \frac{1}{\sqrt{\Delta}}$.

Proof. The parts a) and c) follow from straightforward calculations. To prove b), using part a), we can easily show that it is enough to prove the following identity:

$$\int_{I^{*2}/I_{in}}^{I^*} \frac{p(I)}{I} dI = \int_{I^*}^{I_{in}} \frac{p(I)}{I} dI. \tag{6.8}$$

This identity follows directly from doing the change of variables $J = I^{*2}/I$ on the right side. □

6.4.1 Dynamics of a light-limited chemostat.

By standard arguments (i.e. $\partial(xg(I_{in}, I_{out}(x, I_{in}))/\partial x$ and $g(I_{in}, I_{out}(x, I_{in}))$ are both bounded by p_{max} for all $x \geq 0$) it can be shown that (6.3) admits a unique global solution for any non-negative initial condition.

It is clear that p (see (6.6)) is differentiable, $p'(I) > 0$ for all $I \in [0, I^*)$, $p'(I) < 0$ for all $I \in (I^*, \infty)$, $p(0) = 0$ and $\lim_{I\to\infty} p(I) = 0$. Let us assume that $I_{in} > I^*$. Following Lemma A1 (see Appendix A), we know that $g(I_{in}, 0) = 0$, $g(I_{in}, I_{in}) = p(I_{in})$ and that there exists $\gamma(I_{in}) < I^*$ such that the function $I_{out} \longmapsto g(I_{in}, I_{out})$ is strictly increasing on $[0, \gamma(I_{in})]$ and strictly decreasing on $[\gamma(I_{in}), I_{in}]$ (see Figure 6.2 a)). Thus, if $m + D > g(I_{in}, \gamma(I_{in}))$, then the equation $m + D = g(I_{in}, I_{out}(x, I_{in}))$ for x has no solution (see Figure

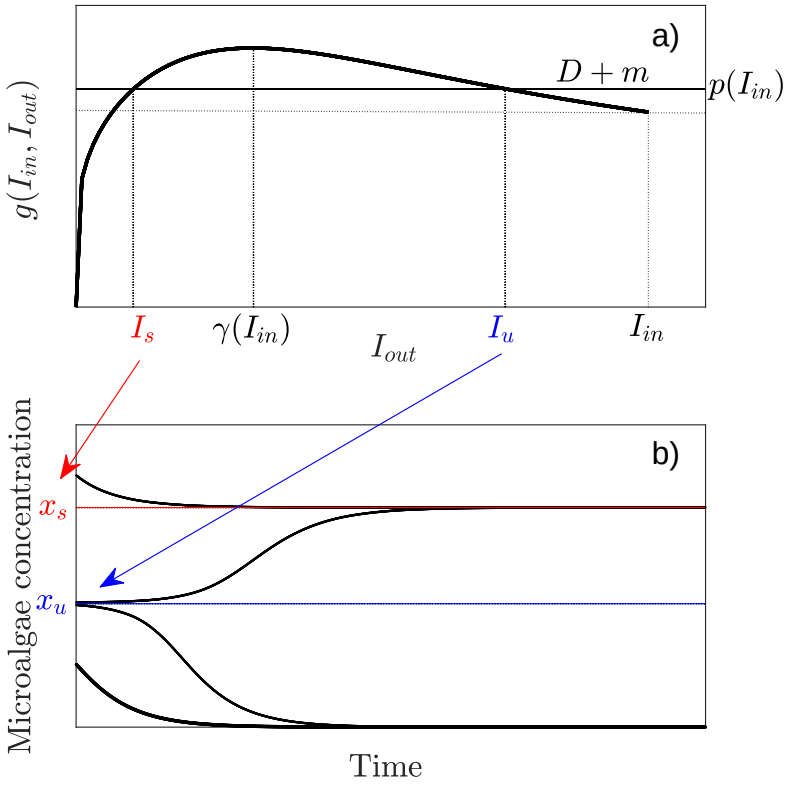

Figure 6.2: **a)** Function g and its intersection with $D + m$. **b)** Graphical representation of bi-stability. The black lines represent solutions of (6.3) for different initial conditions.

6.2 a)) and $x_s = 0$ is the unique equilibrium of (6.3) which is globally stable. Let us assume that:

$$0 < m + D \leq g(I_{in}, \gamma(I_{in})). \tag{6.9}$$

Then, there exists a unique I_s such that:

$$g(I_{in}, I_s) = D + m, \text{ and } I_s \leq \gamma(I_{in}). \tag{6.10}$$

Thus, we have the positive equilibrium x_s of (6.3):

$$x_s := \frac{1}{kL} \ln\left(\frac{I_{in}}{I_s}\right), \tag{6.11}$$

If $D + m \leq p(I_{in})$, then x_s is the unique positive equilibrium of (6.3) and is globally stable. If

$$p(I_{in}) < D + m, \tag{6.12}$$

then there exists another equilibrium x_u given by:

$$x_u = \frac{1}{kL} \ln\left(\frac{I_{in}}{I_u}\right), \tag{6.13}$$

with I_u satisfying:

$$g(I_{in}, I_u) = D + m, \text{ and } \gamma(I_{in}) \leq I_u. \tag{6.14}$$

In this situation x_s attracts any solution of (6.3) with an initial concentration higher than x_u, and $x = 0$ attracts any solution with an initial concentration lower than x_u (see Fig. 6.2b)). In this case we say that the system faces bi-stability. This behavior is due to photoinhibition. If the initial biomass

concentration is high enough, self-shading reduces this effect of inhibition. We note that if $D + m = g(I_{in}, \gamma(I_{in}))$ then $x_u = x_s$.

6.4.2 Maximizing biomass productivity

Let us assume that condition (6.9) holds. Then (6.3) admits a positive locally stable steady state (see (6.11)). We define the *steady-state micro-algal biomass surface productivity* as $P := DLx_s$. We will simply speak of productivity when referring to P. The productivity represents the quantity of microalgae that is produced per unit of area and time when the system reaches its steady state. Recalling (6.10) we can rewrite the productivity as:

$$P = \frac{D}{k} \ln\left(\frac{I_{in}}{I_s}\right). \tag{6.15}$$

From (6.10) we note that I_s is strictly increasing w.r.t. m (see Figure 6.2 a)), therefore the productivity is decreasing w.r.t. m. However, the dependence of P on D and I_{in} is not trivial. By combining equations (6.10) and (6.15), we obtain that:

$$\begin{aligned} P &= \frac{1}{k}(g(I_{in}, I_s) - m) \ln\left(\frac{I_{in}}{I_s}\right) \\ &= \frac{1}{k} \int_{I_s}^{I_{in}} \frac{p(I) - m}{I} dI. \end{aligned} \tag{6.16}$$

Let $\hat{I}_{in}$ be such that:

$$p(\hat{I}_{in}) = m, \ \hat{I}_{in} > I^*. \tag{6.17}$$

Then, the integral in (6.16) reaches its maximum value when:

$$I_s = \sigma(\hat{I}_{in}) \text{ and } I_{in} = \hat{I}_{in}, \tag{6.18}$$

because in that way the integral is calculated over the maximal interval where the function to be integrated is non-negative. In the following theorem we show that by taking $D = \hat{D}$ with:

$$\hat{D} = g(\hat{I}_{in}, \sigma(\hat{I}_{in})) - m, \tag{6.19}$$

then I_s satisfies (6.18).

Theorem 6.4.2. *The productivity is maximal when $D = \hat{D}$ and $I_{in} = \hat{I}_{in}$ with $\hat{D}$ and $\hat{I}_{in}$ satisfying (6.17) and (6.19). The maximal productivity is given by:*

$$P_{max} := \frac{1}{k} \int_{\sigma(\hat{I}_{in})}^{\hat{I}_{in}} \frac{p(I) - m}{I} dI. \tag{6.20}$$

Under these conditions, the model (6.3) faces bi-stability, that is, the solutions of (6.3) reach the stable equilibrium if and only if the initial microalgae concentration x_0 satisfies $x_0 > \hat{x}_u$ with:

$$\hat{x}_u = \frac{1}{kL} \ln\left(\frac{I_{in}}{I^*}\right). \tag{6.21}$$

Proof. Let $\hat{I}_{in} > I^*$ defined by (6.17) and $\hat{D}$ defined by (6.19). We note that $\hat{D} > 0$, indeed:

$$\hat{D} = \frac{1}{\ln\left(\frac{\hat{I}_{in}}{\sigma(\hat{I}_{in})}\right)} \int_{\sigma(\hat{I}_{in})}^{\hat{I}_{in}} \frac{p(I) - m}{I} dI > 0. \tag{6.22}$$

From the definition of $\hat{D}$ and Lemma 6.4.1 b), we have that

$$\hat{D} + m = g(\hat{I}_{in}, \sigma(\hat{I}_{in})) = g(\hat{I}_{in}, I^*).$$

Since $\sigma(\hat{I}_{in}) < I^*$, we conclude that $I_s = \sigma(\hat{I}_{in})$ and that (6.3) faces bi-stability with $I_u = I^*$. Finally, by using (6.13) we conclude that the unstable equilibrium is given by (6.21). □

Theorem 6.4.2 not only gives the maximal productivity but an expression for the minimal initial microalgae concentration $\hat{x}_u$ to avoid the washout. Expression (6.21) shows that $\hat{x}_u$ increases by reducing the depth of the reactor. Thus, even if the productivity does not depend on the depth of the reactor, the depth should be chosen such that $\hat{x}_u$ is not too big. The condition $x_0 > \hat{x}_u$ can be rewritten as $I^* > I_{out,0} := I_{in}e^{-ax_0L}$. Thus, the result related to bi-stability can be stated as follows: the system will washout only if at the beginning the light intensity at the bottom of the reactor is higher than I^* (i.e. if all microalgae in the culture are suffering from photoinhibition).

For evaluating the optimal parameters and the maximal productivity we take the kinetic parameters from Table 2.1. Figure 6.3 shows that for small values of m the optimal incident light intensity takes high values; if $m = 0.1d^{-1}$ then $\hat{I}_{in} = 2151\,\mu mol\,m^{-2}\,s^{-1}$. In fact, as m approaches to zero, the optimal incident light intensity goes to infinity. To see how $\hat{I}_{in}$ varies with other parameters, we note that $\hat{I}_{in}$ is the biggest solution of the following equation for I:

$$\frac{(I - I^*)^2}{I^{*2}} = \alpha \left(\frac{1}{m} - \frac{1}{p_{max}} \right) I. \tag{6.23}$$

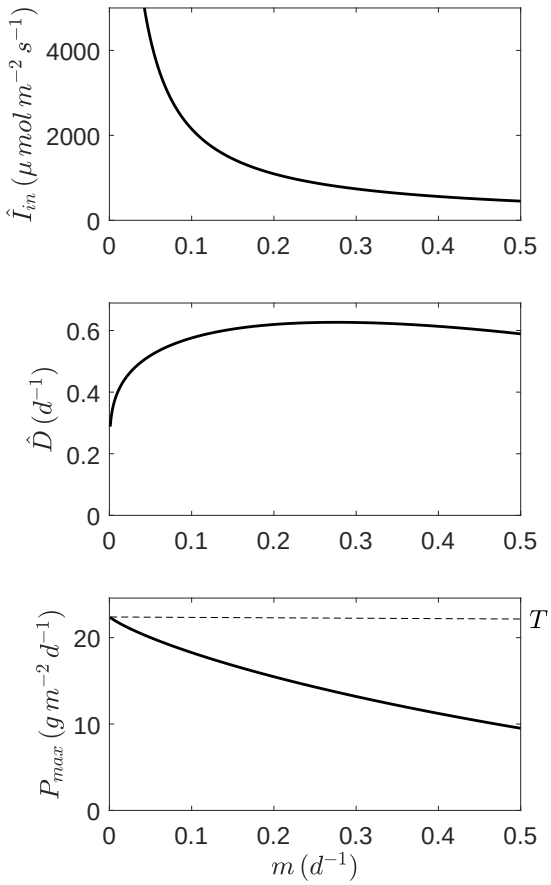

Figure 6.3: Plot of the optimal incident light intensity, the optimal dilution rate, and the maximal productivity as functions of the mortality rate. The function p is given by (6.6) with kinetic parameters of *C. vulgaris* given in Table 2.1, and $k = 0.2m^2\,g^{-1}$.

The solutions of this equation correspond to the intercepts of a parabola (left side of (6.23)) and a line (right side of (6.23)). Figure 6.4 shows this situation. Thus, any increase in the slope of the line results in an increase of the value of $\hat{I}_{in}$. In particular, this occurs when m decreases or when α or p_{max} increases. On the other hand, any increase on I^* will open wider and translate to the right the parabola. Thus, any increase on I^* increases the value of $\hat{I}_{in}$.

Figure 6.3 shows that the maximal productivity approaches a finite value, that we denote T, when m approaches to zero. The following proposition gives a simple expression for evaluating T.

Proposition 6.4.3. *The maximal productivity is bounded from above by:*

$$T = \frac{2p_{max}}{k\sqrt{\Delta}} \left\{ \frac{\pi}{2} - \arctan\left[\frac{1}{\sqrt{\Delta}} \left(1 - \frac{2p_{max}}{\alpha I^*} \right) \right] \right\}, \tag{6.24}$$

when $\Delta > 0$.

Proof. By taking derivative with respect to m in (6.23), we obtain:

$$\frac{\partial \hat{I}_{in}}{\partial m} = \frac{-\alpha \hat{I}_{in}}{m^2 \frac{\hat{I}_{in} - I^*}{\hat{I}_{in}^{*2}} \left[1 + \frac{I^*}{\hat{I}_{in}} \right]}. \tag{6.25}$$

By applying L'Hopital's rule and using (6.25) we conclude that:

$$\lim_{m \to 0^+} m \ln \left(\frac{\hat{I}_{in}}{\sigma(\hat{I}_{in})} \right) = 0. \tag{6.26}$$

Now, by using (6.20) and noting that $\hat{I}_{in} \to \infty$ and $\sigma(\hat{I}_{in}) \to 0$ as $m \to 0^+$,

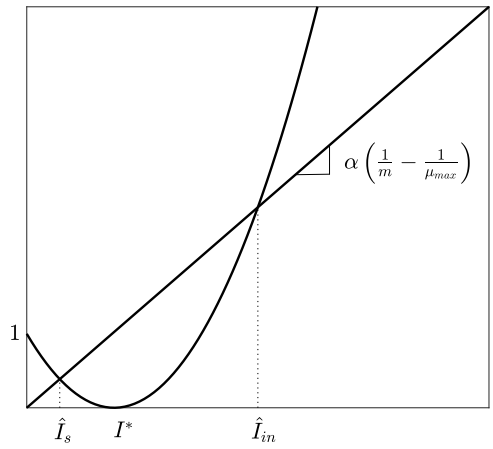

Figure 6.4: Plots of the parabola $y = \frac{(I-I^*)^2}{I^{*2}}$ and the line $y = \alpha\left(\frac{1}{m}-\frac{1}{p_{max}}\right)I$.

we obtain that:

$$T := \lim_{m\to 0^+} P_{max} = \frac{1}{k}\int_0^\infty \frac{p(I)}{I}dI. \tag{6.27}$$

Finally, using (6.7) to evaluate the integral in (6.27) we obtain the result of the proposition. □

In the example of Figure 6.3, we have that $T = 22.35g\,m^{-2}\,d^{-1}$. Thus, according to the parameters in this chapter, *C. vulgaris* could never reach a higher productivity than $22.35g\,m^{-2}\,d^{-1}$ in a photobioreactor operated at constant dilution rate and constant incident light.

6.5 Maximizing microalgae productivity by shading outdoor cultures

In this section, we assume that μ is differentiable, that there exists I^* such that $\mu'(I) > 0$ for all $I < I^*$ and $\mu'(I) < 0$ for all $I > I^*$, and that $\mu(0) = 0$. This section begins with the construction of a control strategy for shading the culture. Then, we study the dynamics of the microalgae culture when the control strategy is applied. Finally, we test the control strategy with numerical simulations.

6.5.1 Control strategy

In order to include the process of shading the microalgae culture, we consider a control variable $u \in [0, 1]$ indicating the percentage of the incident photon flux arriving to the culture surface. We will refer to u as *exposure factor*. The problem of optimizing the biomass productivity can be stated as the following optimal control problem:

$$\begin{aligned} \max \quad & P = \int_{t_i}^{t_f} LD(t)x(t)dt, \\ s.t. \quad & \dot{x}(t) = (\mu(x, u(t)I_{in}(t)) - D(t) - m(t))x, \\ & x(0) = x_0 \ , \ u(t) \in [0, 1], \end{aligned} \tag{6.28}$$

where P is the areal biomass productivity on the interval of time $[t_i, t_f]$, L is the depth of the culture, and x_0 is the initial microalgal concentration. P represents the quantity of biomass that is harvested during the interval of time $[t_i, t_f]$ per unit of area. We assume that I_{in}, D and m are continuous

functions of time.

We note that the objective function P does not depend directly on u and is linear in x. Thus, knowing the monotony of μ as a function of I_{in} we can construct a feedback control for u. With respect to the monotony of μ, we have the following lemma.

Lemma 6.5.1. *For any $x > 0$ there exists $\mathcal{I}(x)$ such that the function $I_{in} \longmapsto \mu(x, I_{in})$ is strictly increasing on $[0, \mathcal{I}(x)]$ and strictly decreasing on $[\mathcal{I}(x), \infty)$. The value of $\mathcal{I}(x)$ is determined by:*

$$p(\mathcal{I}(x)) = p(\mathcal{I}(x)e^{-kxL}). \tag{6.29}$$

Proof. See Proposition A2c) in Appendix A. □

Note that when p is given by (6.6), then $\mathcal{I}(x) = I^* e^{\frac{kxL}{2}}$. The following lemma gives some properties of $\mathcal{I}(x)$.

Lemma 6.5.2. *Let $\mathcal{I}(x)$ be given by Lemma 6.5.1. Then:*

a) $\mathcal{I}$ is strictly increasing.

b) $\mathcal{I}'(x) \leq kL\mathcal{I}(x)$ for all $x > 0$

c) $\lim_{x\to\infty} \mathcal{I}(x) = \infty$ and $\lim_{x\to 0^+} \mathcal{I}(x) = I^*$.

Proof. Let $x > 0$ be given. From the definition of $\mathcal{I}(x)$ we have that:

$$p(\mathcal{I}(x)) = p(\mathcal{I}(x)e^{-kxL}). \tag{6.30}$$

By using the implicit function theorem, we obtain that:

$$\mathcal{I}'(x) = \frac{k\mathcal{I}(x)e^{-kxL}}{\gamma(x) + e^{-kxL}}, \tag{6.31}$$

with $\gamma(x) = \frac{-p'(\mathcal{I}(x))}{p'(\mathcal{I}(x)e^{-kxL})}$. From (6.30) we have that $\mathcal{I}(x)e^{-kxL} < I^* < \mathcal{I}(x)$, from where it is clear that $\gamma(x) > 0$. Thus, from (6.31) we obtain directly the parts a) and b).

For the part c), since $\mathcal{I}$ is strictly increasing, $\lim_{x\to\infty}\mathcal{I}(x) = \infty$ or $\lim_{x\to\infty}\mathcal{I}(x) = l > I^*$. If $\lim_{x\to\infty}\mathcal{I}(x) = l$, since p is a continuous function, we can take the limit when $x \to \infty$ in (6.30) and conclude that $p(l) = 0$, which is a contradiction. Hence, $\lim_{x\to\infty}\mathcal{I}(x) = \infty$. Finally, from Lemma 6.5.1, we have that $I^* < \mathcal{I}(x) < I^*e^{kxL}$, which implies that $\lim_{x\to 0^+}\mathcal{I}(x) = I^*$. □

In the following theorem we construct an optimal feedback control for (6.28).

Theorem 6.5.3. *Let $\mathcal{I}(x)$ be given by Lemma 6.5.1 with $\mathcal{I}(0) = I^*$. Then, P is maximal when $u = \epsilon(x, I_{in})$ with ϵ defined as:*

$$\epsilon(x, I_{in}) = \begin{cases} 1 & if \quad I_{in} \leq \mathcal{I}(x), \\ \frac{\mathcal{I}(x)}{I_{in}} & if \quad I_{in} > \mathcal{I}(x), \end{cases} \tag{6.32}$$

for all $x, I_{in} \in \mathbb{R}^2_+$.

Proof. If a function $\epsilon : \mathbb{R}^2_+ \longrightarrow \mathbb{R}_+$ satisfies:

$$\mu(x, \epsilon(X, I_{in})I_{in}) = \max\{\mu(x, \delta I_{in})\,;\, \delta \in [0, 1]\}, \tag{6.33}$$

for all $x, I_{in} \geq 0$, and $u = \epsilon(x, I_{in})$ satisfies the restrictions of (6.28), then, u is a solution of (6.28), and ϵ is an optimal feedback control.

Lemma 6.5.1 shows that, if the incident light I_{in} is greater than $\mathcal{I}(x)$, we should reduce I_{in} with a factor $\epsilon(x, I_{in}) := \mathcal{I}(x)/I_{in}$ in order to illuminate the system with optimal light for the total growth rate. Conversely, if I_{in} is lower than $\mathcal{I}(x)$, since $\mu(x, \cdot)$ is strictly increasing on $(0, \mathcal{I}(x))$, any decrease in the incident light will decrease the total growth rate, so we should take $\epsilon(x, I_{in}) := 1$. Thus, we have defined ϵ for any $x > 0, I_{in} \geq 0$ by:

$$\epsilon(x, I_{in}) = \begin{cases} 1 & if \quad I_{in} \leq \mathcal{I}(x), \\ \frac{\mathcal{I}(x)}{I_{in}} & if \quad I_{in} > \mathcal{I}(x). \end{cases} \tag{6.34}$$

Since $\epsilon(x, I_{in}) = 1$ for any $I_{in} < I^*$, we define $\epsilon(x, 0) := 1$ for any $x \in \mathbb{R}_+$.

Now we have to prove that the differential equation in (6.28) admits a unique solution on $[t_i, t_f]$ when $u = \epsilon(x, I_{in})$. Lemma 6.5.2 shows that the function $\mathcal{I} : [0, \infty) \longrightarrow [I^*, \infty)$ is a bijection. As usual, we will denote $\mathcal{I}^{-1}$ the inverse function of $\mathcal{I}$. Now, we can write ϵ in the following way:

$$\epsilon(x, I_{in}) := \begin{cases} 1 & if \quad \hat{x}(I_{in}) \leq x, \\ \frac{\mathcal{I}(x)}{I_{in}} & if \quad \hat{x}(I_{in}) > x, \end{cases} \tag{6.35}$$

where:

$$\hat{x}(I_{in}) := \begin{cases} 0 & if \quad I_{in} \leq I^*, \\ \mathcal{I}^{-1}(I_{in}) & if \quad I_{in} > I^*. \end{cases} \tag{6.36}$$

We define the function $\mu_\epsilon : \mathbb{R}_+^2 \longrightarrow \mathbb{R}_+$ by:

$$\mu_\epsilon(x, I_{in}) = \mu(x, \epsilon(x, I_{in})I_{in}), \tag{6.37}$$

for all $x, I_{in} \in \mathbb{R}_+$. Thus, when $u = \epsilon(x, I_{in})$, the ODE in (6.28) can be written:

$$\dot{x} = (\mu_\epsilon(x, I_{in}) - m + D)X. \tag{6.38}$$

From expression (6.35), we obtain that $\frac{\partial}{\partial x}\epsilon(x, I_{in}) = 0$ when $\hat{x}(I_{in}) < x$, while for $\hat{x}(I_{in}) > x$, by using Lemma 6.5.2, we have that:

$$\frac{\mathcal{I}'(x)}{I_{in}} \leq kL\frac{\mathcal{I}(x)}{I_{in}} \leq kL\frac{\mathcal{I}(\hat{x}(I_{in}))}{I_{in}} = kL. \tag{6.39}$$

Following this result, ϵ is Lipschitz with respect to x with Lipschitz constant aL. Since μ is a Lipschitz function, it follows directly that μ_ϵ is Lipschitz with respect to x. Thus, (6.38) admits a unique solution on $[t_i, t_f]$ for any non-negative initial condition. □

Remark 6.5.4. *Expression (6.35) shows that when the microalgae concentration is higher than the threshold $\hat{x}(I_{in})$ the culture must be under full exposure to solar radiation. This is consistent with the assumption that in high dense cultures the light intensity is a limiting factor [1]. We also note that when p is a Haldane-type function, then $\hat{x}(I_{in}) = \frac{2}{aL}\ln\left(\frac{I_{in}}{I^*}\right)$.*

6.5.2 Dynamics of the controlled culture

Let us consider the function μ_ϵ defined in (6.37). The following proposition shows that μ_ϵ is strictly decreasing i.e. the shading has removed the Allee

effect.

Proposition 6.5.5. *For any $I_{in} > 0$, the function $x \longmapsto \mu_\epsilon(x, I_{in})$ is strictly decreasing.*

Proof. From Chapter 3, we know that $x \longmapsto \mu(x, I_{in})$ is strictly increasing on $[0, \tilde{x}(I_{in})]$ and strictly decreasing on $[\tilde{x}, \infty)$ with $\tilde{x}(I_{in})$ defined by:

$$\tilde{x}(I_{in}) := \begin{cases} \frac{1}{kL} \ln\left(\frac{I_{in}}{\gamma(I_{in})}\right) & if \quad I_{in} > I^*, \\ 0 & if \quad I_{in} \leq I^*. \end{cases} \tag{6.40}$$

where $\gamma(I_{in})$ is determined by:

$$p(\gamma(I_{in})) = g(I_{in}, \gamma(I_{in})), \tag{6.41}$$

with g defined in (6.7). If $I_{in} < I^*$, then $\hat{x}(I_{in}) = \tilde{x}(I_{in}) = 0$. Thus, $\mu_\epsilon = \mu$ and we conclude that μ_ϵ is strictly decreasing on x. Let us assume that $I_{in} > I^*$. Then $\hat{x}(I_{in})$ is determined from the equation $p(I_{in}) = p(I_{in}e^{-k\hat{x}(I_{in})L})$. Since $g(I_{in}, \gamma(I_{in})) > p(I_{in})$ (see Chapter 3), we obtain that $p(\gamma(I_{in})) > p(I_{in}e^{-a\hat{x}(I_{in})L})$, from where $\gamma(I_{in}) > I_{in}e^{-k\hat{x}(I_{in})L}$, which implies that $\tilde{x}(I_{in}) < \hat{x}(I_{in})$. Thus, for $x \geq \hat{x}(I_{in})$ we have that $\mu_\epsilon = \mu$ and we conclude that μ_ϵ is strictly decreasing on x. For $x < \hat{x}(I_{in})$ we have that:

$$\frac{\mu_\epsilon(x, I_{in})}{\partial x} = -\frac{1}{x}\mu(x, I_{in}) + \frac{1}{kxL}\frac{p((x))}{\mathcal{I}(x)}(1 - e^{kxL}) < 0.$$

Thus, μ_ϵ is strictly decreasing on x. □

In outdoor cultures, the light source varies with a light phase (day) and a dark phase (night). Thus, in a first approach, we can assume that I_{in} is

ω-periodic with $\omega > 0$ the length of the day. In the following proposition, we prove that the periodic fluctuations lead the controlled culture to a periodic state that is attained by any initial biomass concentration i.e. solutions of (6.38) converges to an ω-periodic solution.

Proposition 6.5.6. *Assume that I_{in}, D and m are ω-periodic with I_{in} and m not identically zero. If*

$$\int_0^\omega \mu_\epsilon(0, I_{in}(t))dt > \int_0^\omega (m(t) + D(t))dt, \tag{6.42}$$

then there exists a unique ω-periodic solution x^* to the differential equation (6.38) which is globally stable on $\mathbb{R}_+\backslash\{0\}$.

Proof. Let us define $f(t,x) = \mu_\epsilon(0, I_{in}(t))$. If $I_{in}(t) = 0$, it is easy to verify that $f(t,x) = -m(t) - D(t)$. If $I_{in}(t) > 0$, from Proposition 6.5.5, we know that f is strictly decreasing in x. Now we note that for $x > \hat{x}(I_{in})$ we have $\mu_\epsilon(x, I_{in}) = \mu(x, I_{in}) < \frac{M\omega}{kxL}$ with $M = \int_0^{\max I_{in}(t)} \frac{p(I)}{I} dI$. Thus, taking $R = \max\{\hat{x}(I_{in}), \frac{M\omega}{kL\int_0^\omega (D(t)+m(t))dt}\}$ we have that $\int_0^\omega f(t,R)dt < 0$. Applying Proposition 5 in [13], we complete the proof. □

6.5.3 Simulations

In this section we evaluate the performance of our control strategy; we determine and compare numerically the productivities and the solutions of the controlled culture (modelled by (6.38) and the non-controlled culture (modelled by (6.3)). We consider that p is given by (6.6), with parameters for *C. vulgaris* given in Table 2.1. We consider that the incident light varies according to $I_{in}(t) = I_{max} \max\{0, \sin(2\pi t)\}^2$ with $I_{max} = 2000\, \mu mol\, m^{-2}\, s^{-1}$.

The attenuation coefficient of microalgae and the mortality rate are taken to be $k = 0.2\, m^2\, g^{-1}$ and $m = 0.1\, d^{-1}$ respectively.

Evaluation of the biomass productivity at different constant dilution rates Here, we evaluate the biomass productivities at different constant dilution rates in a period of 30 days with an initial microalgae areal concentration of $10\, g\, m^{-2}$. Figure 6.5 shows a plot of these evaluations. We can see that, at small dilution rates, the productivities are the same, in contrast with high dilution rates where the productivity of the controlled culture is clearly higher. In particular, the maximal productivity in the controlled culture is a 20.3% higher than the maximal productivity in the non-controlled case.

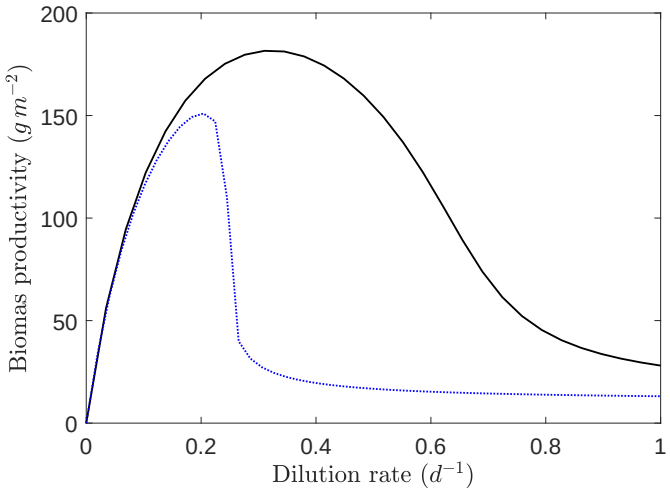

Figure 6.5: Biomass productivities of the controlled culture (continuous line) and the non-controlled culture (dotted line) at different dilution rates.

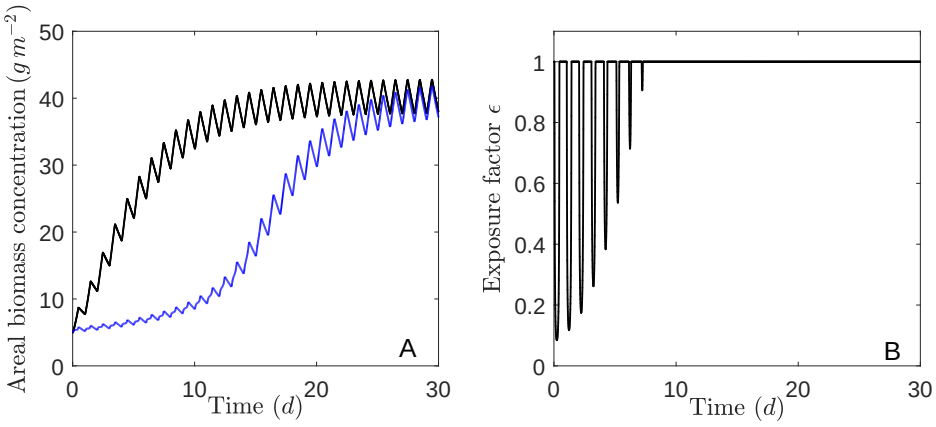

Figure 6.6: **A)** Comparison of the evolution of biomass concentration of the controlled culture (continuous line) and the non-controlled culture (dotted line) at a dilution rate $D = 0.13d^{-1}$. **B)** Evolution of the exposure factor.

Reaching rapidly a high density by shading Figure 6.6A shows the evolution of the microalgae concentrations for an initial concentration $X_0 = 5g\,m^{-2}$ and a dilution rate $D = 0.13\,d^{-1}$. The controlled culture is clearly denser than the other one during the first 25 days. After that, both cultures reach the same periodic state. The productivity over the 30 days is $131.4g\,m^{-2}$ and $82.4\,g\,m^{-2}$ for the controlled and the non-controlled culture respectively. In Figure 6.6B, we can see that the exposure factor is regulated only during the first seven days, then, the microalgae population is dense enough ($x > \hat{x}(I_{in})$) to protect itself from high light intensities. With such a strategy, two weeks are gained in the culturing.

Shading the culture to avoid washout Consider a dilution rate $D = 0.3\,d^{-1}$. If we start at an areal initial concentration of $10g\,m^{-2}$, the controlled culture converges to a periodic state while the non-controlled culture washouts as it is shown in Figure 6.7A. According to Proposition 6.5.6, the

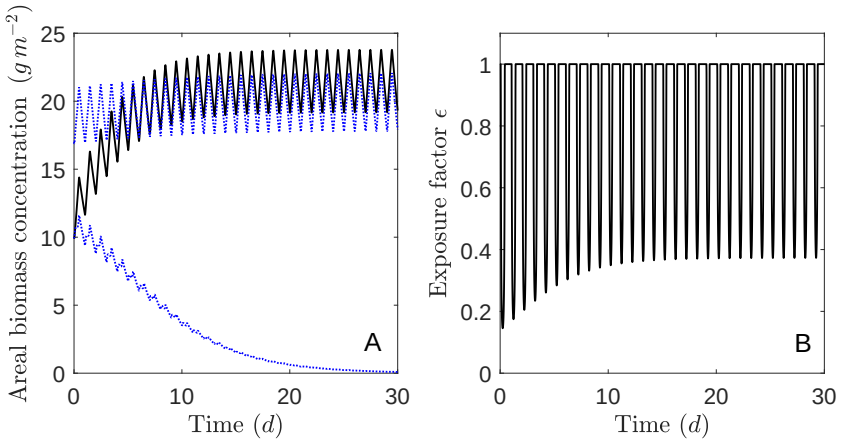

Figure 6.7: **A)** Comparison of the evolution of biomass concentration of the controlled culture (continuous line) and the non-controlled culture (dotted line) for different initial concentrations at a dilution rate $D = 0.3d^{-1}$. **B)** Evolution of the exposure factor.

controlled culture will reach the same periodic state, regardless of the initial biomass concentration. The washout in the non-controlled culture is due to photoinhibition. This washout can be avoided by starting at a higher initial concentration ($17\,g\,m^{-2}$). In that case, the non-controlled culture reaches a positive periodic state. However, this periodic state is lower than that of the controlled culture. Figure 6.7B shows that in this case, shading is necessary during the whole culture.

6.6 Conclusions.

We determined the maximal microalgal productivity that can be reached in a light-limited chemostat operated at constant dilution rate and constant incident light intensity. A simple criterion is obtained: the biomass productivity is maximal when the incident light intensity and the light intensity at

the bottom of the culture are such that the growth rates at the top and at the bottom equal the loss rate. Under these optimal conditions the system faces bi-stability i.e. the system washouts when the density is below a certain threshold. We provided a simple expression for determining this threshold.

We also determined a control strategy to shadow a culture illuminated with natural light in order to maximize the biomass productivity. This control strategy also allows to avoid washout due to photoinhibition - by removing the Allee effect - and to gain time in culturing

Bibliography

[1] J. S. Burlew. Current status of the large-scale culture of algae. *Algal culture from laboratory to pilot plant. Carnegie Institute of Washington Publication*, 600:3–23, 1953.

[2] A. P. Carvalho, S. O. Silva, J. M. Baptista, and F. X. Malcata. Light requirements in microalgal photobioreactors: an overview of biophotonic aspects. *Applied Microbiology and Biotechnology*, 89(5):1275–1288, Mar 2011.

[3] J.-S. Deschnes and A. V. Wouwer. Dynamic optimization of biomass productivity in continuous cultures of microalgae isochrysis galbana through modulation of the light intensity. *IFAC-PapersOnLine*, 48(8):1093 – 1099, 2015.

[4] F. Grognard, A. R. Akhmetzhanov, and O. Bernard. Optimal strategies for biomass productivity maximization in a photobioreactor using natural light. *Automatica*, 50(2):359 – 368, 2014.

[5] S. P. Long, S. Humphries, and P. G. Falkowski. Photoinhibition of photosynthesis in nature. *Annual Review of Plant Physiology and Plant Molecular Biology*, 45(1):633–662, 1994.

[6] F. Mairet and O. Bernard. The photoinhibistat: Operating microalgae culture under photoinhibition for strain selection. *IFAC-PapersOnLine*, 49(7):1068 – 1073, 2016.

[7] F. Mairet, R. Muñoz-Tamayo, and O. Bernard. Driving species competition in a light-limited chemostat. *IFAC Proceedings Volumes*, 46(23):175 – 180, 2013.

[8] C. Martínez, O. Bernard, and F. Mairet. Maximizing microalgae productivity by shading outdoor cultures. *IFAC-PapersOnLine*, 50(1):8734–8739, 2017.

[9] C. Martínez, O. Bernard, and F. Mairet. Maximizing microalgae productivity in a light-limited chemostat. *IFAC-PapersOnLine*, 51(2):735–740, 2017.

[10] P. Masci, F. Grognard, and O. Bernard. 11th ifac symposium on computer applications in biotechnology microalgal biomass surface productivity optimization based on a photobioreactor model. *IFAC Proceedings Volumes*, 43(6):180 – 185, 2010.

[11] H. Qiang, H. Guterman, and A. Richmond. Physiological characteristics of spirulina platensis (cyanobacteria) cultured at ultrahigh cell densities1. *Journal of Phycology*, 32(6):1066–1073, 1996.

[12] A. Vonshak and R. Guy. Photoadaptation, photoinhibition and productivity in the blue-green alga, spirulina platensis grown outdoors. *Plant, Cell Environment*, 15(5):613–616, 1992.

[13] F. Zanolin. Continuation theorems for the periodic problem via the translation operator. *Rend. Sem. Mat. Univ. Politec. Torino*, 54(1):1–23, 1996.

CHAPTER 7

Optimization of microalgae processes under light and substrate limitation

Contents

7.1 Chapter presentation

This chapter relies on a conference article accepted in the 12th IFAC Symposium on Dynamics and Control of Process Systems (DYCOPS 2019). The original article includes a brief description of the dynamics of the periodically forced light-limited Droop which was included in Chapter 4 and therefore is omitted here.

In the context of microalgae production with wastewater, we study numerically an optimal control problem to determine the optimal operation of a high rate algal pond (HRAPs). We briefly recall the light-limited Droop model and we propose an optimal control problem that is solved numerically with the software BOCOP developed by INRIA-Saclay (team Commands).

Martínez, C., Mairet, F., P. Martinon & Bernard, O. (2019). *Dynamics and control of a periodically forced microalgae culture.* (Proceedings of the Dycops conference)

Abstract : *Microalgae cultivation with wastewater is a promising way of reducing the energetic needs for wastewater treatment and the costs of biofuel production. However, the very turbid medium is not favorable for the development of microalgae. Indeed, light, the key element for photosynthesis, rapidly vanishes along depth due to absorption and scattering. Therefore it is crucial to understand the effects of the depth on turbid cultures. In this work, we study theoretically the long-term behavior of a continuous culture of microalgae exposed to a periodic source of light. By allowing periodic variations of the depth and the hydraulic retention time, we show that the microalgae population is forced to a periodic regime. Finally, we address numerically the problem of determining the optimal variations of the depth and the hydraulic retention time for maximizing the productivity of the culture in the periodic regime.*

7.2 Introduction

Microalgae grown as a by-product of wastewater treatment in high rate algal ponds (HRAPs) represent a great opportunity for reducing costs of biofuel production [7, 17]. Moreover, HRAPs show a great potential for nutrient removal in wastewater treatment [1]. One problem with the cultivation of algae in wastewater systems is that light, one of the main factors affecting microalgae growth, rapidly becomes limiting after its decrease due to absorption and scattering by algal cells and the high content of particulate matter and colored substances [5, 15]. We refer to the light extinction due to all non-microalgae components as background turbidity. In the standard analyses of microalgae cultures, background turbidity is neglected. However, in [14] (or Chapter 3), it was shown theoretically that background turbidity results in a reduction of the productivity when increasing the depth of the system. Indeed, according to [12], HRAP depths between 15 and 50 cm are generally recommended.

The objective of this chapter is to give some insights in the optimization of biomass productivity by playing with the depth of the culture and considering a natural light source. In our approach, we combine the modelling approaches of [9] and [11] to build a model accounting for light and substrate limitation. The model is periodically forced by the incident light with a period of one day. Following Chapter 4, we know that under periodic operation of the HRAP, any solution of the model reaches a 1-day periodic regime i.e. approaches asymptotically a periodic solution. Thus, we study

the productivity of the system in a periodic regime by controlling the input and output flow rates, or equivalently, the depth of the system and the hydraulic retention time.

7.3 Model description

Let us consider a perfectly mixed microalgae culture of depth L illuminated from above with an incident light I_{in}. We assume that light is attenuated exponentially according to the Lambert-Beer law i.e. at a distance $z \in [0, L]$ from the illuminated surface, the corresponding light intensity $I(x, z)$ satisfies:

$$I(x, z) = I_{in} e^{-(kx+K_{bg})z}, \tag{7.1}$$

with x the microalgae concentration, $k > 0$ the specific light attenuation coefficient of microalgae, and $K_{bg} \geq 0$ the background turbidity. We assume that microalgae growth is limited by light and a substrate s. Based on the model of Droop [9], we assume that the specific growth rate μ depends on an internal cell quota q. The latter corresponds to an internal pool of nutrient per unit of biomass. Following the model presented by Bernard [3] (see (2.25)), we describe the co-limitation by a multiplicative function:

$$\mu(\cdot) = \left(1 - \frac{q_0}{q}\right) \frac{1}{L} \int_0^L p(I(z))dz - r, \tag{7.2}$$

where $r > 0$ is the respiration rate, $q_0 > 0$ represents the value of q at which growth ceases, and p is a Monod type function describing the limitation by

light:

$$p(I) = p_{max}\frac{I}{K_I + I},$$

with $K_I > 0$ a half-saturation constant, and $p_{max} > 0$ the maximal specific growth rate.

Cell quota q decreases with cell growth and increases with nutrient uptake, whose rate function is taken to be:

$$\rho(q,s) = \begin{cases} \rho_{max}\frac{s}{K_s+s}d(q) & if \quad q \leq q_L, \\ 0 & if \quad q > q_L, \end{cases} \tag{7.3}$$

where ρ_{max} is the maximal uptake rate of nitrogen, q_L is the hypothetical maximal quota, and K_s is a half-saturation constant. $d(q) \in [0,1]$ is a down regulation term. While $d(q)$ is usually taken as a linear function [6, 16], here we take $d(q)$ as:

$$d(q) = \left(\frac{q_L - q}{q_L - q_0}\right)^2 \left(\frac{q_L - q}{q_L - q_0} + 3\frac{q - q_0}{q_L - q_0}\right) \tag{7.4}$$

We note that d is the unique cubic function satisfying:

$$d(q_0) = 1\,, d(q_L) = 0\,, \text{ and } d'(q_0) = d'(q_L) = 0. \tag{7.5}$$

The volume (V) of the culture varies with the supply flow rate (Q_{in}) and the withdrawal rate (Q_{out}) according to:

$$\dot{V} = Q_{in} - Q_{out}. \tag{7.6}$$

The area (A) of the transversal section of the HRAP is constant in time and along the depth of the culture. After dividing both sides in (7.6) by A, we obtain the following equation for the depth of the culture:

$$\dot{L} = F_{in} - F_{out}, \tag{7.7}$$

with $F_{in} := Q_{in}/A$ and $F_{out} := Q_{out}/A$ linear flows. Mass balances in the culture give the following equations (see Chapter 2 in [8] and [6])

$$\begin{aligned} \dot{x} &= [\bar{\mu}(t,x,q,L) - \frac{F_{in}}{L}]x \\ \dot{q} &= \rho(q,s) - \bar{\mu}(t,x,q,L)q \\ \dot{s} &= \frac{F_{in}}{L}(s_{in} - s) - \rho(q,s)x, \end{aligned} \tag{7.8}$$

where s_{in} is the (constant) nutrient supply concentration.

7.4 Maximizing microalgae productivity

We are interested in the quantity of biomass that can be produced in a single day when initial conditions at the beginning of the day equal the final conditions at the end of the day. The biomass productivity (areal) on the interval of time $[0, \omega]$ is defined by:

$$P = \int_0^{\omega} L(t)\mu(\cdot)x(t)dt. \tag{7.9}$$

A more suitable expression for P is obtained as follows. From the first equation in (7.8) and (7.7) we have that:

$$d(xL)/dt = \mu(\cdot)xL - F_{out}x. \tag{7.10}$$

Then, integrating (7.10) on $[0, \omega]$ we obtain:

$$P = \int_0^\omega F_{out}(t)x(t)dt. \tag{7.11}$$

This means that in a periodic regime, P corresponds also to the quantity of biomass that is harvested during one day per unit of area. Now, we are ready to state an optimal control problem for maximizing P. The control variables are $u_1 = F_{in}$ and $u_2 = F_{out}$, and the problem is:

$$\begin{aligned}
\max \quad & P(u_1, u_2) = \int_0^\omega u_2(t)x(t)dt, \\
s.t. \quad & \dot{x} = [\mu(t, x, q, L) - u_1/L]x, \\
& \dot{q} = \rho(q, s) - \mu(t, x, q, L)x, \\
& \dot{s} = u_1/L(s_{in} - s) - \rho(q, s), \\
& \dot{L} = u_1 - u_2, \\
& x(0) = x(\omega) > 0,\ q(0) = q(\omega), s(0) = s(\omega), L(0) = L(\omega), \\
& L(t) > 0, u_1(t) \in [0, F_{in,max}]\,, u_2(t) \in [0, F_{out,max}].
\end{aligned} \tag{7.12}$$

We solve numerically the problem (7.12), with a direct method implemented in the software BOCOP [4] (version 2.10). The problem is discretized by a two-stage Gauss-Legendre method of order 4 with 200 time steps. We consider a constant initialization, and the tolerance for IPOPT NLP solver

Table 7.1: Parameters used to solve the optimization problem (7.12)

Parameter	Value	Unit	Reference
p_{max}	1.72	d^{-1}	[11]
K_I	107	$\mu mol\, m^{-2}\, s^{-1}$	[11]
k	0.2	$m^2\, gC^{-1}$	[2]
ρ_{max}	11.2	$gN\, gC^{-1}\, d^{-1}$	[6]
q_L	0.28	$gN\, gC^{-1}$	[6]
q_0	0.07	$gN\, gC^{-1}$	[6]
K_s	0.0007	$gN\, m^{-3}$	[6]
r	0.1	d^{-1}	-
s_{in}	$7-25$	$gN\, m^{-3}$	-
I_{max}	2000	$\mu mol\, m^{-2}\, s^{-1}$	-
K_{bg}	$0-10$	m^{-1}	-
$F_{in,max}$	1000	$L\, m^{-2}\, d^{-1}$	-
$F_{out,max}$	1000	$L\, m^{-2}\, d^{-1}$	-

is set at 10^{-12}.

To evaluate the impact of the background turbidity in the medium, we first consider two culture mediums; one without background turbidity i.e. $K_{bg} = 0$, and another one with a background turbidity $K_{bg} = 10\, m^{-1}$. For both cases, $s_{in} = 15\, gN\, /m^3$ while the rest of parameters are given in Table 8.3. Figure 7.1 shows the results. In both cultures, algae concentration increases only during the first half of the period, while it decreases during the night night and by the end of illuminated period (see Figure 7.1A). In presence of background turbidity the microalgae concentration is higher, and consequently the nutrient in the medium is lower (see Figure 7.1C), but the quota dynamis are very similar. However, the daily microalgae productivity is $2.1\, gC\, m^{-2}$ in contrast to the culture without background turbidity that reaches a daily microalgae productivity of $4.0\, gC\, m^{-2}$ (i.e. $8.0\, gDW\, m^{-2}$).

The control structures are Bang-Singular (u_1) and Bang-Bang (u_2) for both cultures (see Figure 7.1D). These controls result in a different depth for each culture. Figure 7.1E shows that there is a difference of around $30\,cm$ during all the period of 24 hours with a lower depth for the culture that accounts for background turbidity.

We solve now (7.12) for a set of values of K_{bg} and s_{in} in the ranges $0-10\,m^{-1}$ and $7-25\,gN/m^3$ respectively. The rest of parameters are given in Table 8.3. Figure 7.2 shows the productivity and the average of different quantities associated to the solution of (7.12). In Figure 7.2A, as expected, we observe that K_{bg} and s_{in} have a negative and positive effect on the areal productivity respectively. Figure 7.2B shows a high impact of the background turbidity on the optimal depth for low nutrient supply. This impact decreases as the nutrient supply increases. We also remark that for nutrient-rich wastewater, maximal productivities are reached for low values of the optimal depth. Figure 7.2C shows that the optimal microalgae concentration varies almost linearly with the nutrient supply why almost no variation is observed with respect to to the background turbidity. The areal microalgae concentration varies in the same way as the productivity as shown in Figure 7.2D. Figure 7.2E shows that under optimal conditions for microalgae optimization, the background turbidity has a positive effect on nutrient removal. Indeed, in presence of background turbidity, the nutrient concentration in the HRAP drops drastically. These results show the quandary of providing enough nutrients for growth, without shading the culture with background turbidity.

Finally, we illustrate with simulations the dynamics of the system over a long time horizon. Consider the controls (u_1, u_2) obtained from the optimization of one periodic day-night cycle (see Figure 7.1D). We apply the respective control to each culture (i.e. to solve (7.7)-(7.8)) repeatedly for a long interval of time. The initial depth for each culture is equal to the initial depth of the respective optimal solution (see Figure 7.1E). The initial microalgae concentration and the initial quota are $5\, gC/m^3$ and $0.28\, gN/gC$ respectively for both cultures. Figure 7.3 shows that the microalgae concentration approaches the optimal periodic microalgae concentration found previously, depicted in Figure 7.1A. For the culture with background turbidity, the microalgae concentration approaches more slowly to the periodic solution. Indeed, it needs 50 days in contrast to 30 days for the culture without background turbidity.

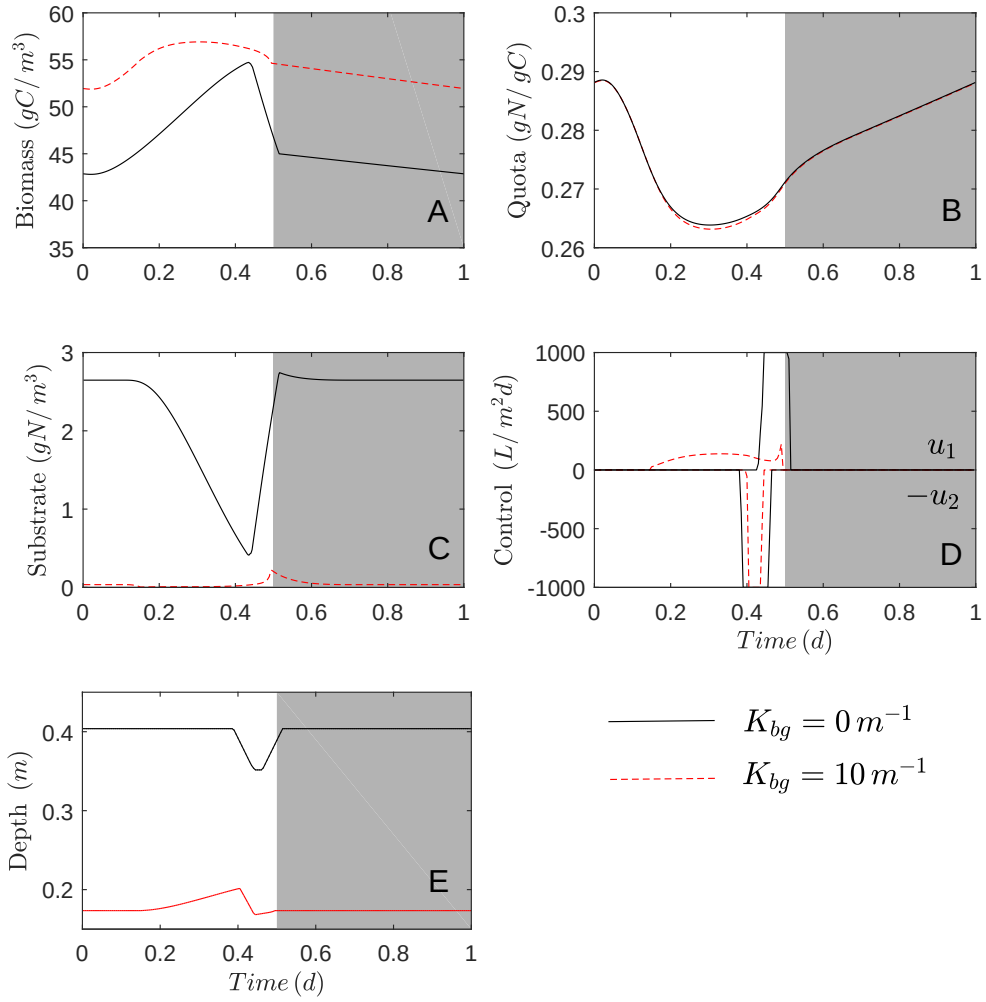

Figure 7.1: Optimal solutions for problem (7.12) obtained numerically with BOCOP for two different background turbidities. A. Microalgae concentration. B. Cell quota. C. Substrate concentration in the medium. D. Control variables. E. Depth of the culture.

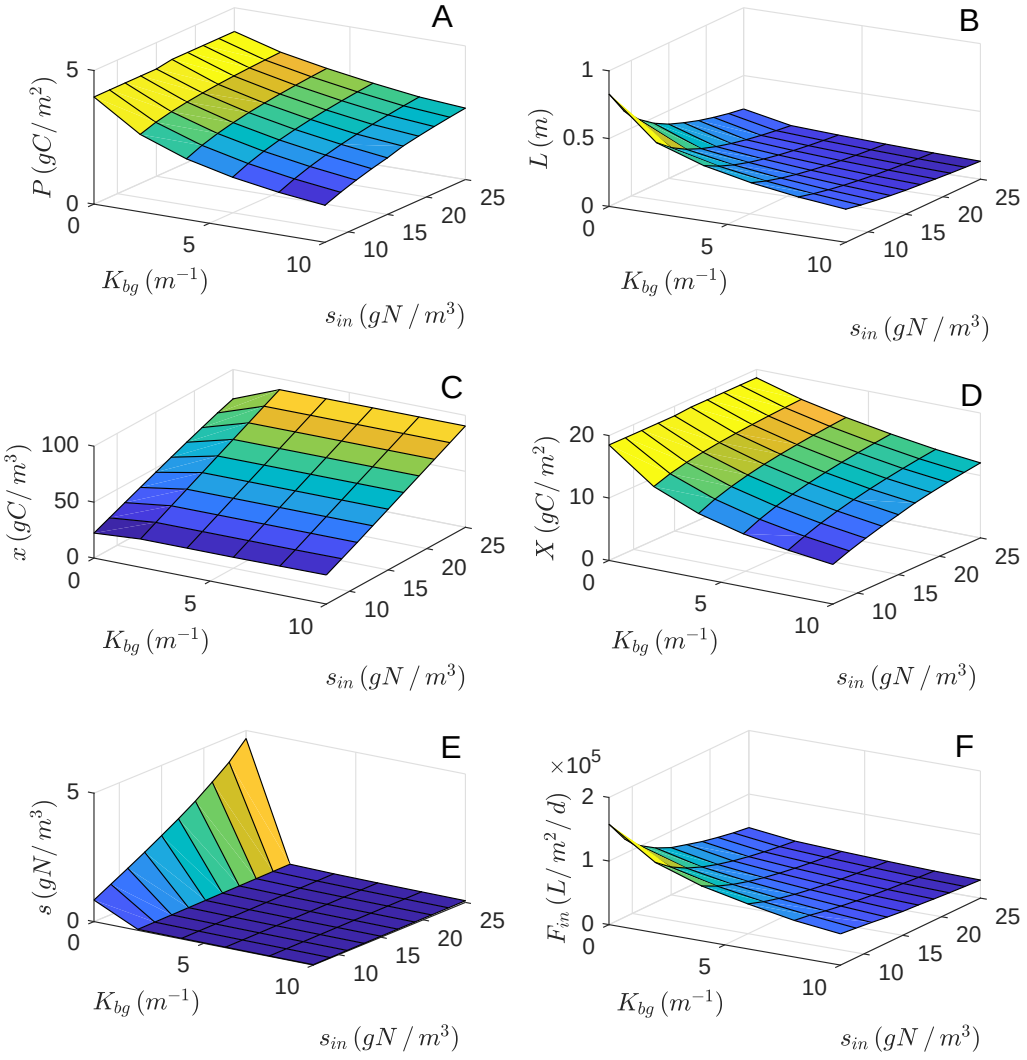

Figure 7.2: Effects of background turbidity and nutrient input concentration on the optimal solution of problem (7.12). A. Biomass productivity. B. Average optimal depth. C. Average biomass concentration. D. Average areal biomass concentration. E. Average substrate concentration. F. Average optimal input flow.

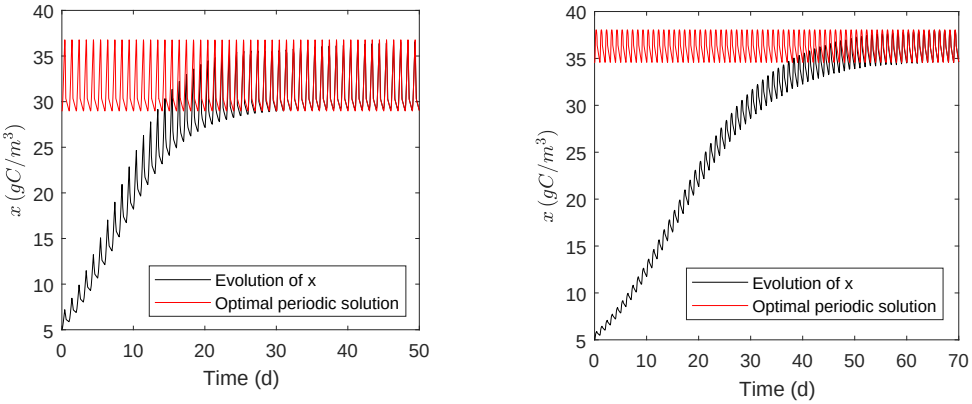

Figure 7.3: Comparison of the optimal 1-day periodic microalgae concentration and the evolution of the microalgae with a low initial concentration when the periodic 1-day optimal periodic control is applied. Left. Culture without background turbidity. Right. Culture with background turbidity.

7.5 Conclusions

A first series of numerical simulations using a direct method illustrates the impact of the background turbidity on the choice of the depth of the culture for maximizing microalgae productivity when both light and nutrient can limit algal growth. We have shown that a background turbidity of $10\,m^{-1}$ can result in a reduction of $30\,cm$ of the optimal depth and a productivity loss of $55\,\%$. Thus, the background turbidity should not be neglected. The choice of the depth is not trivial and should be adapted to the overall turbidity, in particular when both light and nutrient limitations can occur. This choice should also include thermal considerations, since low depth induces lower thermal inertia.

Photoinhibition should be included in a future work. Low depths of the culture could enhance the photoinhibitory process resulting in a lower productivity, and for low initial microalgae concentrations the population could go extinct [10, 13].

In this chapter, we emphasized the productivity of microalgae using wastewater streams without considering additional constraints associated to wastewater treatment. In a future work, other optimization problems will be studied, e.g. the maximization of nitrogen removal with restrictions over the volume of wastewater to be treated.

Bibliography

[1] N. Abdel-Raouf, A. Al-Homaidan, and I. Ibraheem. Microalgae and wastewater treatment. *Saudi journal of biological sciences*, 19(3):257–275, 2012.

[2] Q. Béchet, A. Shilton, and B. Guieysse. Modeling the effects of light and temperature on algae growth: state of the art and critical assessment for productivity prediction during outdoor cultivation. *Biotechnology advances*, 31(8):1648–1663, 2013.

[3] O. Bernard. Hurdles and challenges for modelling and control of microalgae for co2 mitigation and biofuel production. *Journal of Process Control*, 21(10):1378–1389, 2011.

[4] J. Bonnans, V. Grelard, and P. Martinon. Bocop, the optimal control solver, open source toolbox for optimal control problems. *URL http://bocop. org*, 2011.

[5] M. A. Borowitzka. Limits to growth. In *Wastewater treatment with algae*, pages 203–226. Springer, 1998.

[6] G. Bougaran, O. Bernard, and A. Sciandra. Modeling continuous cultures of microalgae colimited by nitrogen and phosphorus. *Journal of theoretical biology*, 265(3):443–454, 2010.

[7] L. Christenson and R. Sims. Production and harvesting of microalgae for wastewater treatment, biofuels, and bioproducts. *Biotechnology advances*, 29(6):686–702, 2011.

[8] D. Dochain. *Automatic control of bioprocesses*. John Wiley & Sons, 2013.

[9] M. R. Droop. Vitamin B 12 and marine ecology. iv. the kinetics of uptake, growth and inhibition in monochrysis lutheri. *Journal of the Marine Biological Association of the United Kingdom*, 48(3):689–733, 1968.

[10] D. J. Gerla, W. M. Mooij, and J. Huisman. Photoinhibition and the assembly of light-limited phytoplankton communities. *Oikos*, 120(3):359–368, 2011.

[11] J. Huisman, H. C. Matthijs, P. M. Visser, H. Balke, C. A. Sigon, J. Passarge, F. J. Weissing, and L. R. Mur. Principles of the light-limited chemostat: theory and ecological applications. *Antonie van Leeuwenhoek*, 81(1-4):117–133, 2002.

[12] K. Larsdotter. Wastewater treatment with microalgae-a literature review. *Vatten*, 62(1):31, 2006.

[13] C. Martínez, O. Bernard, and F. Mairet. Maximizing microalgae productivity by shading outdoor cultures. *IFAC-PapersOnLine*, 50(1):8734–8739, 2017.

[14] C. Martínez, F. Mairet, and O. Bernard. Theory of turbid microalgae cultures. *Journal of theoretical biology*, 456:190–200, 2018.

[15] A. Morel and A. Bricaud. Theoretical results concerning light absorption in a discrete medium, and application to specific absorption of phytoplankton. *Deep-Sea Res*, 28(11):1375–1393, 1981.

[16] F. M. Morel. Kinetics of nutrient uptake and growth in phytoplankton 1. *Journal of phycology*, 23(1):137–150, 1987.

[17] J. Park, R. Craggs, and A. Shilton. Wastewater treatment high rate algal ponds for biofuel production. *Bioresource technology*, 102(1):35–42, 2011.

CHAPTER 8

Microalgae growth limited by light, nitrogen, and phosphorus

Contents

8.1 Chapter presentation

This chapter relies on a conference article submitted to the 8th IFAC Conference on Foundations of Systems Biology in Engineering (FOSBE 2019). We propose a model accounting for co-limitation by light, phosphorus, and nitrogen, taking into account photoacclimation. The performance of the model is illustrated with experimental data from [15], where the authors grow a microalgal consortium that was isolated in a natural pond in contact with used water. By numerical simulations, we evaluate the capacity of microalgae to remove nutrients from raw wastewater.

Martínez, C., Mairet, F., Plaza L., Sciandra, A., & Bernard, O. (2019). *Quantifying the potential of microalgae culture systems to remove nutrients from wastewater.* (Submitted to Proceedings of the FOSBE conference)

Abstract : *The main resources limiting microalgae growth are typically phosphorus, nitrogen, and light. Based on the theory of the light limited chemostat, the variable cell quota approach, and photoacclimation models, we build a mathematical model for describing microalgae growth under limitation by these resources. The model is then calibrated with a data set from the literature. Then, by numerical simulations, we find that under constant operation of the culture and constant environmental conditions (illumination, temperature, pH, etc.), solutions of the model approach towards either a positive or an extinction steady state. Based on the positive steady state, and in the context of wastewater treatment, we evaluate the capacity of microalgae to remove contaminants. We show that the hydraulic retention time and the depth of the culture have a crucial role on the optimization of the nutrient removal efficiency.*

8.2 Introduction

A major requirement in wastewater treatment is the removal of nutrients to acceptable limits prior to discharge and reuse. Microalgae growth in high rate algal ponds (HRAPs) have shown a great potential for nitrogen and phosphorus removal in wastewater treatment ([1, 14]). Technical and economical constraints still exist for the implementation of full scale HRAPs for wastewater treatment. Among the challenges to be solved include maintaining optimal operation despite fluctuations in light, temperature, and influent nutrients.

Here, we propose a computational analysis to determine the capacity of a HRAP to remove nitrogen and phosphorus from raw wastewater. In our approach, first we build a mathematical model for describing microalgae growth under colimitation by light, nitrogen, and phosphorus, including photoacclimation dynamics. Nutrient limitation is described with the variable cell quota model proposed by Droop [9], light limitation is described using the theory of the light limited chemostat developed by Huisman [11], and photoacclimation is described with the model proposed by Bernard [3]. The resulting model fits experimental data from the literature. Through numerical simulations, we study the long-term behavior of the solutions of the model. Finally, we compute the removal capacities of the system for different hydraulic retention times and depths at steady state operation.

This article is organized as follows. In section 2, we introduce the model.

In section 3, we calibrate the model. In section 4, we briefly discuss the dynamics of the model and we determine numerically the nutrient removals at steady state operation. Finally, in section 5, we discuss our results.

8.3 Model description

Mass balances:

The evolution of the microalgae biomass is given by:

$$\frac{dx}{dt} = [\mu(\cdot) - D - m]x, \tag{8.1}$$

where μ is the microalgae growth rate (gross growth), m is the mortality rate, and D is the dilution rate. Based on the Droop model [6, 9] and on the model presented by Bernard [4] for photoacclimation, the evolution of the quotas of nitrogen, phosphorus, and chlorophyll is described by:

$$\begin{aligned} \frac{dq_N}{dt} &= \rho_{NH_4}(\cdot) + \rho_{NO_3}(\cdot) - \mu(\cdot)q_N, \\ \frac{dq_P}{dt} &= \rho_{PO_4}(\cdot) - \mu(\cdot)q_P, \\ \frac{d\theta}{dt} &= \mu(\cdot)[\theta^*(\cdot) - \theta], \end{aligned} \tag{8.2}$$

Here, $\rho_{NH_4}(\cdot)$, $\rho_{NO_3}(\cdot)$, and $\rho_{PO_4}(\cdot)$ represent the uptake rate of NH_4, NO_3, and PO_4 respectively, and $\theta^*(\cdot)$ represents the chlorophyll quota at which microalgae tend to adapt. We define the total amounts of nitrogen, phos-

phorus, and chlorophyll in the biomass by $x_N := q_N x$, $x_P := q_P x$, and $y = \theta x$ respectively. These new variables satisfy the following equations:

$$\begin{aligned}
\frac{dx_N}{dt} &= \rho_{NH_4}(\cdot)x + \rho_{NO_3}(\cdot)x - mx_N - Dx_N, \\
\frac{dx_P}{dt} &= \rho_{PO_4}(\cdot)x - mx_P - Dx_P, \\
\frac{dy}{dt} &= \mu(\cdot)[\theta^*(\cdot)x - y] + (\mu(\cdot) - m - D)y.
\end{aligned}$$

Phosphorus and nitrogen biomass change with the uptake of nutrients and mortality rate, but they do not change with microalgae growth, which only distributes phosphorus and nitrogen over a larger biomass.

The evolution of the external concentrations of ammonium, nitrate, and phosphate is given by:

$$\begin{aligned}
\frac{ds_{NH_4}}{dt} &= D(s_{NH_4,in} - s_{NH_4}) - \rho_{NH_4}(\cdot)x + b(1 - f_{IN})q_N x. \\
\frac{ds_{NO_3}}{dt} &= D(s_{NO_3,in} - s_{NO_3}) - \rho_{NO_3}(\cdot)x \qquad (8.3) \\
\frac{ds_{PO_4}}{dt} &= D(s_{PO_4,in} - s_{PO_4}) - \rho_{PO_4}(\cdot)x + b(1 - f_{IP})q_P x.
\end{aligned}$$

Here, f_{IN} and f_{IP} correspond to the fraction of nitrogen and phosphorus biomass that is transformed into organic matter. Finally, the evolution of

Variable	Definition	Unit
x	Algal biomass	$mgCOD\,L^{-1}$
x_N	Nitrogen biomass	$mgN\,L^{-1}$
x_P	Phosphorus biomass	$mgP\,L^{-1}$
y	Chlorophyll content	$mgChl\,L^{-1}$
s_{NH_4}	NH_4 external concentration	$mgN\,L^{-1}$
s_{NO_3}	NO_3 external concentration	$mgN\,L^{-1}$
s_{PO_4}	PO_4 external concentration	$mgP\,L^{-1}$
x_I	Inert particulate organic matter	$mgCOD\,L^{-1}$
x_{IN}	Inert particulate organic nitrogen	$mgN\,L^{-1}$
x_{IP}	Inert particulate organic phosphorus	$mgP\,L^{-1}$
q_N	Nitrogen cell quota	$mgN\,mgCOD^{-1}$
q_P	Phosphorus cell quota	$mgP\,mgCOD^{-1}$
θ	chlorophyll quota	$mg\,Chl\,mg\,COD^{-1}$

Table 8.1: List of variables involved in the model. COD stands for Chemical oxygen demand that corresponds to the total amount of oxidisable organics (biodegradable and nonbiodegradable and both dissolved and particulate), measured by the amount of oxygen in the form of oxidising agent required for the oxidation of organic matters by heating the sample in strong sulphuric acid containing potassium dichromate [7].

j	i **Process**	1 x $\frac{gCOD}{m^3}$	2 x_N $\frac{gN}{m^3}$	3 x_P $\frac{gP}{m^3}$	4 y $\frac{gChl}{m^3}$	5 s_{NH_4} $\frac{gN}{m^3}$	6 s_{NO_3} $\frac{gN}{m^3}$	7 s_{PO_4} $\frac{gP}{m^3}$	8 x_I $\frac{gCOD}{m^3}$	9 x_{IN} $\frac{gN}{m^3}$	10 x_{IP} $\frac{gP}{m^3}$
1	Algae growth	1			θ						
2	Uptake of NH_4		1			-1					
3	Uptake of NO_3		1				-1				
4	Uptake of PO_4			1				-1			
5	Decay	-1	$-q_N$	$-q_P$	$-\theta$	$(1-f_{IN})q_N$		$(1-f_{IP})q_P$	1	$f_{IN}q_N$	$f_{IP}q_P$
6	Photoacclimation				1						

Table 8.2: Stoichiometry of the growth and decay processes of algae.

the inert particulate organic matter is given by:

$$\begin{aligned} \frac{dx_I}{dt} &= D(x_{I,in} - x_I) + bx. \\ \frac{dx_{IN}}{dt} &= D(x_{IN,in} - x_{IN}) + bf_{IN}q_N x. \\ \frac{dx_{IP}}{dt} &= D(x_{IP,in} - x_{IP}) + bf_{IP}q_P x. \end{aligned} \tag{8.4}$$

Table 8.2 shows the Gujer matrix associated to the variables x, x_N, x_P, y, s_{NH_4}, s_{NO_3}, s_{PO_4}, x_I, x_{IN}, and x_{IP}. The total amount of nitrogen and phosphorus in the system are given by $N = x_N + s_{NH_4} + s_{NO_3} + x_{IN}$ and $P = x_P + s_{PO_4} + x_{IP}$. N and P satisfy the following equations:

$$\frac{dN}{dt} = D(N_{in} - N), \text{ and } \frac{dP}{dt} = D(P_{in} - P), \tag{8.5}$$

with $N_{in} = s_{NH_4,in} + s_{NO_3,in} + x_{IN,in}$ and $P_{in} = s_{PO_4,in} + x_{IP,in}$.

Growth rate and uptake functions:

The growth rate under limitation by light and nutrients has been described by the multiplicative model, the threshold model (law of minimum), or the combination of both models. Here, we combine the models of [10] and [6] i.e. nutrient co-limitation is described by the law of minimum and then multiplied by a function representing light limitation:

$$\mu(\cdot) = \min\left\{\frac{1-\frac{q_{N0}}{q_N}}{1-\frac{q_{N0}}{q_{Nexp}}}, \frac{1-\frac{q_{P0}}{q_P}}{1-\frac{q_{P0}}{q_{Pexp}}}\right\}\mu_I(\cdot), \tag{8.6}$$

with q_{N0} and q_{P0} the subsistence quotas of nitrogen and phosphorus respectively, q_{NL} and q_{PL} hypothetical maximal quotas of nitrogen and phosphorus respectively, and μ_I the growth rate when nutrient limitation is ignored. μ_I is given by:

$$\mu_I(\cdot) = \frac{1}{L}\int_0^L p(I(z),\theta)dz, \tag{8.7}$$

with p the specific production rate, or P-I curve, of microalgae and $I(z)$ the light intensity at a distance z from the illuminated surface. $I(z)$ is determined by using the Beer-Lambert law:

$$I(z; I_{in}) = I_{in}e^{-(kx+K_{bg})z}, \tag{8.8}$$

with k and K_{bg} light attenuation coefficients associated to microalgae and to the background medium respectively. The specific microalgae extinction

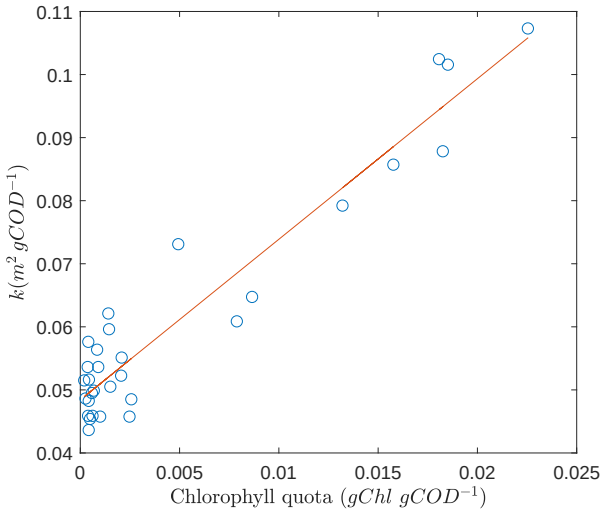

Figure 8.1: Correlation between the chlorophyll quota θ and the specific light attenuation coefficient of microalgae k. Experimental data is taken from the work of [15]. The linear regression is given by $k = 2.5459 \times \theta + 0.0484$.

coefficient depends on θ [5] (see Figure 8.1):

$$k = k_1\theta + k_2, \tag{8.9}$$

with k_1 and k_2 non-negative coefficients. p is taken as:

$$p(I,\theta) = p_{max}\frac{I}{I + \frac{p_{max}}{\alpha_0\theta/\theta_0}\left(\frac{I}{I^*} - 1\right)^2}, \tag{8.10}$$

where I^* and p_{max} are the irradiance at which production rate is maximal and the specific maximum gross growth rate, and α_0 is the initial slope of the light response curve for a chlorophyll quota θ_0. The parameter θ_0 must be chosen.

For the uptake rate functions we have:

$$\rho_{NH_4}(\cdot) = \begin{cases} \rho_{max,NH_4} \dfrac{s_{NH_4}}{K_{NH_4} + s_{NH_4}} \dfrac{q_{NL} - q_N}{q_{NL} - q_{N0}} \dfrac{q_P - q_{P0}}{q_{PL} - q_{P0}} & if \quad q \leq q_{NL}, \\ 0 & if \quad q > q_{NL}. \end{cases} \tag{8.11}$$

where ρ_{max,NH_4} is the maximal uptake rate of NH_4, and K_{NH_4} is a half-saturation constant. Similarly, we have:

$$\rho_{NO_3}(\cdot) = \begin{cases} \rho_{max,NO_3} \dfrac{K_{NH_4}}{K_{NH_4} + s_{NH_4}} \dfrac{s_{NO_3}}{K_{NO_3} + s_{NO_3}} \dfrac{q_{NL} - q_N}{q_{NL} - q_{N0}} \dfrac{q_P - q_{P0}}{q_{PL} - q_{P0}} & if \quad q \leq q_{NL}, \\ 0 & if \quad q > q_{NL}. \end{cases}$$

As reported in [8], we consider that microalgae prefer NH_4 over NO_3. The uptake of N is enhanced by the phosphorus cell quota [6]. The phosphate uptake rate is given by:

$$\rho_{PO_4}(\cdot) = \begin{cases} \rho_{max,PO_4} \dfrac{s_{PO_4}}{K_{PO_4} + s_{PO_4}} \dfrac{q_{PL} - q_P}{q_{PL} - q_{P0}} & if \quad q \leq q_{PL}, \\ 0 & if \quad q > q_{PL}. \end{cases} \tag{8.12}$$

Finally, following [3] we assume that algal photoacclimation is driven by the nitrogen quota and the average light intensity:

$$\theta^*(\cdot) = \gamma_m q_N \frac{k_I}{\bar{I} + k_I}, \tag{8.13}$$

with k_I and γ_m positive constants, and $\bar{I} := \frac{1}{L}\int_0^L I(z)dz$ the average light intensity in the medium.

Nomenclature	**Value**	**Unit**
γ_m	0.01*	$gChl\,gCOD^{-1}$
k_I	97 [13]	$\mu mol\,m^{-2}\,s^{-1}$
δ_0	0.41*	d^{-1}
k_1	2.54 (Fig. 8.1)	$m^2\,gChl^{-1}$
k_2	0.048 (Fig. 8.1)	$m^2\,gCOD^{-1}$
K_{bg}	7.2 [11]	m^{-1}
θ_0	0.01	$gChl\,gCOD^{-1}$
α	0.0145*	$\mu mol^{-1}\,m^2\,s\,d^{-1}$
I^*	331.7*	$\mu mol\,m^{-2}\,s^{-1}$
p_{max}	3.6 [16]	d^{-1}
q_{N0}	0.0264	$gN\,gCOD^{-1}$
q_{NL}	0.0833	$gN\,gCOD^{-1}$
$\rho_{NH_4,max}$	0.2185*	$gN\,gCOD^{-1}\,d^{-1}$
$\rho_{NO_3,max}$	0.1773*	$gN\,gCOD^{-1}\,d^{-1}$
K_{NH_4}	6.7 [16]	$gN\,m^{-3}$
K_{NO_3}	6.87 [16]	$gN\,m^{-3}$
q_{P0}	0.0027	$gP\,gCOD^{-1}$
q_{PL}	0.0058	$gP\,gCOD^{-1}$
$\rho_{PO_4,max}$	0.0158*	$gP\,gCOD^{-1}\,d^{-1}$
K_{PO_4}	4.7 [16]	$gP\,m^{-3}$
f_{IN}	1	-
f_{IP}	1	-
m	0.0432*	d^{-1}

Table 8.3: List of parameters involved in the model. The quotas q_{N0} and q_{P0} were estimated as the minimum of the experimental values of the respective quota, and the quotas q_{NL} and q_{PL} were estimated as a 10% higher that the maximum value of the respective quota. * Parameters estimated with *fminsearch* in Matlab.

8.4 Fitting of the model

We estimate parameters of the model with experimental data from [15]. Experiments were carried out in a 8-L batch reactor with mixed green microalgal consortium consisting mainly of *Chlorella sorokiniana* and *Scenedesmus sp.*. Constant aeration with CO_2 enriched air (5% CO_2) at a flow rate of $20\,L/h$ was used to mix biomass and to provide CO_2. The reactor is illuminated from above (flat-surface) with an incident light intensity of $1500 \pm 150\,\mu mol\,m^{-2}\,s^{-1}$. The temperature and the pH vary in the ranges $23-24\,°C$ and $6.8-7.9$ respectively.

The measured variables are the microalgae concentration x, the nitrogen biomass ($x_N := xq_N$), the phosphorus biomass ($x_P := xq_P$), the chlorophyll quota θ, and the external nutrient concentrations. The quotas q_{N0} and q_{P0} are estimated as the minimum of the experimental values of the respective quota, and the quotas q_{NL} and q_{PL} were estimated as a 10% higher than the maximum value of the respective quota. The parameters γ_m, δ_0 α, I^*, $\rho_{NH_4,max}$, $\rho_{NO_3,max}$, $\rho_{PO_4,max}$, and m are determined with the optimization solver of MATLAB *fminsolve*. The objective function to minimize is the square error normalized to the range of the observed data *i.e.*

$$\sum_{Y=x,x_N,x_P,\ldots} \sum_{i=1}^{N} \left(\frac{Y_{model,i} - Y_{obs,i}}{Y_{obs,max} - Y_{obs,min}} \right)^2 \tag{8.14}$$

The solver is initialized with parameters from literature [13, 16]. Results are given in Table 8.3 and Figure 8.2.

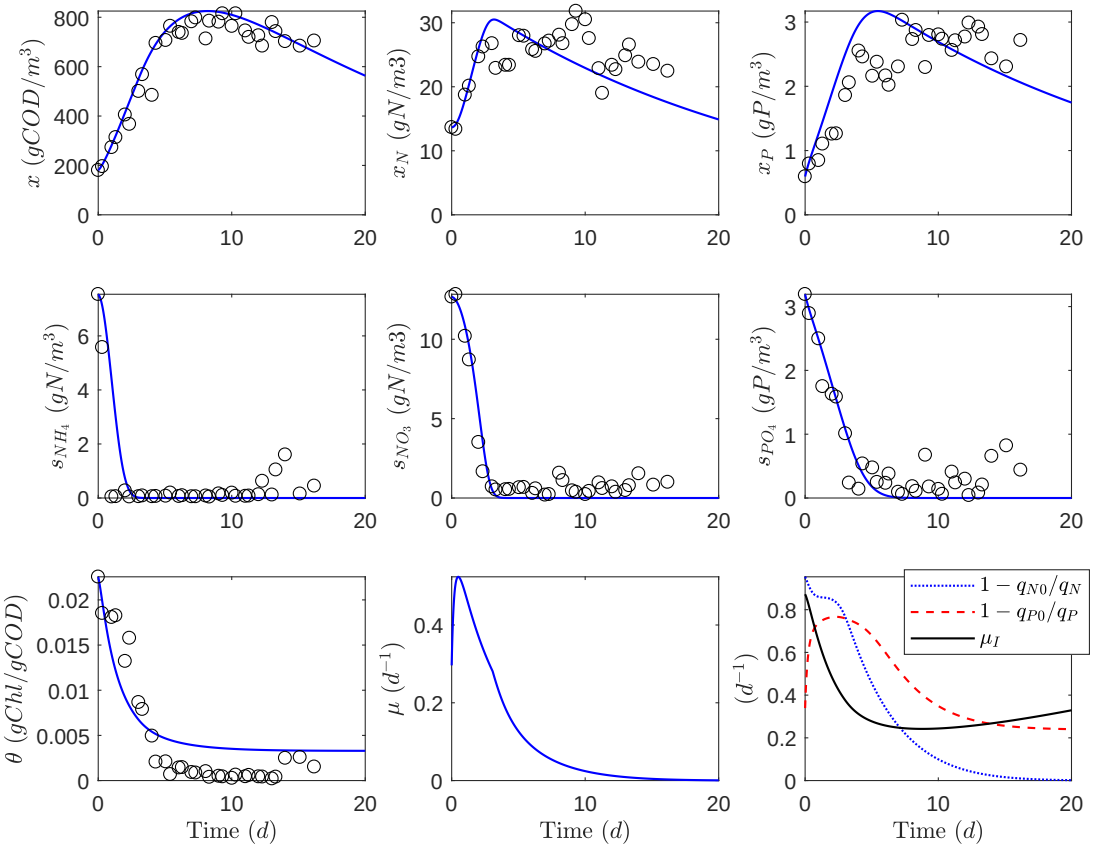

Figure 8.2: Simulation with parameters from Table 8.3.

8.5 Removal capacity of the system

Simulations of the model for different initial conditions show that trajectories approach towards a steady state; either the washout characterized by the absence of microalgae, or a positive steady state characterized by the presence of microalgae. In some cases, the positive steady state is reached by any solution starting with a positive initial microalgae concentration. In other cases, the model faces bi-stability, i.e. depending on the initial conditions, the solutions of the model approach to the washout or the positive steady state. This is consistent with the results presented in Chapter 5 . Figure 8.3 illustrates this situation. We define the steady state areal removal rate of the nutrient Y (with Y representing NH_4, NO_3, or PO_4) by:

$$R_Y := DL(s_{Y,in} - s'_Y), \tag{8.15}$$

with s'_Y the concentration of the nutrient Y associated to the positive steady state. R_Y indicates the quantity of nutrient Y that is removed per day per unit of area of the reactor.

To evaluate the removal rate at steady state operation, we run the model for 500 days with high initial microalgae concentrations ($300\, gCOD/m^3$) to avoid the extinction if bistability occurs. Thus, s'_Y is given by the evaluation of the simulated s_Y at the day 500. The results of these evaluations for different values of the dilution rate D and the depth L are shown in Figure 8.4 (for $I_{in} = 100\, \mu\, mol\, m^{-2}\, s^{-1}$), Figure 8.5 (for $I_{in} = 500\, \mu\, mol\, m^{-2}\, s^{-1}$), and

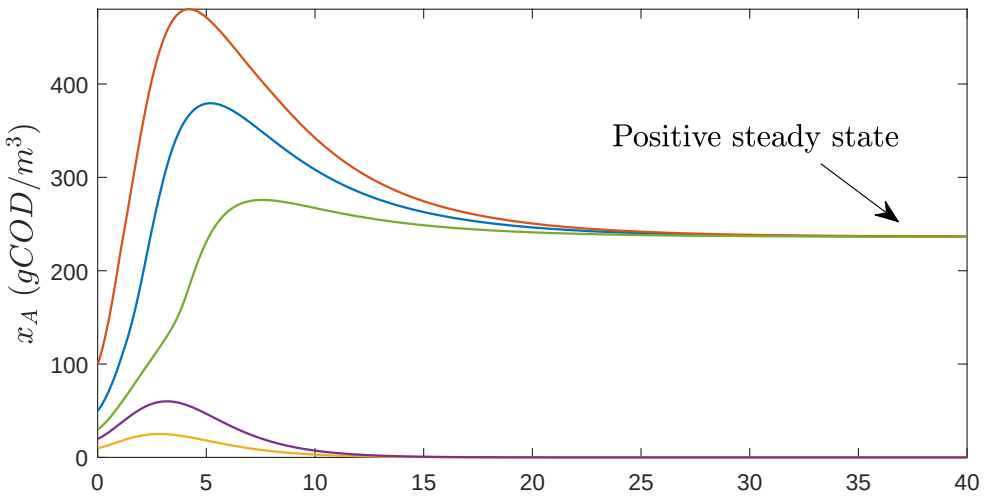

Figure 8.3: Simulated microalgae evolution for different initial microalgae concentrations. If the initial microalgae concentration is over a certain threshold then a positive steady state is reached, otherwise, microalgae go extinct. Kinetic parameters are taken from Table 8.3. Operational parameters are $I_{in} = 1500\,\mu\,mol\,m^{-2}\,s^{-1}$, $D = 0.5\,d^{-1}$, $L = 0.2\,m$.

Figure 8.6 (for $I_{in} = 2000\,\mu\,mol\,m^{-2}\,s^{-1}$). Input nutrient concentrations are $s_{NH_4,in} = 25\,gN/m^3$, $s_{NO_3,in} = 5\,gN/m^3$, and $s_{PO_4,in} = 25\,gP/m^3$

Figure 8.4 shows that the removal rates of nutrient are better for depths of 10 or 20 cm. A recent experimental study [12] with a HRAP illuminated with $I_{in} = 100\,\mu\,mol\,m^{-2}\,s^{-1}$ confirms our prediction. In this study, it is shown that a depth 20 cm is better than depths of 30 and 40 cm. However, Figures 8.5 and 8.6 show that for a incident light intensities of $500\,\mu\,mol\,m^{-2}\,s^{-1}$ and $2000\,\mu\,mol\,m^{-2}\,s^{-1}$ respectively, there is a positive relation between removal rates and the depths in the range 0-0.8 m. This is also consistent with other studies. For example in [2], under periodic illumination ($250\,\mu\,mol\,m^{-2}\,s^{-1}$ under a 14 : 10 h light:dark cycle) a depth of 30 cm is more efficient than 15 cm. We also observe that the highest removal rates are reached for $I_{in} = 500\,\mu\,mol\,m^{-2}\,s^{-1}$. For $I_{in} = 100\,\mu\,mol\,m^{-2}\,s^{-1}$ the HRAP is highly photo-limited while for $I_{in} = 2000\,\mu\,mol\,m^{-2}\,s^{-1}$ it is photoinhibited.

In Figures 8.4 and 8.5 we observe that nitrogen nutrients (NH_4 and NO_3) in the HRAP increase with the dilution rate, while in Figure 8.6 the nitrogen nutrients reach a minimum concentration at an intermediate, and very low, dilution rate. In all cases, PO_4 concentration reaches a minimum value at an intermediate dilution rate. Thus, determining operational parameters is not trivial for keeping all the concentration under a certain threshold. While NH_4 is very low (D close to zero), PO_4 may be close to the input concentration (Figure 8.6).

A last observation is that the range of dilution rates at which the HRAP removes nutrients is highly dependent on the water depth and on the incident light. In Figure 8.4, the maximum dilution rate for a positive equilibrium cannot be higher than $0.15\,d^{-1}$ while in Figure 8.5 can be higher than $0.9\,d^{-1}$ for a depth of $10\,cm$.

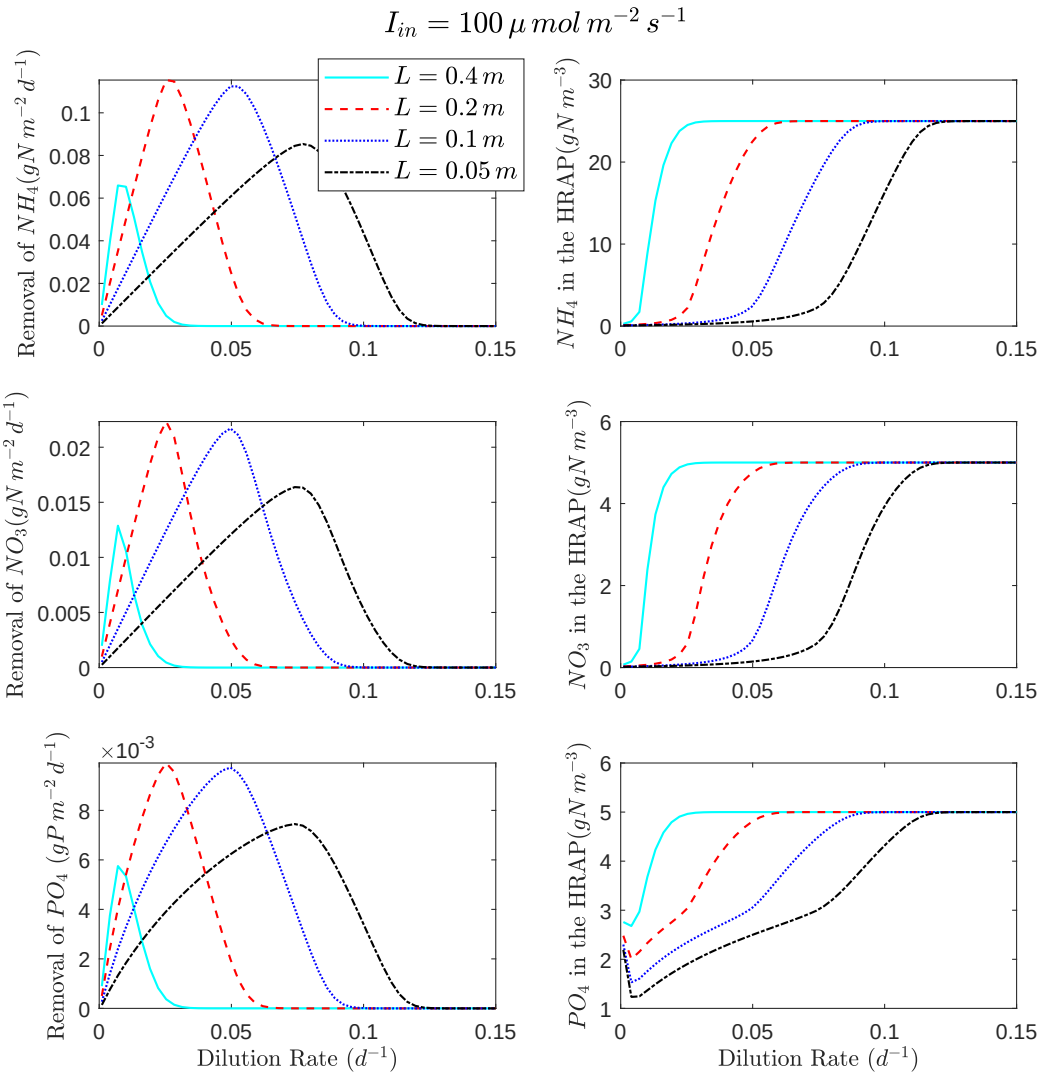

Figure 8.4: Removal rates and concentrations in the HRAP of NH_4, NO_3, and PO_4, for different values of D and $L.I_{in} = 100\,\mu\,mol\,m^{-2}\,s^{-1}$, $K_{bg} = 10\,m^{-1}$. The rest of parameters are taken from Table 8.3.

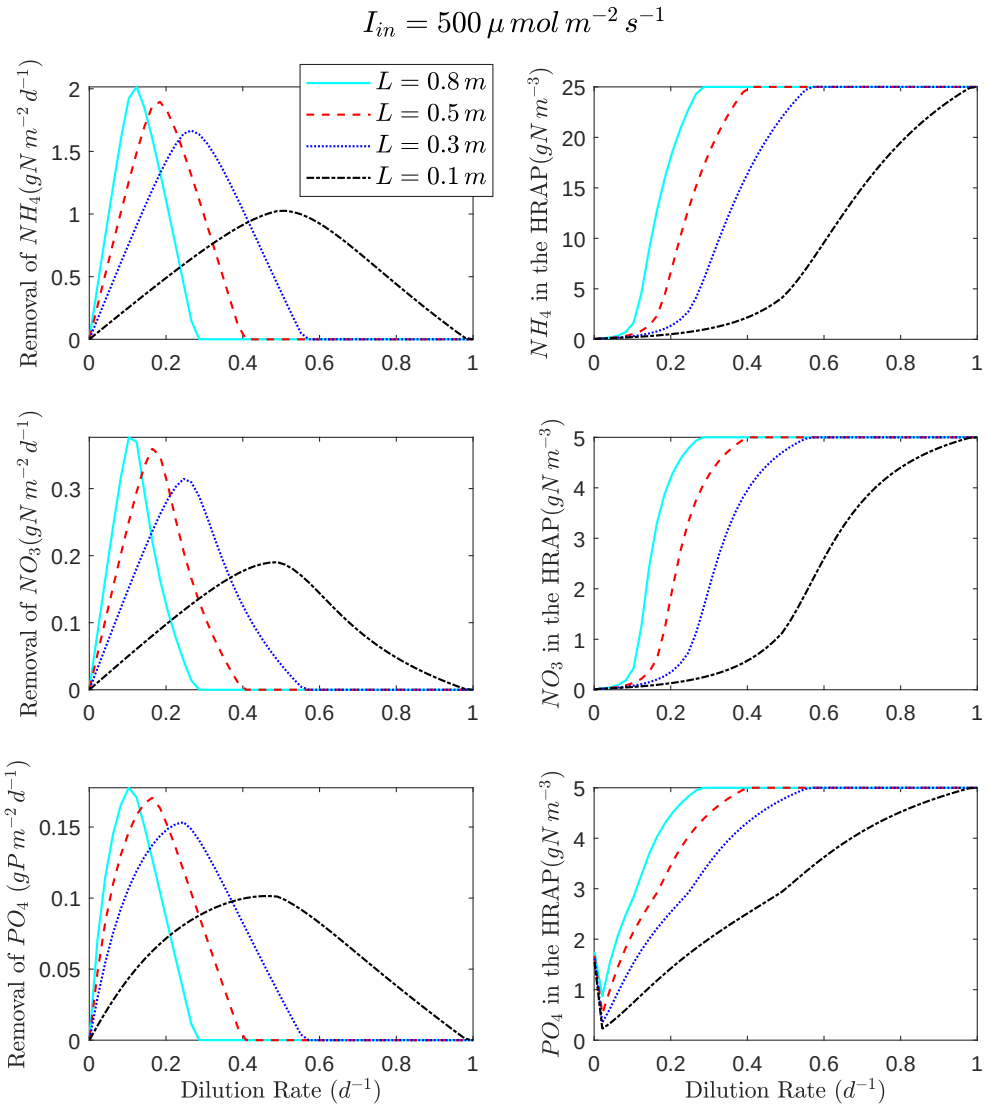

Figure 8.5: Removal rates and concentrations in the HRAP of NH_4, NO_3, and PO_4, for different values of D and L.$I_{in} = 500\,\mu mol\,m^{-2}\,s^{-1}$, $K_{bg} = 10\,m^{-1}$. The rest of parameters are taken from Table 8.3.

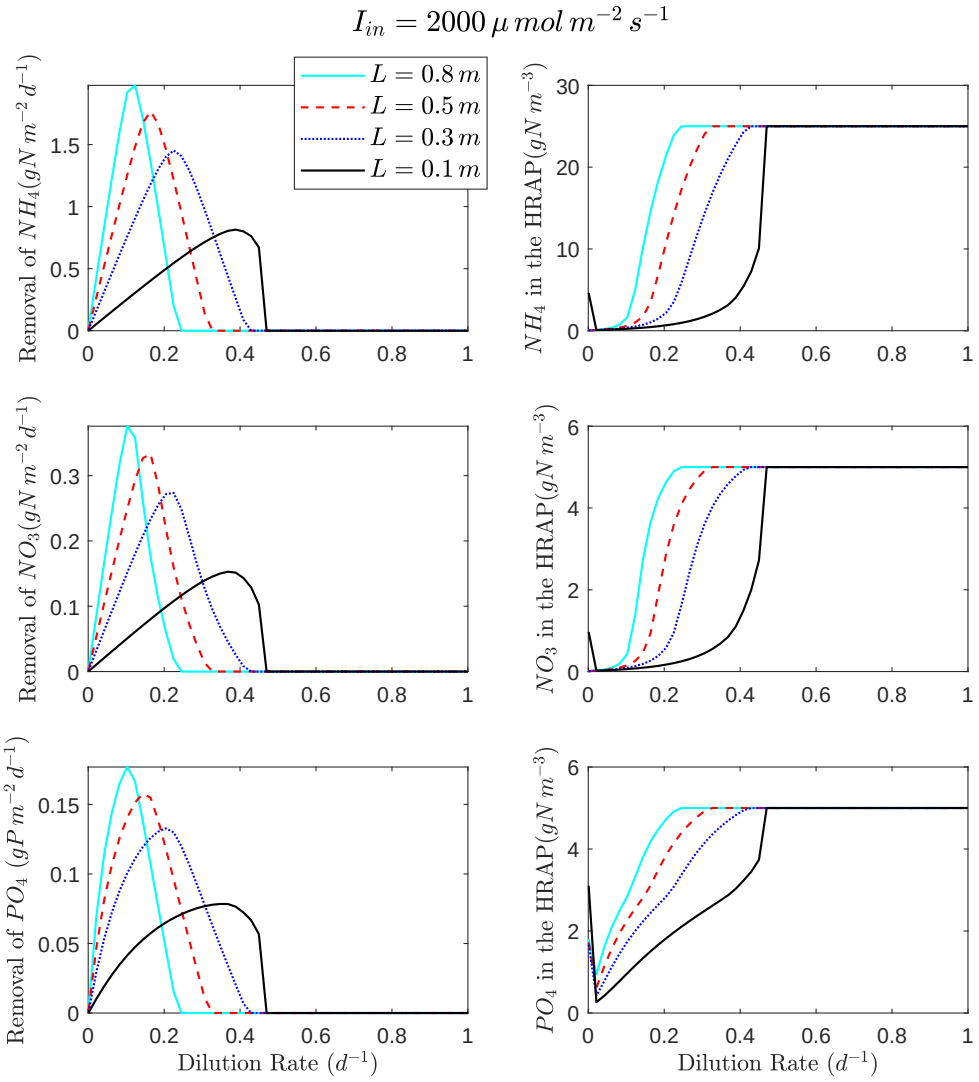

Figure 8.6: Removal rates and concentrations in the HRAP of NH_4, NO_3, and PO_4, for different values of D and $L.I_{in} = 2000\,\mu mol\,m^{-2}\,s^{-1}$, $K_{bg} = 10\,m^{-1}$. The rest of parameters are taken from Table 8.3.

8.6 Conclusions

We built a mathematical model for describing microalgae growth in HARPs under limitation by light, phosphorus, and nitrogen. The model shows a good performance in reproducing experimental data of a batch experiment, describing accurately the consumption of the different nutrients in the medium.

We showed that the incident light intensity, the depth of the HRAP, and the dilution rate are all crucial parameters on the operation of a HRAP for nutrient removal. For low incident light intensities, an optimal depth is observed, while for high light intensities deeper HRAPs are better. However, the operational range for the dilution rate decreases for very high light intensities and for too deep HRAPs.

As a future work, temperature of the medium should be considered to evaluate a possible overheating of the HARP at low depths. High temperatures may have a negative effect on micralgae growth.

Bibliography

[1] N. Abdel-Raouf, A. Al-Homaidan, and I. Ibraheem. Microalgae and wastewater treatment. *Saudi Journal of Biological Sciences*, 19(3):257 – 275, 2012.

[2] Z. Arbib, I. de Godos, J. Ruiz, and J. A. Perales. Optimization of

pilot high rate algal ponds for simultaneous nutrient removal and lipids production. *Science of the Total Environment*, 589:66–72, 2017.

[3] O. Bernard. Hurdles and challenges for modelling and control of microalgae for co2 mitigation and biofuel production. *Journal of Process Control*, 21(10):1378–1389, 2011.

[4] O. Bernard, F. Mairet, and B. Chachuat. Modelling of microalgae culture systems with applications to control and optimization. In *Microalgae Biotechnology*, pages 59–87. Springer, 2015.

[5] O. Bernard, F. Mairet, and B. Chachuat. *Modelling of Microalgae Culture Systems with Applications to Control and Optimization*, pages 59–87. Springer International Publishing, Cham, 2016.

[6] G. Bougaran, O. Bernard, and A. Sciandra. Modeling continuous cultures of microalgae colimited by nitrogen and phosphorus. *Journal of theoretical biology*, 265(3):443–454, 2010.

[7] P. S. Davies. The biological basis of wastewater treatment. *Strathkelvin Instruments Ltd*, 3, 2005.

[8] Q. Dortch. The interaction between ammonium and nitrate uptake in phytoplankton. *Marine ecology progress series. Oldendorf*, 61(1):183–201, 1990.

[9] M. R. Droop. Vitamin B 12 and marine ecology. iv. the kinetics of uptake, growth and inhibition in monochrysis lutheri. *Journal of the Marine Biological Association of the United Kingdom*, 48(3):689–733, 1968.

[10] J. S. Guest, M. C. van Loosdrecht, S. J. Skerlos, and N. G. Love. Lumped pathway metabolic model of organic carbon accumulation and mobilization by the alga chlamydomonas reinhardtii. *Environmental science & technology*, 47(7):3258–3267, 2013.

[11] J. Huisman, H. C. Matthijs, P. M. Visser, H. Balke, C. A. Sigon, J. Passarge, F. J. Weissing, and L. R. Mur. Principles of the light-limited chemostat: theory and ecological applications. *Antonie van Leeuwenhoek*, 81(1):117–133, Dec 2002.

[12] B.-H. Kim, J.-E. Choi, K. Cho, Z. Kang, R. Ramanan, D.-G. Moon, H.-S. Kim, et al. Influence of water depth on microalgal production, biomass harvest, and energy consumption in high rate algal pond using municipal wastewater. *J. Microbiol. Biotechnol.*, 28(4):630–637, 2018.

[13] F. Mairet, O. Bernard, P. Masci, T. Lacour, and A. Sciandra. Modelling neutral lipid production by the microalga isochrysis aff. galbana under nitrogen limitation. *Bioresource Technology*, 102(1):142–149, 2011.

[14] B. S. Sturm and S. L. Lamer. An energy evaluation of coupling nutrient removal from wastewater with algal biomass production. *Applied Energy*, 88(10):3499–3506, 2011.

[15] D. S. Wágner, B. Valverde-Pérez, and B. G. Plósz. Light attenuation in photobioreactors and algal pigmentation under different growth conditions–model identification and complexity assessment. *Algal research*, 35:488–499, 2018.

[16] D. S. Wágner, B. Valverde-Pérez, M. Sæbø, M. B. de la Sotilla, J. Van Wagenen, B. F. Smets, and B. G. Plósz. Towards a consensus-based biokinetic model for green microalgae–the asm-a. *Water research*, 103:485–499, 2016.

CHAPTER 9

Conclusions

In this thesis, we have proposed a deeper insight into the dynamics of microalgae culture at high density, with four main contributions.

Main contributions.

First, in Chapter 3, we have expanded on the work in [14] and [13] in order to better understand and characterize the impact of light on microalgae cultures for which all the nutrients were in excess. The difficulty is that such processes can be at the same time photolimited (in the darkest area of the reactor and on average) and photoinhibited at the periphery of the reactor. We have shown that this typically can give rise to an Allee effect associated with bistability. This phenomenon persists when considering more realistic periodic patterns reflecting daily light variations, but also temperature fluctuations which both drive the growth dynamics in outdoor conditions. We have also better characterized the impact of the reactor geometry on the resulting productivity, and shown that some geometries are more adapted to certain situations.

Then we have explored how microalgae growth is affected by additional limiting elements (Chapters 4 and 5) focusing on the dynamics of microalgae cultures under co-limitation by light and nutrients. This part consists in a mathematical analysis based on different tools from the theory of dynamical systems. The behaviour of such systems turns out to be complex and multistability situations appear.

The co-limitation situation thus reveals quite tricky, and appears for a large range of external light intensities and influent nutrient concentrations. It is therefore very likely that, in many experimental situations where authors focus on nutrient limitation, the impact of light must also be considered whenever cell density is large enough to generate a marked light gradient.

Then, in Chapters 6 and 7, we have explored control strategies for maximizing microalgae productivity. From our understanding of the mechanisms driving these dynamical systems, it became clear that shadowing the culture was beneficial in some situations, especially at the inoculum phases, to avoid the Allee effect. We have also shown that playing with culture depth (when accounting for background turbidity) was at the same time a powerful and a simple way to improve productivity. We have also initiated some work towards dynamical optimal control, but much remain to be done on the theoretical side to derive a control strategy when dealing with light fluctuation.

Chapter 8 was dedicated to another extension of the model. We proposed a new model accounting for co-limitation by light, phosphorus, and nitrogen, including photoacclimation dynamics. This model accurately reproduced experimental data, but its high dimension leads to a very challenging level of mathematical complexity. Understanding all the potential behaviour of its dynamics will still necessitate a lot of work. But we do believe that the theoretical developments carried out in the previous chapters can greatly help in understanding such systems. Of course, the model is interesting for its genericity and its ability to describe a broad range of situations including

the cases when three limitations simultaneously appear.

Most of our work has been carried out considering generic model hypotheses. The conclusions are therefore rather independent from the exact form of the functions, and, of course, of the chosen parameters. In some cases, we did not assume differentiability hypotheses, so that Liebig's law of the minimum, for example, can be considered.

Increasing microalgae productivity.

Production of microalgae is still challenging, especially in full-scale systems subjected to permanent fluctuations of light intensity and temperature. To attain maximum productivity in these systems, a crucial parameter is light that must be provided at an appropriate intensity to enhance growth [7]. Low light intensities will become growth-limiting, notably in dense cultures due to self-shading, while too high levels may lead to photoinhibition [17]. In this context, we gave some new insights on the optimization of biomass productivity.

For cultures illuminated under constant light intensity, some authors proposed that maximal productivities can be attained by maintaining the light intensity such that the growth rate at the bottom equals the loss rate [9, 18, 25]. We have revisited and extended this strategy proposing that the incident light intensity should be chosen such that the growth rate at the top of the reactor should also equal the loss rate. In that way, the range of

light intensities inside the culture corresponds to the maximal range resulting in a non-negative net growth. This strategy is only valid when background turbidity is neglected. This aspect should be considered in a future work.

In outdoor cultures, the incident light intensity, or sunlight, cannot be directly controlled. It might be believed that in outdoor cultures light is always a limiting factor. However, a loss of productivity due to an excess of sunlight during the midday was shown experimentally in [26]. We proposed a strategy for shadowing microalgae cultures in order to decrease the negative effects of photoinhibition. This strategy not only results in an increase of productivity (see Figure 6.5), but avoids possible extinction of microalgae (see Figure 6.7), by eliminating the Allee effect, and allows to gain time in culturing (see Figure 6.6). According to Figure 6.5, high productivities can be reached even for high dilution rates. For example, similar productivities are reached for dilution rates of $0.2\,d^{-1}$ and $0.6\,d^{-1}$. This suggests an intensifying strategy where the same productivity could be reached reducing the reactor size to one-third which could significantly decrease production costs. Shading systems are used nowadays for plant cultures in greenhouse [12]. Some projects have even explored the combination of microalgae with photovoltaic panels producing electricity so that the shadowing of the culture can at the same time produce a fraction of the energy needed for mixing or harvesting [24]. As a future work, this optimal strategy should be adapted to deal with technical constraints of such shading systems for real implementation.

Wastewater treatment with microalgae.

Microalgae cultivation in high rate algal ponds (HRAP) has been well known for decades for removing contaminants from wastewater effluents [21]. This can also reduce costs of biomass production when green chemistry is targeted, including biofuel, with concomitant carbon dioxide sequestration [19, 20]. However, raw wastewater is characterized by a high background turbidity (turbidity due to organic matter and colored substances) which can highly limit the availability of light for microalgae. Our results suggest that background turbidity may have a positive effect in eliminating the Allee effect (due to photoinhibition), but strongly reduces the productivity of microalgae. This negative effect increases with the depth of the HRAP (see Figure 3.10) which is a first indication that many industrial systems are too deep. Designing HRAPs with a much lower depth must be considered as a way to significantly improve microalgae productivity and thus oxygen production rate to support the bacterial activity. Nevertheless, this may result in very high dense cultures which will rapidly suffer from nutrient limitation. Thus the depth of the HRAPs system is a crucial design parameter, and when intensifying the process, the impact of nutrient limitation must be jointly considered in the study and the optimization. The more complicated model presented in the last chapter can therefore be used, at least to determine if a double, or a triple, limitation is likely to occur.

When considering more realistic outdoor conditions such as periodic fluc-

tuations of environmental factors such as light or medium temperature together with prolonged continuous periodic culture operation (periodic dilution rate and nutrient supply), we demonstrated that periodic concentrations can be maintained in the culture. We formulated an optimization problem, and a strategy to solve it. This algorithm provides the optimal values of the depth to maximize microalgae productivity in a periodic regime. Numerical results suggest an optimal depth of around $20\,cm$ when background turbidity is taken into account. However, typically HRAPs are designed with a depth of about $30 - 35\,cm$ [10, 22]. Our findings are confirmed by a recent experimental study [15] that showed that a depth of $20\,cm$ is better than deeper ponds in terms of productivity and nutrient removals. In [1] a depth of $30\,cm$ was better than $15\,cm$, which is probably due to overarming at too low depths. More comparative experimental studies should be carried out considering the impact of depth for corroborating our theoretical results.

As future work, the choice of the optimal depth should include thermal considerations. Temperature is a factor which also deeply influences microalgae development [23]. One of the problems of microalgae is overheating during the most sunny hours of the day, especially during summer. Lower pond depth means lower thermal inertia and therefore a rapid temperature increase under strong solar fluxes. Processes with low depth are likely to overwarm very rapidly in hot seasons [11] and a trade-off between light and temperature performances should be found.

Phytoplankton blooms in the oceans.

Prediction of phytoplankton blooms in lakes and oceans has been a recurrent subject of research. This question is of utmost importance, when dealing with harmful algal blooms that cause environmental damage, economic losses, and disease outbreaks [3]. A fundamental understanding of this problem is still lacking, since many factors are known to influence where and when phytoplankton blooms occur. Water temperature, density, and salinity, hydrography of the region, availability of nutrients and sunlight levels are the most important factors. The determinism of the blooms stays unclear and the range of environmental conditions under which blooms occur makes them somewhat difficult to study. Existing physical prediction models have difficulties distinguishing between each factor when predicting algal blooms, and many variable data sources are required for the analysis [16].

Among the results that we get, some could help understanding how suddenly a single species massively dominates the ecosystem. The Allee effect that we demonstrated explains, for chemostat models, why a population of phytoplankton can stay at a minimal level even if all the conditions for growth seem to be available. Photoinhibition has been shown to be the key factor, which prevents the algal development. Once a population can reach a large enough density, because of the advection of cells, or due to temporal reduction of light, it might cross the Allee gap, and then the population would

explode. Of course, such an explanation has been rigorously shown only in a perfectly mixed chemostat, where the patterns are constant or periodic. The extrapolation to the oceanic environment must be taken with care where temperature and spatial gradients may play a determinant role. But there is a chance that our results can be extrapolated to a cascade of reactors (considering each reactor as an ocean layer), and that this Allee effect can still appear in this more complicated situation. Developing new models, more suitable for the natural environment would be very helpful for integrating temperature and space in the theory. The analysis of such spatial models (which can be limited in a first stage to a series of coupled dynamical systems) may further confirm the explanations and the related theory extracted from our simple chemostat models.

Dynamical systems and microalgae.

The theory of differential equations and dynamical systems have shown to be very useful in the study of the dynamics of light-limited chemostat models. An important property in our analysis, especially for the Droop model, was the cooperativity between the microalgae concentration and the concentration of stored element. This property was used to show that any solution of the model asymptotically approaches a steady state solution (Chapter 5) or a periodic solution in the case of periodic forcing (Chapter 4). As far as we know, this kind of cooperativity has not been exploited before to derive dynamical properties of photobioreactors.

In the absence of Allee effect, as in the case of Chapter 4, we used some ideas from the theory of sub-homogeneous dynamical systems (developed in Chapter 2 in [29]) to prove the uniqueness of non-trivial periodic solutions (see Theorem 4.5.2). Classical techniques fail due to the dependence of the growth rate on the microalgae population density.

In both Chapters 4 and 5, conditions for the persistence of the microalgae population were given. In the autonomous case, we gave a threshold result on the persistence (see Theorem 5.4.5), but in the periodic case we only found sufficient conditions (see Theorem 4.5.1). A detailed discussion about this is given in Section 4.7. Under periodic forcing, the proof of the persistence result was mainly based on persistence results for periodic Kolmogorov equations [27] and on the theory of asymptotically periodic semiflows [28], while in the autonomous case an analysis of the local stability of the washout steady state sufficed.

Perspectives: impact of photoacclimation on the reactor dynamics.

In Chapter 8, we introduced photoacclimation of algae, *i.e.* their ability to modulate their pigment content so that they can more efficiently use the available light. Photoacclimation will subsequently modify the light distribution in the reactor. Accounting for the photoacclimation dynamics may therefore modulate some of our theoretical results. First, let us remark that, at high density, the average light in the reactor represents less than 15% of

the incident light [4]. It has been shown [8] that microalgae photoacclimate to the average light intensity they perceive, so that in these conditions, the cells are most of the time acclimated to low light. Numerical simulations in Chapter 8 suggest that some theoretical results from the previous chapters remain valid: existence of bi-stability, existence of optimal values of the depth and/or the dilution rate, existence of stable equilibria etc. However further studies are needed to understand the influence of the photoacclimation dynamics, and identify the situations complexifying the dynamics of the chemostat with photosynthetic organisms. But better understanding photoacclimation is also an opportunity to control this mechanism, and eventually end-up with more transparent microalgae, with better light transmission properties and eventually a higher productivity.

Perspectives: including the effect of temperature.

In our study, the impact of medium temperature on microalgae growth has been tackled indirectly, by considering periodic kinetic functions. This first approach does not consider all the possible effects of temperature. Actually, temperature has been shown for example to strongly influence the cellular chemical composition of microalgae [5]. Temperature also highly affects photoacclimation and therefore the transparency of the microalgae. It is worth remarking that temperature is somehow strongly linked to light. The most sunny conditions which are likely to produce strong photoinhibition are also susceptible to warmup the growth medium up to temperatures which become lethal for the cells [2]. In that sense, it makes the problem

of high light even more critical than just considering it under the angle of photoinhibition. Reducing temperature of a large scale cultivation system is very expensive and impacting from the environmental point of view, and this strategy cannot by itself address the problem. If temperature similarly affects all the biological processes through a certain positive function $\phi(T)$ which multiplies all the model kinetics, it is worth remarking that a time change would eliminate such term and the model could be reduced to a dynamical model independent of temperature, but with a temperature dependant time. Temperature fluctuations have nevertheless other consequences, such as synchronizing cell division [6], which may modify the population dynamics. Upgrading our model by including temperature, and validating it with experimental data where both light and temperature fluctuate is therefore an important milestone to more extensively capture the dynamics of solar photobioreactors. Temperature plays also a key role in nature, and such models would also be useful to face *in situ* topics. Revisiting the presented theories when considering temperature fluctuations will highly extend the scope of our results and definitely encompass a very large range of realistic situations. But increasing the dimension of a nonlinear dynamical model, adding even just one more state variable, often leads to rapid mathematical bottlenecks, and several PhD theses will still be necessary to more exhaustively explore the subject and eventually produce a clear picture of the dynamics.

Bibliography

[1] Z. Arbib, I. de Godos, J. Ruiz, and J. A. Perales. Optimization of pilot high rate algal ponds for simultaneous nutrient removal and lipids production. *Science of the Total Environment*, 589:66–72, 2017.

[2] Q. Béchet, M. Laviale, N. Arsapin, H. Bonnefond, and O. Bernard. Modeling the impact of high temperatures on microalgal viability and photosynthetic activity. *Biotechnology for biofuels*, 10(1):136, 2017.

[3] J. M. Beman, K. R. Arrigo, and P. A. Matson. Agricultural runoff fuels large phytoplankton blooms in vulnerable areas of the ocean. *Nature*, 434(7030):211, 2005.

[4] O. Bernard, F. Mairet, and B. Chachuat. Modelling of microalgae culture systems with applications to control and optimization. In *Microalgae Biotechnology*, pages 59–87. Springer, 2015.

[5] O. Bernard and B. Rémond. Validation of a simple model accounting for light and temperature effect on microalgal growth. *Bioresource technology*, 123:520–527, 2012.

[6] H. Bonnefond, N. Moelants, A. Talec, O. Bernard, and A. Sciandra. Concomitant effects of light and temperature diel variations on the growth rate and lipid production of dunaliella salina. *Algal research*, 14:72–78, 2016.

[7] A. P. Carvalho, S. O. Silva, J. M. Baptista, and F. X. Malcata. Light requirements in microalgal photobioreactors: an overview of biophotonic

aspects. *Applied Microbiology and Biotechnology*, 89(5):1275–1288, Mar 2011.

[8] C. Combe, P. Hartmann, S. Rabouille, A. Talec, O. Bernard, and A. Sciandra. Long-term adaptive response to high-frequency light signals in the unicellular photosynthetic eukaryote dunaliella salina. *Biotechnology and bioengineering*, 112(6):1111–1121, 2015.

[9] J.-F. Cornet. Calculation of optimal design and ideal productivities of volumetrically lightened photobioreactors using the constructal approach. *Chemical Engineering Science*, 65(2):985–998, 2010.

[10] R. Craggs, D. Sutherland, and H. Campbell. Hectare-scale demonstration of high rate algal ponds for enhanced wastewater treatment and biofuel production. *Journal of Applied Phycology*, 24(3):329–337, 2012.

[11] R. De-Luca, F. Bezzo, Q. Béchet, and O. Bernard. Exploiting meteorological forecasts for the optimal operation of algal ponds. *Journal of Process Control*, 55:55–65, 2017.

[12] M. P. Gent. Effect of degree and duration of shade on quality of greenhouse tomato. *HortScience*, 42(3):514–520, 2007.

[13] D. J. Gerla, W. M. Mooij, and J. Huisman. Photoinhibition and the assembly of light-limited phytoplankton communities. *Oikos*, 120(3):359–368, 2011.

[14] J. Huisman, H. C. Matthijs, P. M. Visser, H. Balke, C. A. Sigon, J. Passarge, F. J. Weissing, and L. R. Mur. Principles of the light-limited

chemostat: theory and ecological applications. *Antonie van Leeuwenhoek*, 81(1-4):117–133, 2002.

[15] B.-H. Kim, J.-E. Choi, K. Cho, Z. Kang, R. Ramanan, D.-G. Moon, H.-S. Kim, et al. Influence of water depth on microalgal production, biomass harvest, and energy consumption in high rate algal pond using municipal wastewater. *J. Microbiol. Biotechnol.*, 28(4):630–637, 2018.

[16] S. Lee and D. Lee. Improved prediction of harmful algal blooms in four major south koreas rivers using deep learning models. *International journal of environmental research and public health*, 15(7):1322, 2018.

[17] S. Long, S. Humphries, and P. G. Falkowski. Photoinhibition of photosynthesis in nature. *Annual review of plant biology*, 45(1):633–662, 1994.

[18] P. Masci, F. Grognard, and O. Bernard. Microalgal biomass surface productivity optimization based on a photobioreactor model. *IFAC Proceedings Volumes*, 43(6):180–185, 2010.

[19] W. Mulbry, S. Kondrad, C. Pizarro, and E. Kebede-Westhead. Treatment of dairy manure effluent using freshwater algae: algal productivity and recovery of manure nutrients using pilot-scale algal turf scrubbers. *Bioresource technology*, 99(17):8137–8142, 2008.

[20] E. J. Olguın. Phycoremediation: key issues for cost-effective nutrient removal processes. *Biotechnology advances*, 22(1-2):81–91, 2003.

[21] W. Oswald. Waste water reclamation through the production of algae. 1959.

[22] J. Park, R. Craggs, and A. Shilton. Wastewater treatment high rate algal ponds for biofuel production. *Bioresource technology*, 102(1):35–42, 2011.

[23] M. Ras, J.-P. Steyer, and O. Bernard. Temperature effect on microalgae: a crucial factor for outdoor production. *Reviews in environmental science and bio/technology*, 12(2):153–164, 2013.

[24] E. Sforza, E. Barbera, and A. Bertucco. Improving the photoconversion efficiency: An integrated photovoltaic-photobioreactor system for microalgal cultivation. *Algal research*, 10:202–209, 2015.

[25] H. Takache, G. Christophe, J.-F. Cornet, and J. Pruvost. Experimental and theoretical assessment of maximum productivities for the microalgae chlamydomonas reinhardtii in two different geometries of photobioreactors. *Biotechnology progress*, 26(2):431–440, 2010.

[26] A. Vonshak and R. Guy. Photoadaptation, photoinhibition and productivity in the blue-green alga, spirulina platensis grown outdoors. *Plant, Cell & Environment*, 15(5):613–616, 1992.

[27] G. S. Wolkowicz, X.-Q. Zhao, et al. n-species competition in a periodic chemostat. *Differential and Integral Equations*, 11(3):465–491, 1998.

[28] X.-q. Zhao. Asymptotic behavior for asymptotically periodic semiflows with applications. In *MR 97i: 58150*. Citeseer, 1996.

[29] X.-Q. Zhao, J. Borwein, and P. Borwein. *Dynamical systems in population biology*, volume 16. Springer, 2003.

Appendix A

This Appendix present the lemmas and propositions used in Chapter 3. We assume that Assumptions 3.4.1 and 3.4.2 hold. The first lemma gives in detail the properties of the function g defined in (3.23). We note that (3.23) does not define g when I_{in} or I_{out} are equal to zero. However, from the definition of the AGR (see (3.5)), it is natural to define

$$g(0, I_{out}) = g(I_{in}, 0) = \mu(0). \tag{1}$$

In the reality I_{out} is never higher that I_{in}. However, we study the behavior of g for any value of I_{out}. This is necessary for proving Lemma A3.

Lemma A1. *(Properties of g) Let $g : \mathbb{R}_+ \times \mathbb{R}_+ \longrightarrow \mathbb{R}$ defined by (3.23) and (1).*

a) (Symmetry) $g(I_{in}, I_{out}) = g(I_{out}, I_{in})$ for all $I_{in}, I_{out} \geq 0$.

b) (Partial continuity) $g(I_{in}, \cdot)$ is continuous on $\mathbb{R}_+$ for all $I_{in} \in \mathbb{R}_+$.

c) (Unimodal function with respect to I_{out}) For any $I_{in} > 0$, there exists a unique $\gamma(I_{in}) > 0$ satisfying

$$g(I_{in}, \gamma(I_{in})) = p(\gamma(I_{in})). \tag{2}$$

It holds that $g(I_{in}, \cdot)$ is strictly increasing on $[0, \gamma(I_{in})]$ and strictly de-

creasing on $[\gamma(I_{in}), \infty)$*, moreover,*

- *if* $I_{in} > I^*$*, then* $\gamma(I_{in}) \in (\sigma(I_{in}), I^*)$*,*
- *if* $I_{in} = I^*$*, then* $\gamma(I_{in}) = I^*$*, and*
- *if* $I_{in} < I^*$*, then* $\gamma(I_{in}) \in (I^*, \sigma(I_{in}))$*.*

Proof. The proof of the part a) follows directly from the definition of g. For the part b), following [1], we can easily determine that $\lim_{I_{out} \to I_{in}} g(I_{in}, I_{out}) = p(I_{in})$ and $\lim_{I_{out} \to 0} g(I_{in}, I_{out}) = p(0)$, which completes the proof.

For the part c), let $I_{in} > 0$ be given. By using (3.23), we can determine the partial derivative of g with respect to I_{out}:

$$\frac{\partial g(I_{in}, I_{out})}{\partial I_{out}} = \frac{1}{I_{out}[\ln(I_{in}) - \ln(I_{out})]^2} \phi(I_{out}), \tag{3}$$

with $\phi(I_{out}) = \int_{I_{out}}^{I_{in}} \frac{p(I) - p(I_{out})}{I} dI$. Since $I_{out}[\ln(I_{in}) - \ln(I_{out})]^2 > 0$ for any $I_{out} \in (0, I_{in})$, the sign of $\frac{\partial g(I_{in}, I_{out})}{\partial I_{out}}$ is determined by the sign of $p(I_{out})$.

Let us assume that $I_{in} > I^*$ and let $I_{out} \in [0, \sigma(I_{in})]$. Since p is strictly increasing on $[0, \sigma(I_{in})]$, we have that $p(I) > p(I_{out})$ for all $I \in [I_{out}, \sigma(I_{in}))$. This implies that $\phi(I_{out}) > 0$. Since I_{out} was chosen arbitrarily we conclude that $\phi(I_{out}) > 0$ for all $I_{out} \in [0, \sigma(I_{in})]$. In the same way we can prove that $\phi(I_{out}) < 0$ for all $I_{out} \in [I^*, \infty)$. By the intermediate value theorem there exists $I' \in (\sigma(I_{in}), I^*)$ such that $\phi(I') = 0$. Suppose there exists another $I'' \in (\sigma(I_{in}), I^*)$ such that $\phi(I'') = 0$. By using elemental properties of

integrals, it can be shown that the equality $\phi(I') = \phi(I'')$ implies

$$\int_{I''}^{I_{in}} \frac{p(I') - p(I'')}{I} dI = \int_{I'}^{I''} \frac{p(I) - p(I')}{I} dI. \tag{4}$$

Suppose that $I'' > I'$. Since p is strictly increasing on $[0, I^*]$, we have that $p(I) \geq p(I')$ for all $I \in [I', I'']$. Thus the left side in (4) is negative, while the right side is positive. This contradiction shows that I' is the unique root of ϕ. Hence ϕ is positive on $[0, I')$ and negative on (I', ∞). Consequently, $g(I_{in}, \cdot)$ is strictly increasing on $[0, I')$ and strictly decreasing on (I', ∞). By taking $\gamma(I_{in}) = I'$ we conclude the proof. The case $I_{in} \leq I^*$ follows the same arguments. □

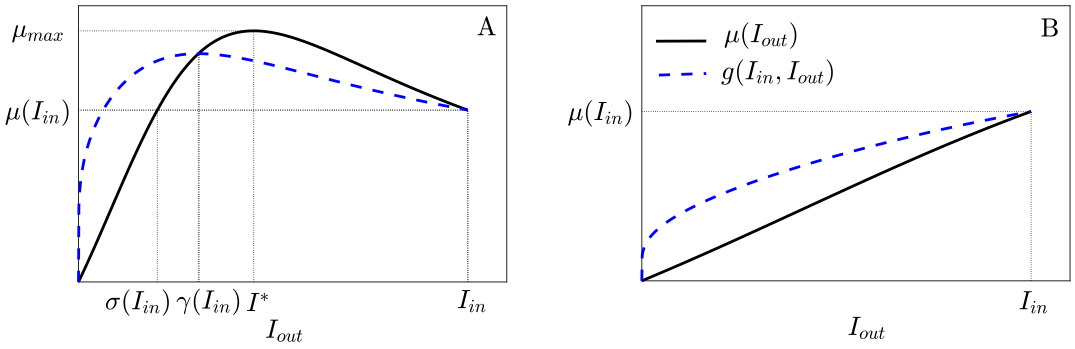

Figure 1: Plot of specific productivity rate p (continuous line) and the function $g(I_{in}, \cdot)$ (dotted line) as functions of I_{out}. a) $I_{in} > I^*$; the function p has a peak at the optimal irradiance I^*, while the function $g(I_{in}, \cdot)$ has a peak at $\gamma(I_{in})$, where intersects p. According to Lemma A1, $\sigma(I_{in}) < \gamma(I_{in}) < I^*$. Both functions reach the same value at I_{in}. b) $I_{in} \leq I^*$; both functions p and $g(I_{in}, \cdot)$ are strictly increasing reaching the same value when $I_{out} = I_{in}$.

Figure 1 shows graphically the part c) of Lemma A1. The following proposition states the main properties of the AGR (see (3.9) or (3.22)) as a

function of the optical depth λ and the incident light intensity I_{in}.

Proposition A2. *(Properties of the AGR)*

a) $\mu(\lambda, 0) = p(0)$ *for all* $\lambda \in \mathbb{R}_+$, *and* $\mu(0, I_{in}) = p(I_{in})$ *for all* $I_{in} \in \mathbb{R}_+$.

b) If $I_{in} > 0$, *then* $\mu(\cdot, I_{in})$ *is strictly increasing on* $[0, \tilde{\lambda}(I_{in})]$ *and strictly decreasing on* $[\tilde{\lambda}(I_{in}), \infty)$ *with* $\tilde{\lambda}(I_{in})$ *defined by (3.28).*

c) If $\lambda > 0$, *then* $\mu(\lambda, \cdot)$ *is strictly increasing on* $[0, \mathcal{I}(\lambda)]$ *and strictly decreasing on* $[\mathcal{I}(\lambda), \infty)$ *with* $\mathcal{I}(\lambda)$ *defined by the equation*

$$p(\mathcal{I}(\lambda)) = p(\mathcal{I}(\lambda)e^{-\lambda}). \tag{5}$$

d) $\lim_{\lambda \to \infty} \mu(\lambda, I_{in}) = p(0)$ *for any* $I_{in} \in \mathbb{R}_+$.

Proof. Part a) follows directly from the definition of the AGR. For the part b), first we note that I_{out} is always decreasing as a function of λ. This implies that for any interval $J \subset [0, I_{in}]$, if $g(I_{in}, \cdot)$ is strictly increasing (decreasing)in J, then $\mu(\cdot, I_{in})$ is strictly decreasing (increasing) in J^{-1} (as a function of λ), where $J^{-1} = \{\lambda \geq 0\,;\, I_{out}(\lambda, I_{in}) \in J\}$. If $I_{in} \leq I^*$, then $\tilde{\lambda}(I_{in}) = 0$, hence we have to prove that $\mu(\cdot, I_{in})$ is strictly decreasing on $\mathbb{R}_+$. From Lemma A1 we have that $g(I_{in}, \cdot)$ is strictly increasing in $J = \mathbb{R}_+$, then $\mu(\cdot, I_{in})$ is strictly decreasing in $J^{-1} = \mathbb{R}_+$. If $I_{in} > I^*$, then $\tilde{\lambda}(I_{in}) = \ln\left(\frac{I_{in}}{\gamma(I_{in})}\right) > 0$. From Lemma A1 we have that $g(I_{in}, \cdot)$ is strictly increasing in $J = [0, \gamma(I_{in})]$, then $\mu(\cdot, I_{in})$ is strictly decreasing in $J^{-1} = [0, \tilde{\lambda}(I_{in})]$. In the same way we prove that $\mu(\cdot, I_{in})$ is strictly increasing in $[\tilde{\lambda}(I_{in}), \infty)$.

For the part c), first we note that for any $\lambda > 0$, $\frac{\partial \mu(\lambda, I_{in})}{\partial I_{in}} = \frac{1}{\lambda I_{in}} h(I_{in})$ with $h(I) = p(I) - p(Ie^{-\lambda})$. Since p is strictly increasing on $(0, I^*]$, we have that

$$h(I) > 0 \text{ for all } I \in (0, I^*]. \tag{6}$$

In the same way, since p is strictly decreasing on $[I^*, \infty)$, we have that

$$h(I) < 0 \text{ for all } I \in [I^* e^{\lambda}, \infty). \tag{7}$$

From (6) and (7), we conclude that there exists $\mathcal{I}(\lambda) \in J := (I^*, I^* e^{\lambda})$ such that $h(\mathcal{I}(\lambda)) = 0$. Now let $I_1, I_2 \in J$ such that $I_1 < I_2$. It is not difficult to note that

$$h(I_2) - h(I_1) = \underbrace{p(I_2) - p(I_1)}_{<0} + \underbrace{p(I_1 e^{-\lambda}) - p(I_2 e^{-\lambda})}_{<0} < 0,$$

from where h is strictly decreasing on J. Combining this result with the inequalities (6) and (7), we conclude that h is positive on $(0, \mathcal{I}(\lambda))$ and negative on $(\mathcal{I}(\lambda), \infty)$. Part c) follows directly from this result.

For the part d), if $\lambda \to \infty$, then $I_{out}(\lambda, I_{in}) \to 0$. Thus, $\mu(\lambda, I_{in}) \to g(0, I_{in}) = p(0)$. □

The following lemma states how γ (defined in Lemma A1) varies with I_{in}. This lemma is necessary for proving Proposition A4.

Lemma A3. *γ is continuous and strictly decreasing as a function of I_{in} on $[I^*, \infty)$.*

Proof. Let $I_{in}, I'_{in} > I^*$ such that $I_{in} < I'_{in}$. For any $I_{out} \in [\gamma(I_{in}), I^*)$, the function $g(I_{out}, \cdot)$ is strictly decreasing on $[\gamma(I_{out}), \infty)$. Since $I_{out} < I^*$, we have that $\gamma(I_{out}) \in (I^*, \sigma(I_{out}))$. We also note that $I_{out} > \gamma(I_{in}) > \sigma(I_{in})$, therefore $\sigma(I_{out}) < I_{in}$. The last inequality implies that the function $g(I_{out}, \cdot)$ is strictly decreasing on $[I_{in}, \infty)$. By symmetry of g, we conclude that the function $g(\cdot, I_{out})$ is strictly decreasing on $[I_{in}, \infty)$. Thus, we have that

$$g(I_{in}, I_{out}) > g(I'_{in}, I_{out}), \text{ for all } I_{out} \in [\gamma(I_{in}), I^*).$$

This shows that $g(I_{in}, \cdot)$ cannot intersect p on $[\gamma(I_{in}), I^*)$, therefore $\gamma(I'_{in}) < \gamma(I_{in})$. Consequently, γ is strictly decreasing on (I^*, ∞).

To prove that γ is continuous, it is enough to prove that γ is a bijection. Since γ is strictly decreasing, it is enough to prove that for any $y \in (0, I^*)$ there exist $I_y \in (I^*, \infty)$ such that $g(I_y, y) = p(y)$. For this purpose, we define the function $G : [I^*, \infty) \longrightarrow \mathbb{R}$ such that

$$\begin{aligned} G(I_{in}) &= \ln(I_{in}/y)[g(I_{in}, y) - p(y)] \\ &= \int_y^{I_{in}} \frac{p(I) - p(y)}{I} dI. \end{aligned}$$

It is clear that $G(I^*) > 0$ (see proof Lemma A1 c)). Let $M(I) = \frac{p(I)-p(y)}{I}$. Since $\lim_{I\to\infty} \frac{M(I)}{1/I} = p(0) - p(y) < 0$, we conclude that $\lim_{I_{in}\to\infty} G(I_{in}) = -\infty$. Thus, since G is continuous, there is $I_y > I^*$ such that $G(I_y) = 0$.

From Lemma A1 c), we have that

$$\lambda(I_{in}) < \gamma(I_{in}) < I^*.$$

By taking the limit when $I \to I^{*+}$ in the later inequality, we conclude that $\gamma(I_{in}) \to I^*$ as $I_{in} \to I^{*+}$. Therefore γ is continuous on $[I^*, \infty]$. □

The following proposition states some properties of the critical optical depth (defined in (3.28)).

Proposition A4. *(Properties of the critical optical depth.)*

a) For any $I_{in} \in [I^*, \infty)$ it holds

$$\ln\left(\frac{I_{in}}{I^*}\right) < \tilde{\lambda}(I_{in}) < \ln\left(\frac{I_{in}}{\sigma(I_{in})}\right). \tag{8}$$

b) $\tilde{\lambda}$ is continuous on $\mathbb{R}_+$, strictly increasing on $[I^*, \infty)$, and $\lim_{I_{in}\to\infty} \tilde{\lambda}(I_{in}) = \infty$.

Proof. From Lemma A1 part c), we have that for any $I_{in} > I^*$,

$$\sigma(I_{in}) < \gamma(I_{in}) < I^*.$$

This implies the inequality (8). For the part b), from Lemma A3 and the definition of $\tilde{\lambda}$ (see 3.28), we conclude that $\tilde{\lambda}$ is strictly increasing on $[I^*, \infty)$. By taking the limit when $I_{in} \to \infty$ in (8), we conclude that $\lim_{I_{in}\to\infty} \tilde{\lambda}(I_{in}) = \infty$. For the continuity, we take the limit when $I_{in} \to I^{*+}$ in (8), we obtain $\lim_{I_{in}\to I^{*+}} \tilde{\lambda}(I_{in}) = 0 = \tilde{\lambda}(I^*)$, from where $\tilde{\lambda}$ is continuous in I^*. The continuity over all $\mathbb{R}_+$ follows directly from the definition of $\tilde{\lambda}$ and Lemma A3. □

The following proposition gives some properties of the critical light intensity

Proposition A5. *(Properties of the critical light intensity) $\mathcal{I}$ is strictly increasing and continuous.*

Proof. From (5), we obtain that

$$\frac{\mathcal{I}(\lambda)}{\sigma(\mathcal{I}(\lambda))} = e^{\lambda}.$$

This equation shows that as λ increases the fraction on the left increases. Since σ is strictly decreasing, this is only possible if $\mathcal{I}(\lambda)$ increases. Thus, $\mathcal{I}$ is strictly increasing as a function of λ. From (9), we also note that $\mathcal{I}$ is a bijection, indeed, it is inverse function $\mathcal{I}^{-1}(I) : [I^*, \infty) \longrightarrow [0, \infty)$ is given by

$$\mathcal{I}^{-1}(I) = \ln\left(\frac{I}{\sigma(I)}\right). \tag{9}$$

Since $\mathcal{I}$ is strictly increasing and bijective, we conclude that is continuous. □

Bibliography

[1] S.-B. Hsu, C.-J. Lin, C.-H. Hsieh, and K. Yoshiyama. Dynamics of phytoplankton communities under photoinhibition. *Bulletin of Mathematical Biology*, 75(7):1207–1232, 2013.

Appendix B

Results on the dynamics of scalar differential equations.

Consider the non-autonomous Kolmogorov equation:

$$\frac{du}{dt} = uF(t,u), \quad u \in \mathbb{R}_+ = [0,\infty), \tag{10}$$

and the ω-periodic Kolmogorov equation:

$$\frac{du}{dt} = uF_0(t,u), \quad u \in \mathbb{R}_+, \tag{11}$$

where $F(t,u) : \mathbb{R}^2_+ \longrightarrow \mathbb{R}$ is continuous, decreasing in u and locally Lipschitz in u, and $F_0(t,u) : \mathbb{R}^2_+ \longrightarrow \mathbb{R}$ is continuous, ω-periodic in t ($\omega > 0$), decreasing in u and locally Lipschitz in u uniformly in $t \in [0,\omega]$. Consider the following assumptions:

Assumption B6. $\lim_{t\to\infty} |F(t,u) - F_0(t,u)| = 0$ *uniformly for* u *in any bounded subset of* $\mathbb{R}_+$.

Assumption B7. $\int_0^\omega F_0(t,R)dt < 0$ *for some* $R > 0$.

Lemma B8. *Assume that Assumptions B6 and B7 hold. Then, solutions of (10) are ultimately bounded.*

Proof. Let $\phi(t,s,u), t \geq s \geq 0$, be the unique solution of (10) with $\phi(s,s,u) = u$. From Assumption B6, there is $t_0 > 0$ such that $|F(t,0) - F_0(t,0)| < 1$ for all $t \geq t_0$. Since F is decreasing in u, we have that

$$F(t,u) \leq F(t,0) < 1 + \max_{t\in[0,\omega]} F_0(t,0), \quad \text{for all } t \in [t_0,\infty), u \in \mathbb{R}_+$$

and

$$F(t,u) \leq \max_{t\in[0,t_0]} F(t,0), \quad \text{for all } t \in [0,t_0), u \in \mathbb{R}_+.$$

From these inequalities we conclude that $F(t,u)$ is bounded from above, and consequently $\phi(t,s,u)$ exists for all $t \geq s \geq 0$.

Let $R > 0$ be according to Assumption B7 and let $\epsilon > 0$ be such that $\epsilon < -\frac{1}{\omega}\int_0^\omega F_0(t,R)dt$. From Assumption B6, there is t^* such that $|F(t,R) - F_0(t,R)| < \epsilon$ for all $t \geq t^*$. Then, for all $t \geq t^*$ we have

$$\int_t^{t+\omega} F(\tau,R)d\tau < -\epsilon_1 := \epsilon\omega + \int_0^\omega F_0(t,R)dt < 0. \tag{12}$$

If $u = 0$ then $\phi(t,0,u) = 0$ for all $t \geq 0$, hence suppose that $u > 0$. In that case $\phi(t,0,u) > 0$ for all $t \in \mathbb{R}_+$. For the rest of the proof we need the following claim:

Claim 1: If there is $t_1 \geq t^*$ such that $\phi(t,0,u) \geq R$ for all $t \in [t_1, t_1+\omega]$ then $\phi(t_1+\omega,0,u) < \phi(t_1,0,u)e^{-\epsilon_1}$.

The proof of the claim follows directly from the following inequality:

$$ln\left(\frac{\phi(t_1+\omega,0,u)}{\phi(t_1,0,u)}\right)=\int_{t_1}^{t_1+\omega}F(t,\phi(t,0,u))dt\leq\int_{t_1}^{t_1+\omega}F(t,R)dt<-\epsilon_1.$$

Let us assume that $\phi(t,0,u)\geq R$ for all $t\geq t^*$. Using Claim 1 we obtain that

$$\phi(t^*+k\omega,0,u)<\phi(t^*,0,u)exp(-k\epsilon_1),\ \text{ for any } k\in\mathbb{N}$$

and a contradiction is achieved letting $k\to\infty$. We may therefore assume without loss of generality that $\phi(t^*,0,u)<R$.

Now suppose that there is $t_1>t^*$ such that $\phi(t_1,0,u)=R$. Let us define $\Delta:=\max\{\delta\geq 0\,;\,\phi(t_1+\delta,0,u)\geq R\}$ and $\mathcal{I}:=[t_1,t_1+\Delta]$. From the Claim 1 we have that $\phi(t_1+\omega,u)<Re^{-k\epsilon_1}<R$, therefore Δ is well defined and smaller than ω. For each $t\in\mathcal{I}$ we have:

$$ln\left(\frac{\phi(t,0,u)}{\phi(t_1,0,u)}\right)=\int_{t_1}^{t}F(t,\phi(\tau,0,u))d\tau\leq(t-t_1)M\leq\omega M,\qquad(13)$$

with M an upper bound for $F(t,u)$. From (13), we conclude that $\phi(t,0,u)\leq Re^{M\omega}$ for all $t\in\mathcal{I}$. This implies that $\phi(t,0,u)\leq\beta=Re^{M\omega}$ for all $t\geq t^*$, and consequently $\limsup_{t\to\infty}\phi(t,0,u)\leq\beta$. □

The following proposition is inspired by part b) of Theorem 2.1 in [1].

Proposition B9. *Assume that Assumptions B6-B7 hold. Let $a>0$ and $J=[a,\infty)$. If $F_0(a,t)\geq 0$ for all $t\geq 0$, then:*

a) The periodic equation (11) admits an ω-periodic solution u^* satisfying $u^*(t)\geq a$ for all $t\in[0,\omega]$.

b) Assume that $F(t,a) \geq 0$ for all $t \geq 0$. If (11) admits a unique ω-periodic solution u^* satisfying $u^*(t) \geq a$, then any solution to (10) with initial condition on J approaches asymptotically to u^*.

Proof. Let $\phi(t,s,u)$ and $\phi_0(t,s,u)$ be the unique solutions of (10) and (11) respectively with $\phi(s,s,u) = \phi_0(s,s,u) = u \in \mathbb{R}_+$. From Lemma B8, solutions of (11) and (10) are ultimately bounded, and hence, uniformly bounded. Let $S : J \longrightarrow J$ be the Poincaré map associated to (11). We note that J is positively invariant with respect to (11), then S is well defined. Let $u \in J$. Since $S^n(u)$ is monotone and bounded, $S^n(u)$ is convergent. Since J is positively invariant with respect to (11), $u_0 = \lim_{n\to\infty} S^n(u) \in J$. Thus, $u^*(t) = \phi_0(t,s,u_0)$ is an ω-periodic solution satisfying $u^*(t) \in J$, and the part a) is proved.

For the part b), let u^* be the unique ω-periodic solution with $u^*(0) \in J$. By Proposition 3.2 in [2], $\phi(t,s,u)$ is asymptotic to the ω-periodic semiflow $T(t) := \phi_0(t,0,\cdot) : \mathbb{R}_+ \longrightarrow \mathbb{R}_+$, and hence $T_n(u) = \phi(n\omega,0,u), n \geq 0$, is an asymptotically autonomous discrete dynamical process with limit discrete semiflow $S^n : \mathbb{R}_+ \longrightarrow \mathbb{R}_+, n \geq 0$. Since $u^*(0)$ is the unique globally stable fixed point of S, by Theorem 2.4 in [2], we conclude that $\lim_{n\to\infty} T_n(u) = u^*(0)$ for any $u \in J$. Applying Theorem 3.1 in [2], we conclude the proof. □

Properties of μ_I

Here, we state some properties of the function μ_I defined in (4.28).

Proposition B10. *Let us consider μ_I given in (4.28). Then*

a) $\lim_{x\to\infty} \mu_I(t,x) = 0$ *uniformly for* $t \in [0,\omega]$.

b) $x \longmapsto \mu_I(t,x)$ *is strictly decreasing for all* $t \in (0,\omega/2)$ *and* $\mu_I(t,x) = 0$ *for all* $t \in [\omega/2,\omega]$.

c) μ_I *is Lipschitz in* x *uniformly in* t.

Proof. We recall that $\mu_I(t,x) = \int_0^L p(I(t,x,z))dz$. By doing the change of variable $I = I(t,x,z)$, we rewrite μ_I as:

$$\mu_I(t,x) = \frac{g(q)}{(kx+K_{bg})L}\int_{I_{out}(t,x)}^{I_{in}(t)} \frac{p(I)}{I}dI \tag{14}$$

where $I_{out}(t,x) = I(t,x,L)$. We can easily verify that:

$$0 \leq \mu_I(t,x) \leq \frac{1}{kxL} I_{max}\mu_{max}. \tag{15}$$

Letting $x \to \infty$ in (15), we prove a). For b), if $I_{in}(t) > 0$ we have:

$$\frac{\partial \mu_I(t,x)}{\partial x} = \frac{g(q)kL}{(kx+K_{bg})^2L^2}\int_{I_{out}(t,x)}^{I_{in}(t)} \frac{p(I_{out}(t,x)) - p(I)}{I}dI. \tag{16}$$

Since p is strictly increasing and $I_{out}(t,x) < I$ for all $I \in (I_{out}(t,x), I_{in}(t)]$ and $x > 0$, we conclude that $\frac{\partial \mu(t,x,q)}{\partial x} < 0$ for all $x > 0$, and consequently μ is strictly decreasing in x. For c), let us define $\theta = (kx+K_{bg})L$. Let l be a

Lipschitz constant of p, then we have:

$$\begin{aligned}\left|\frac{\partial \mu_I(t,x)}{\partial x}\right| &\leq \frac{kL}{\theta^2}\int_{I_{out}(t,x)}^{I_{in}(t)} \frac{|p(I)-p(I_{out}(t,x))|}{I}dI \\ &\leq \frac{klL}{\theta^2}\int_{I_{out}(t,x)}^{I_{in}(t)} \frac{|I-I_{out}(t,x)|}{I}dI \\ &\leq lkLI_{max}\frac{1-e^{-\theta}}{\theta} \leq lkLI_{max}.\end{aligned}$$

Thus μ_I is Lipschitz in x uniformly in t and c) is proved. □

Bibliography

[1] G. S. Wolkowicz, X.-Q. Zhao, et al. n-species competition in a periodic chemostat. *Differential and Integral Equations*, 11(3):465–491, 1998.

[2] X.-q. Zhao. Asymptotic behavior for asymptotically periodic semiflows with applications. In *MR 97i: 58150*. Citeseer, 1996.

List of publications:

- **(2019) (Submitted)** Carlos Martínez, Francis Mairet, Olivier Bernard. "Dynamics of the periodically forced light-limited Droop model." *Journal of Differential Equations.*

- **(2019) (Submitted)** Carlos Martínez, Francis Mairet, Luis Plaza, Antoine Sciandra, Olivier Bernard. "Quantifying the potential of microalgae culture systems to remove nutrients from wastewater." *Proceedings of the FOSBE conference.*

- **(2019) (In preparation)** Carlos Martínez, Francis Mairet, Olivier Bernard. "Effects of photoinhibition on the dynamics of the light-limited Droop model." *Journal of Differential Equations.*

- **(2019) (Accepted)** Carlos Martínez, Olivier Bernard, Pierre Martinon, Francis Mairet. "Dynamics and Control of a Periodically Forced Microalgae Culture", *Proceedings of the DYCOPS conference.*

- **(2018)** Carlos Martínez, Olivier Bernard, and Francis Mairet. "Theory of turbid microalgae cultures", *Journal of Theoretical Biology, 456, 190-200.*

- **(2018)** Carlos Martínez, Olivier Bernard, and Francis Mairet. "Maximizing Microalgae Productivity in a Light-Limited Chemostat", *IFAC-PapersOnLine 51(2), 735-740.*

- **(2017)** Carlos Martínez, Olivier Bernard, and Francis Mairet. "Maximizing microalgae productivity by shading outdoor cultures." *IFAC-PapersOnLine 50.1 (2017): 8734-8739.*

Modeling, analysis, and control of microalgae growth in dense cultures.

Abstract

Microalgae are photosynthetic microorganisms with a high biotechnological potential. They have many industrial applications, including food, fine chemicals, biofuel and wastewater treatment. Nevertheless, controlling optimal growth conditions for full-scale outdoor cultivation of microalgae is challenging. Mathematical models based on ordinary differential equations are of great help to better manage this complex, nonlinear and dynamical system. The aim of this thesis is to better understand how different factors such as the availability of light and nutrients affect microalgae growth in high density cultures. In a first part, we study the impacts of photo-inhibition and medium turbidity when microalgae growth is only limited by light. Then, we analyse the long-term behaviour of a microalgae population model accounting both for nutrient and light limitations. We determine the conditions to avoid the extinction of the population. In particular, we show that continuous periodic culture operation (periodic dilution rate and nutrient supply) under periodic fluctuations of environmental conditions (such as the light source or temperature) lead to a periodic behaviour. In a third part, we show how to maximize microalgae productivity. We determine a strategy for shading outdoor cultures to protect microalgae from excess light. We find the

optimal incident light for photobioreactors operated at steady state. In the context of wastewater treatment, we determine numerically optimal values of the depth of a culture limited by light and nutrient. Finally, the last part of this work proposes and validates a mathematical model accounting for light, nitrogen, and phosphorus limitations, including photoacclimation dynamics.

Keywords: microalgae, mathematical modelling, biomass productivity, photoinhibition, quota model, dynamical system, asymptotic behavior, control, Droop, chemostat, photobioreactor

Résumé

Les microalgues sont des microorganismes photosynthétiques avec un grand potentiel biotechnologique. Elles ont différentes applications industrielles, parmi lesquelles l'alimentation humaine ou animale, la production de composés pour la chimie verte, les biocarburants et le traitement des eaux usées. Néanmoins, contrôler les conditions optimales de cultures de microalgues à grande échelle reste un défi difficile. L'objectif de cette thèse est de mieux comprendre ces systèmes à l'aide de modèles mathématiques basés sur des équations différentielles ordinaires décrivant la croissance microalgale dans des cultures à haute densité en fonction de différents facteurs comme la disponibilité en lumière et en nutriments. Dans une première partie, on étudie l'impact de la photoinhibition et de la turbidité du milieu sur la croissance microalgale limitée par la lumière. Ensuite, le comportement à long terme d'une population microalgale colimitée par un nutriment et la lumière est analysé. Des conditions pour éviter l'extinction de la population sont identifiées. En particulier, on montre que le fonctionnement en continu, avec entrées périodiques (concentrations dans l'alimentation et taux de dilution périodiques) sous variations périodiques de l'environnement (source de lumière et température), conduit la population à un état périodique. Dans une troisième partie, une stratégie est proposée pour maximiser la productivité microalgale en extérieur, basée sur un contrôle de l'ombrage. Finalement, dans le contexte du traitement des eaux usées, on détermine numériquement la profondeur optimale pour une culture limitée par la lumière

et par un substrat (à dépolluer). Dans une dernière partie, un modèle est proposé et validé pour rendre compte de la limitation par la lumière, l'azote et le phosphore, tout en incluant la dynamique de photoacclimatation.

Mots-clés: microalgues, modélisation mathématique, productivité, photoinhibition, modèle à quota, système dynamique, comportement asymptotique, contrôle, Droop, chémostat, photobioréacteur